3-22-2012

Optimization of Nanoscale Zero-Valent Iron for the Remediation of Groundwater Contaminants

Andrew W. E. McPherson

OPTIMIZATION OF NANOSCALE ZERO–VALENT IRON FOR THE REMEDIATION OF GROUNDWATER CONTAMINANTS

THESIS

Andrew W.E. McPherson, Second Lieutenant, USAF

AFIT/GES/ENV/12-M01

DEPARTMENT OF THE AIR FORCE
AIR UNIVERSITY

AIR FORCE INSTITUTE OF TECHNOLOGY

Wright-Patterson Air Force Base, Ohio

AFIT/GES/ENV/12-M01

OPTIMIZATION OF NANOSCALE ZERO–VALENT IRON FOR THE REMEDIATION OF GROUNDWATER CONTAMINANTS

THESIS

Presented to the Faculty

Department of Systems and Engineering Management

Graduate School of Engineering and Management

Air Force Institute of Technology

Air University

Air Education and Training Command

In Partial Fulfillment of the Requirements for the

Degree of Master of Science in Environmental Engineering and Science

Andrew W.E. McPherson, B.S.

Second Lieutenant, USAF

March 2012

AFIT/GES/ENV/12-M01

OPTIMIZATION OF NANOSCALE ZERO–VALENT IRON FOR THE REMEDIATION OF GROUNDWATER CONTAMINANTS

Andrew W.E. McPherson, B.S.

Second Lieutenant, USAF

Approved:

■ S IG N E D --	5 Mar 12
Mark Goltz, Lt Col (Ret.), USAF, P.E., Ph.D. (Co-Chairman)	Date
S I G N E D --	6 Mar 12
Abinash Agrawal, Ph.D., WSU (Co-Chairman)	Date
S I G NE D --	6 Mar 12
Leeann Racz, Maj, USAF, P.E., Ph.D. (Member)	Date

Abstract

Nanoscale zero-valent iron (nZVI) is an emerging material used for the remediation of groundwater contaminants. The nanoparticles are capable of reductively destroying or immobilizing a wide range of contaminants. Their extremely small size results in a high surface area to mass ratio, making them much more reactive compared to their more-coarse predecessors. Their small size also allows nZVI particles to be injected directly into contaminated areas via a well, limiting the above-ground footprint and allowing access to contaminated areas that are beyond the reach of some conventional methods, such as excavation. nZVI application has the potential to facilitate remediation in difficult situations, improve remediation outcomes, and reduce remediation costs.

Using bench-scale laboratory experiments, this research investigates three methods for improving the reactivity and transport properties of nZVI, including: optimizing the nanoparticle synthesis process, adding a polyelectrolyte stabilizer to minimize nanoparticle aggregation and decrease their size, and amending the particles with a palladium catalyst. Increasing the amount of iron-reducing chemical during nZVI synthesis improved reactivity by 72%. Addition of a polyelectrolyte stabilizer at an optimized concentration of 8.0 g/L further increased nZVI reactivity by 452%, while decreasing the mean particle size from 29.3 to 4.6 nm and inhibiting aggregation, which should improve subsurface transport. Finally, amendment of nZVI with an optimized amount of 3.3% (w/w) palladium catalyst increased reactivity by another 375% while decreasing the formation of toxic byproducts during contaminant degradation.

To the community of the Silver Valley of Idaho,
may the soilings of yesterday's spoils be
washed away by the knowledge and hope of tomorrow.

Acknowledgments

I appreciate the AFIT Faculty Research Council for their funding of this work and Dr. Nancy Ruiz of the Naval Facilities Engineering Service Center for her sponsorship. I am very thankful for my thesis advisors, Dr. Mark Goltz, Dr. Abinash Agrawal, and Maj. Leeann Racz, for their work and sustained support and guidance throughout this research endeavor. Their patience, knowledge, and critique proved indispensable.

I would also like to thank my coworkers, Kelsey Danner, Dr. Garrett Struckhoff, Dr. Sushil Kanel, Madelyn Smith, and Ke Qin. Their collaboration, instruction, and friendship in the laboratory were essential to my research efforts and enriched my time as a student. Also, thanks go to Elizabeth Maurer of the 711th Human Performance Wing for her help performing DLS analysis and to Barbara Miller of the University of Dayton's Nanoscale Engineering Science & Technology (NEST) laboratory for conducting TEM imaging.

To my fellow AFIT students, I am thankful for your support, friendship, and good humor. Your company made the pains and frustrations of graduate school less difficult. Your mentorship made me a wiser officer and better friend.

I am ever thankful to my loving family for their constant support and understanding. You are a source of motivation and perspective in challenging times. I am especially thankful for my wonderful fiancé, whose patience and love is a constant source of happiness and renewal.

Andrew W.E. McPherson

Table of Contents

Page

Page

List of Figures

Page

List of Tables

Page

OPTIMIZATION OF NANOSCALE ZERO–VALENT IRON FOR THE REMEDIATION OF GROUNDWATER CONTAMINANTS

I. Introduction

Background

Zero-valent iron (ZVI) is a strongly reducing material. ZVI is capable of degrading or immobilizing a wide range of contaminants, including organic chemicals and heavy metals, making it a versatile remediation tool. ZVI was originally utilized for the remediation of groundwater contaminants in permeable reactive barriers (PRBs), stationary trenches filled with reactive media that remove contaminants as natural groundwater flow passes through them [4]. Iron filings left over from industrial manufacturing and more-coarse iron particles are typically used in PRBs due to their wide availability and low cost. However, PRBs are a passive remediation technology. At best they can only contain contamination, necessitating continued site monitoring and, in some cases, periodic replacement of the reactive media. Also, the need for trench excavation limits the depth to which PRBs can reach, prohibiting their use in many cases.

In 1997, the development of smaller, more reactive nanoscale zero-valent iron (nZVI) brought with it the promise of more rapid and complete remediation of contaminants [10]. Because of their small size, nZVI particles could potentially be injected into the subsurface and subsequently be transported to and mixed with the target contaminants. This possibility transformed zero-valent iron from an immobile, passive technology to one capable of active remediation of both contaminant plumes and source zones. Active remediation is desirable because it may better protect human health and the

environment while reducing the high costs of long-term monitoring and hydraulic containment (i.e. pump and treat) of groundwater contamination. As an *in situ* technology, nZVI injection is also attractive because it avoids the high cost of extracting and treating large volumes of water with dilute concentrations of contamination above ground. The high reactivity of nZVI is a result of the high surface area to mass ratio achieved at such small scales; more of the particle mass is located on the outside and is available for reaction. nZVI is applied by the direct injection of a nanoparticle slurry into the subsurface via a well; both direct push wells and pairs of recirculation wells have been used [7:274-275]. Because no excavation is needed, nZVI can be applied at greater depths than PRBs and at sites where buildings or ongoing operations prohibit more invasive methods.

The target contaminants studied here, chlorinated methanes and ethenes, are two classes of chlorinated organic contaminants widely found at hazardous waste sites. Because of their broad use as industrial solvents on military installations and improper disposal in the past, they are among the most common groundwater contaminants at Department of Defense (DOD) managed sties. The DOD is responsible for 6,400 different hazardous waste sites [5:1826]. Of these, nearly 6,000 require groundwater remediation [9:1]. Between 1995 and 2005, the DOD spent nearly $20 billion remediating these contaminated sites [9:6]. Future cleanup through 2033 is estimated to cost an additional $33 billion [5:1826]. As an emerging remediation tool, nZVI injection has already seen successful use by the DOD at Cape Canaveral Air Force Station, Hunters Point Shipyard, Naval Air Station Jacksonville, and Naval Air Engineering Station Lakehurst [6:ii-iii; 7:276-277]. nZVI was characterized by Naval Facilities

Engineering Command contractors as a "promising option for treatment of [contamination] source zones" [6:iv].

Problem Statement

Despite impressive advances in nZVI technology within the last decade and its limited commercialization, several barriers have prevented it from becoming a widely-adopted remediation option. Initial hopes that nZVI would be readily transported in the subsurface, allowing for improved targeting of contaminants and the treatment of large areas without the need to drill many costly wells, continue to be disappointed. Also, compared to other remediation options, nZVI remains relatively expensive due to the energy- and chemical-intensive methods used to synthesize it [2:10]. Finally, although nZVI clearly outperforms its micro- and milli-scale predecessors in terms of reactivity, chlorinated byproduct formation during degradation remains an issue (see Chapter II). Maximizing nZVI utility while minimizing cost will be a step forward in addressing these issues. The objective of this thesis is to identify and optimize the most promising methods for improving nZVI reactivity while decreasing particle size and improving stability for better nanoparticle transport.

Research Questions

Below is a list of questions and sub-questions which guided this research effort:

1. What aspects of nZVI synthesis may be optimized to improve nanoparticle reactivity?
    i. What are the most widely used nZVI synthesis methods?
    ii. What physical and chemical processes are involved in nZVI synthesis and how might they affect the outcome of synthesis?

2. How might stabilizer use be optimized to improve nZVI reactivity and transport characteristics?
    i. Based on past research, which stabilizers perform best with nZVI?
    ii. What physical effects do stabilizers have on nanoparticle formation and stabilization?
    iii. What is the optimal amount of stabilizer to use in order to maximize nZVI performance?
3. How might catalyst use be optimized to improve nZVI reactivity and minimize formation of toxic chlorinated organic byproducts?
    i. Based on past research, which catalysts most improve the reactivity of nZVI?
    ii. Which catalysts best facilitate the degradation of chlorinated organic contaminants to completely dechlorinated, non-toxic byproducts?
    iii. What physical-chemical processes are involved in catalytic degradation of chlorinated organic contaminants?
    iv. What is the optimal amount of catalyst to use to maximize nZVI performance?
4. What are the chemical pathways and kinetic rates of contaminant degradation by stabilized, catalyzed nZVI?
    i. What degradation byproducts are observed?
    ii. How may the degradation of contaminants be modeled?
    iii. How does observed performance compare to previously reported degradation pathways and kinetic rates by nZVI?

Scope and Research Approach

Research was conducted using bench-scale laboratory experiments, with the degradation of a few common groundwater contaminants in sealed batch reactors monitored over time. Degradation rates versus time were determined and compared for nZVI synthesized under different conditions and targeting various contaminants. To further understand the physical differences at play, physical characterization of the nanoparticles was also performed using dynamic light scattering (DLS) particle size measurement and transmission electron microscope (TEM) imaging. The controlled environment of bench-scale batch reactors is useful for testing the effects of individual parameters on nZVI performance. However, by the same token, the controlled environment cannot completely account for the complex, variable conditions encountered in the subsurface environment. Parameters such as groundwater pH, organic carbon concentration, dissolved oxygen concentration, salinity, temperature, biotic activity, and nZVI injection scheme can all be expected to affect the real-world performance of nZVI particles. Laboratory research findings, although useful in understanding reactivity and transport characteristics, may not be predictive of field performance.

Preview

This thesis uses the scholarly article format. Chapter II is a critical review of the literature pertaining to polyelectrolyte stabilization and catalysis of nZVI, to be submitted for publication in the journal *Environmental Technology Reviews*. This critical review article replaces the traditional Literature Review thesis section, while offering possibilities for future research to both the graduate school and the larger academic

community. Chapter III is a research article, to be submitted for publication in the journal *Environmental Science & Technology*. Together, these articles form the body of this thesis and include all the elements of a traditional thesis, presented in layouts prescribed by the peer-reviewed journals to which they will be submitted. Chapter IV offers a final discussion of the articles, their findings, and opportunities for future research. Included in the appendices are graphs and figures which are to be included in the Supporting Information section that accompanies the research article.

II. Scholarly Article: Critical Review of Literature

To be submitted to *Environmental Technology Reviews*

Polyelectrolyte Stabilization and Bimetal Catalyzation of Nanoscale Zero-Valent Iron: A Critical Review

Abstract

Nanoscale zero-valent iron (nZVI) is an attractive new groundwater remediation tool which offers increased reactivity toward and improved access to subsurface contaminants. Polyelectrolyte stabilization and bimetal catalyzation are two of the most promising methods for increasing the performance of nZVI. Addition of polyelectolyte stabilizers to nZVI decrease particle agglomeration and reduce particle size, increasing net reactivity and enhancing transport in column studies. Amendment of nZVI with metallic catalysts improves reactivity toward almost all groundwater contaminants and, in the case of chlorinated organic compounds, reduces the formation of toxic byproducts. Here, these two methods are reviewed in depth. Physical processes involved are explored, the state-of-the-art is presented, and opportunities for future research are discussed. A general lack of comparability between past studies and the need for greater standardization of nZVI testing procedures is identified. For polyelectrolyte stabilization, prospects for future research include comparative studies that evaluate the performance of many polyelectrolytes side-by-side, use of engineered co-polymers to improve nonaqueous phase liquid (NAPL) targeting by nZVI, and resolution of poor nZVI transport observed at flowrate, ionic strength, and hydraulic conductivity heterogeneity conditions representative of the

subsurface. For bimetal catalyzation, opportunities for future research include comparative studies that evaluate the performance of many catalysts side-by-side, assessment of untested or largely overlooked catalysts such as Ag, and resolution of economic and health issues associated with the use of costly or toxic catalysts such as Pd and Ni, respectively.

Introduction

Nanoscale zero-valent iron (nZVI) is an exciting and rapidly developing new groundwater remediation tool. Its potential includes improved access to the subsurface, rapid source zone remediation, economy over traditional remediation techniques, and site-specific tailoring of the particles to enhance performance. Synthesizing such small particles, only 10^{-9} m in diameter, vastly increases their reactive surface area per gram of iron. The specific surface area of nZVI is typically tens of square meters per gram, one to two orders of magnitude higher than micro-scale particles [1]. The result is particles that are highly reactive compared to their larger predecessors and well-suited for *in situ* remediation of a variety of contaminants. nZVI effectively remediates halogenated organics, pesticides, antibiotics, organophosphates, organic dyes, explosive compounds, heavy metals, perchlorate, and nitrate [2,3]. The methods of remediation, which include reduction, sorption, complexation, and co-precipitation, are contaminant-dependent [2,3]. Furthermore, it has been hypothesized that smaller, colloidal particles could be mobile in the subsurface, thereby facilitating their transport to target contaminants following subsurface injection. The majority of interest in nZVI is focused on its use to remediate contaminated source areas, particularly those inaccessible to conventional remediation methods due to depth or site-use, via direct injection or recirculating wells [2,4-6]. nZVI may also be injected to form permeable reactive barriers [2,7,8].

A wide variety of methods are used to synthesize nZVI particles, but they can generally be separated into two categories: top-down, in which coarser iron is refined into nano-scale particles, and bottom-up, in which nano-scale particles are grown from Fe ion precursors. Examples of top-down synthesis include laser ablation, spark discharge generation, and milling. Examples of bottom-up synthesis include vacuum sputtering, electrodeposition of iron ions, and the reduction of oxide compounds [2,3]. For laboratory-scale and smaller field-scale use, the borohydride reduction method originally proposed by Wang and Zhang in 1997 is most-widely used [1,5,6]. In contrast, two of the leaders in commercial-scale synthesis of nZVI, Golder Associates Inc. and Toda Kogyo Ltd., use different methods. Golder uses a top-down ball mill system while Toda Kogyo uses hydrogen to reduce pre-synthesized iron oxide nanoparticles [2,9]. A large number of laboratory-scale studies employ Toda Kogyo nanoparticles due to their commercial availability.

Many thorough reviews of nZVI technology were previously published, which include discussions of surface chemistry, particle characterization, potential toxicity, target contaminants for remediation, *in situ* implementability, use in permeable reactive barriers (PRBs), and small-scale field studies [2-4,7,9-19]. Given the rapid pace of nZVI research within the last decade however, some of these reviews are unavoidably dated or limited in scope. Two recent developments that have seen significant attention and which hold great promise, but have not been comprehensively reviewed, are improving reactivity and transport characteristics of nZVI particles through polyelectrolyte stabilization and increasing contaminant destruction through bimetal catalyzation of nZVI particles. The purpose of this review is to review the literature relevant to these two aspects of nZVI synthesis and application while identifying prospects for future research.

Polyelectrolyte Stabilization of nZVI

Perhaps the most significant challenge to applying nZVI for subsurface remediation is the rapid agglomeration of individual particles into discrete micro-scale aggregates or larger chain aggregates [20]. Agglomeration occurs due to attractive interparticle van der Waals and magnetic forces [19,20]. The effect of agglomeration is two-fold; first, the available reactive surface area of the nZVI particles is significantly reduced, negatively impacting reactivity, and second, transport of the larger aggregates in porous media is severely restricted [19]. Modifying the surface of the nZVI particles with a polyelectrolyte coating has been conclusively shown to overcome interparticle attractive forces, inhibiting aggregation and thereby improving stability, transport, and reactivity [21-24]. Use of polyelectolytes to stabilize nZVI was pioneered by Mallouk and co-workers beginning in 2000, where carbon nanoparticles and PAA resin were used as supports for nZVI [25,26]. Beginning in 2004 with the work of Schrick et al., the last decade has seen rapid growth in the use of polyelectrolyte coated, or stabilized, nZVI [21]. To date, no fewer than 17 different stabilizing agents have been used, as detailed in Table 2.1. Benefits of using polyelectrolytes to stabilize nZVI include their low cost, wide availability, ease of implementation, non-toxic nature, and the possible promotion of long-term biotic degradation *in situ* [6]. Several polyelectrolytes, such as carboxymethyl cellulose (CMC) and xanthan gum, are food-grade additives [22,27,28]. Some, such as chitosan and soy protein, are derived from natural sources [28,29].

Polyelectrolyte nZVI Stabilizers	
Polyelectrolyte	**Reference(s)**
CMC (Carboxymethyl Cellulose)	6,22-24,27,31-34,39,41, 44,56-58,60,73,84,87
PAA (Polyacrylic Acid)	21,23,28,32,39,40,47,104
PAP (Polyaspartate)	20,31,34,43,49,51,55
PSS (Polystyrene Sulfonate)	20,23,31,43,48,50,104
PAM (Polyacrylamide)	23
PVP (Polyvinylpyrrolidone)	24
PV3A (Polyvinyl alcohol-co-vinyl acetate-co-itaconic acid)	28,53
OMA (Olefin Maleic Acid)	41,42,106
Triblock ($PMAA_{42}$-$PMMA_{26}$-PSS_{462})	51,52
Triblock ($PMAA_{48}$-$PMMA_{17}$-PSS_{650})	49,51,52
Triblock ($PMAA_{15}$-$PBMA_{43}$-PSS_{811})	50
Guar Gum	24,54,105
Xanthan Gum	36,37
Cellulose Acetate	92
Starch	22,56
Soy Proteins	28
Chitosan	29,80

Table 2.1. Summary of polyelectrolytes used to stabilize nZVI.

As their name suggests, polyelectrolytes are chains of individual polymers, with each repeating polymer unit bearing an electrolyte group. The long-chained polymers typically have a very high molecular weight, on the order of thousands of grams per mole. When introduced to water, the electrolyte groups disassociate, leaving the polymer units either positively or negatively charged and releasing their complementary ions to solution [30]. Polymer adhesion to nZVI occurs through either physisorption, driven by dispersive or electrostatic forces, or chemisorption, by covalent bonding to the surface [31]. The charged polymer units aid the polyelectrolyte's adsorption to the nZVI surface via physisorption. In contrast, studies on CMC and polyacrylic acid (PAA) stabilization of nZVI report adsorption occurs via chemisorption, specifically mono- and bidentate chelating, bidentate bridging, and hydrogen bonding [27,32]. Because polyelectrolyte chains are flexible, they may adsorb to nZVI particles at several points

per chain, resulting in high adsorption energies and slow desorption. Kim et al. (2009) showed that for polyaspartate (PAP), CMC, and polystyrene sulfonate (PSS), less than 30% (w/w) desorbed over four months [31]. This rate is insignificant in the context of both laboratory and field-scale use of nZVI, where the reactive particles are oxidized within hours to weeks. Although polyelectrolyte coatings are generally identified by type, several are further identified by molecular weight. The distinction is an important one; variability in performance between different molecular weight polyelectrolytes of the same type may be as much or greater than between type [20,24,31,33,34].

Polyelectrolyte coatings successfully stabilize nZVI by increasing the repulsive forces between individual particles, and in some cases by also forming gel-like networks between the particles [35-37]. The colloidal stability of stabilized nZVI solutions is commonly understood through DLVO theory, under which repulsive steric and electrostatic double layer (EDL) forces oppose attractive van der Waals and magnetic forces. Because these forces act over different distances, their sum, which predicts whether aggregation will occur or not, is dependent on the distance between particles. EDL forces arise when the charged surface of a nanoparticle attracts oppositely charged ions from the surrounding fluid. This “cloud” or double layer of charged ions around a particle forms a repulsive electrical force towards similarly charged particles. Polyelectrolytes, with their ionic polymer units, increase the charge surrounding the nanoparticle, and subsequently, the repulsive force. Steric repulsion arises from the interaction of the polyelectrolyte coating with that of another particle, or with a surface, and the associated thermodynamic penalty [20,32]. Often, the combined effect of EDL and steric forces is referred to as electrosteric repulsion [20,31].

In addition to the stabilization effect of polyelectrolytes on nZVI, the presence of polyelectrolytes during the precipitation-synthesis of nanoparticles affects particle nucleation and, subsequently, particle size. When nanoparticles are precipitated in aqueous solution, many small crystallites initially form which act as nuclei for further growth. Polyelectrolytes mediate faster and more numerous nucleation and slow particle growth, which yields more numerous, smaller diameter particles [38]. For nZVI, this effect was reported twice by He et al. [27,33]. In contrast to these studies, Cirtiu et al. (2011) reported that the presence of CMC, PAA, PSS, and polyacrylamide (PAM) polymers, although inhibiting agglomeration, increased individual particle size compared to bare nZVI [23]. It was hypothesized that the polymers chelated aqueous Fe ions, resulting in an artificial increase in Fe concentration within polymer-zone microcosms prior to precipitation.

Particle size and stability are used as predictors of transport performance through porous media. In terms of particle size, CMC of various molecular weights is shown to produce smaller nZVI particles than PAP, PSS, PAA, polyvinylpyrrolidone (PVP), PAM, and guar gum. Cirtiu et al. (2011) investigated the differences between pre- and post-synthesis stabilization of nZVI by CMC, PAM, PSS, and PAA [23]. They found that although post-synthesis stabilization generally resulted in smaller particle diameters, more stable colloidal suspensions were produced when nZVI was pre-stabilized. That pre- versus post-synthesis can have this effect confounds comparisons of different polyelectrolytes in terms of particle size and colloidal stability, as both pre- and post-synthesis methods were used in past studies [20,23,24,31,39]. In post-synthesis stabilized studies, CMC performs poorest in terms of colloidal stability, with either PSS or PAP proving best [20,31]. However, pre-synthesis stabilized studies suggest that CMC outperforms PAA, PAM, and PSS, though not guar gum, in terms of stability [23,24,39].

Transport of Polyelectrolyte Stabilized nZVI.

The transport of polyelectrolyte stabilized nZVI through saturated porous media has been increasingly studied in the last 5 years. In 1-D column and 2-D cell laboratory studies, the transport of stabilized nZVI is conclusively superior to bare nZVI [19,28,31,32,40-42]. Transport performance across different polyelectrolyte types is largely similar [28,31,32,39]. Small differences between types may be attributable to differences in the adsorbed polyelectrolyte layer thickness which, if too thin, allows *in situ* agglomeration [41,43]. However, extrapolation of laboratory column study results to predict *in situ* transport is in question. For example, He et al. (2009) conclude that although CMC stabilized nZVI shows excellent transport in a variety of media-filled columns, modeling suggests that at a realistic groundwater flowrate of 0.1 m/day, 99% of the nZVI would be removed within 16 cm [44]. Field studies, to be discussed later, support this conclusion of limited *in situ* transport [6,45].

In column studies, four factors worsen transport of stabilized nZVI. The first of these is zero-valent iron content. Zero-valent iron is inherently magnetic, whereas its oxides are less so [46]. By comparing the stability and transport of less-magnetic hematite particles to nZVI, it was shown that magnetic attractive forces between nZVI particles increase agglomeration, significantly reducing their transport [41,47,48]. This is explained by the fact that magnetic forces are stronger than and act over longer distances than van der Waals forces, thus playing a dominant role in causing aggregation [47].

The second factor is nZVI concentration. Phenrat et al. (2009) found that at a low concentration of 0.30 g/L all particles were mobile, but at high concentrations of 1.0 and 6.0 g/L agglomeration during transport occurred [48]. Raychoudhury et al. (2010) report similar results, with increased retardation and, in the case of PAA stabilized particles, decreased effluent

concentrations as the nZVI concentration was increased from 0.1 to 3.0 g/L [39]. Particle agglomeration, followed by straining is the most likely mechanism for capture of nZVI at high concentrations within porous media.

The third cause of decreased nZVI transport is increased ionic strength, which reduces the interparticle repulsive force, leading to agglomeration. Saleh et al. (2008) conducted a focused study of this effect for PAP and triblock-copolymer (discussed below) stabilized nZVI [49]. Transport was reduced between 7 and 38 fold when cation concentrations were raised from 10 mM to 100 mM. In the presence of cations, triblock-copolymer clearly outperformed PAP, with 20 to 59 fold better transport. Lin et al. (2010) reported that a cation concentration of 40 mM decreased transport of PAA-stabilized nZVI by about 40%, but had no effect on CMC-stabilized nZVI [32].

Finally, decreased flow velocity is shown to inhibit the transport of stabilized nZVI. Unfortunately, the majority of column studies were conducted at flow velocities that are artificially high (>1.0 m/day) compared to typical groundwater flow [28,31,48]. Lin et al. (2010) showed that even at these high velocities, decreasing the flowrate from 38.2 to 6.28 m/day decreased transport by ~5% [32]. Raychoudhury et al. (2010) further showed that decreasing flow from 14.4 m/day to a realistic value of 0.29 m/day decreased transport 20% to 30% [39]. This effect is explained by an increase in stagnant zones in the pore spaces and decreased drag torques which, when high, result in adsorbed particle detachment from collector surfaces [32,39,48].

Two-dimensional cell studies have further elucidated the fate and transport of stabilized nZVI under conditions more-representative of the subsurface. The first of these, by Kanel et al. (2008), showed that although a 4 g/L PAA-stabilized nZVI suspension was transported without

retardation in homogeneous porous media, the greater density of the nZVI caused it to travel downward as well as laterally [40]. Phenrat et al. (2010) found that in heterogeneous porous media, stabilized nZVI follows preferential flowpaths and collects in pore spaces that have insufficient fluid shear [41]. In 2011, the same research group reported that stabilized nZVI is capable of targeting NAPL entrapped in porous media, likely due to partitioning to the NAPL-water interface [42].

A series of studies from Carnegie Mellon University investigated the use of a combination of polymers, so-called triblock copolymers, that work in concert to stabilize nZVI and preferentially deliver the particles to water and NAPL interfaces [49-52]. The first polymer, poly(methacrylic acid) (PMAA), strongly adsorbs to iron oxide surfaces, anchoring the copolymer in place. The second, poly(methyl methacrylate or butyl methacrylate) (PMMA or PMBA, respectively), has low polarity, imparting hydrophobicity and an affinity for NAPL phases. Finally, PSS, an anion, ensures strong electrostatic repulsion from other particles and the predominantly negatively charged surfaces of groundwater media. Experiments showed improved nZVI stability and transport in sand columns, but limited NAPL targeting and a 2 to 10 fold decrease in reactivity toward TCE [51,52]. Although the utilization of specially designed copolymer coatings represents a novel approach to nZVI delivery, the issues of decreased reactivity and poor targeting have not been resolved.

A polyelectrolyte that has shown noteworthy performance in improving particle stability and nZVI transport is xanthan gum. At a concentration of 6 g/L, it stabilized nZVI concentrations as high as 15 g/L for up to 10 days, preventing both aggregation and sedimentation [36]. In contrast to other stabilizers, which depend on establishing steric and electrostatic repulsion between particles, xanthan gum works by forming a polymer network

between particles. In packed sand column studies, xanthan-gum-stabilized nZVI reached a steady-state elution of 88% of the original 20 g/L inlet concentration, with a 92% overall mass recovery [37]. The transport of such high concentrations of nZVI with little loss to the porous media suggests exciting possibilities for *in situ* mobility.

Reactivity of Polyelecrolyte Stabilized nZVI.

Reactivity of nZVI toward contaminants is actually inhibited by polyelectrolyte coatings. Phenrat et al. (2009) studied this effect for nZVI coated with PSS, CMC, and PAP and found reactivity toward TCE decreased between 4 and 25 fold [34]. Inhibition was explained by the blocking of reactive sites and partitioning of the TCE to the polyelectrolyte coatings, effectively decreasing the aqueous TCE concentration. However, it is crucial to recognize that loss of reactivity was measured on a surface-area-normalized basis. Polyelectrolyte stabilization of nZVI also decreases mean particle size and prevents aggregation, both of which increase the overall reactive surface area [22,24,53-55]. The net effect is impressive gains in nZVI reactivity on a mass-normalized basis, making polyelectrolyte-coated nZVI a "new class" of particles altogether [22,24,27,56-60].

The majority of studies investigating the effect of polyelectrolyte coatings on nZVI reactivity were done for only one polyelectrolyte type, making comparison across many types difficult. However, in addition to Phenrat et al. (2009), two additional studies have compared reactivity across several polyelectrolytes. Sakulchaicharoen et al. (2010) evaluated the effect of CMC, PVP, and guar gum coatings on TCE degradation [24]. All three coatings resulted in smaller nanoparticles relative to bare nZVI, however improvements in reactivity were mixed. Use of guar gum at 0.05% (w/w) improved reactivity ~2 fold, but an increase to 0.10% decreased reactivity ~3 fold. Similarly, PVP360K (PVP, MW = 360,000 g/mol) improved reactivity 10

fold, but lower molecular weight PVP40K reduced reactivity ~4 fold. Notably, CMC90K, CMC250K, and CMC700K all outperformed bare nZVI and the other coatings both in terms of nanoparticle size and reactivity, with CMC250K proving best. In a study of perchlorate degradation by Xiong et al. (2007), starch and CMC stabilizers improved degradation by 1.8 and 5.5 fold over bare nZVI, respectively [56].

Bimetal Catalyzation of nZVI

As of 2011, approximately 40% of nZVI remediation projects in the U.S. employed catalyzed nZVI [2]. It is well established that catalyzing nZVI with another metal improves nanoparticle reactivity toward almost all contaminants when compared to bare nZVI [2,61-65]. Catalyzation can also enable reduction of particularly recalcitrant contaminants that otherwise would not degrade, change degradation pathways, and, in the case of chlorinated organic compounds, result in fewer harmful chlorinated intermediaries [2,66]. In fact, due to its high reactivity, and subsequent poor longevity, catalyzed nZVI may only be suitable for active treatment (i.e., source zone remediation) and not for use in passive measures such as permeable reactive barriers [2,8]. Use of catalyzed nZVI has been discussed in part elsewhere [2,13,67]; however, no article has yet reviewed and presented in full the breadth of studies focused on this nZVI enhancement. Prior to the development of nZVI, a great number of studies investigated the catalyzation of metallic iron surfaces, iron filings, and micro-scale zero-valent iron (ZVI). Much of this earlier work guided initial efforts at catalyzing nZVI. However, the drastic increase in specific surface area characteristic of nZVI may limit the relevance of earlier studies. As such, this review focuses nearly exclusively on the catalyzation of nZVI.

To catalyze nZVI, typically a lesser amount of a second metal, anywhere from 0.1% to 25% (w/w), is precipitated onto the surface of the nanoparticles. A galvanic cell is established

between the two metals, with Fe acting as a sacrificial anode, transferring electrons to and thereby protecting the catalyst cathode from oxidation [2,68]. This relationship can be predicted by the standard reduction-oxidation (redox) potential of each metal. As shown in Table 2.2, with the exception of Zn, Fe has a higher redox potential than the metals used to catalyze nZVI, meaning that it is thermodynamically favored to be oxidized. As will be shown, Ag, Pd, and Pt are highly effective catalysts, which may owe in part to their exclusive ability to not only accept two electrons from Fe^0, but to recruit an additional electron from the already reduced Fe^{2+} as well. In the case of heavy metals, which cannot be degraded *per se*, redox potential may be used to predict how effective nZVI might be at remediating them. For metals with a standard redox potential for oxidation close to or higher than Fe, such as Cd, removal is by sorption or surface complexation only. However, for metals with a potential much lower the Fe, such as Pb, sorption followed by reduction is likely [2].

Half-Reaction	Standard Redox Potential, mV
$Co^{2+} \rightarrow Co^{3+} + e^-$	-1820
$Pt^0 \rightarrow Pt^{2+} + 2e^-$	-1200
$Pd^0 \rightarrow Pd^{2+} + 2e^-$	-990
$Ag^0 \rightarrow Ag^+ + e^-$	-797
$Fe^{2+} \rightarrow Fe^{3+} + e^-$	-769
$Cu^0 \rightarrow Cu^+ + e^-$	-520
$Cu^0 \rightarrow Cu^{2+} + 2e^-$	-340
$Ni^0 \rightarrow Ni^{2+} + 2e^-$	250
$Co^0 \rightarrow Co^{2+} + 2e^-$	280
$Fe^0 \rightarrow Fe^{2+} + 2e^-$	441
$Zn^0 \rightarrow Zn^{2+} + 2e^-$	760

Table 2.2. Standard reduction-oxidation potentials of Fe and its catalysts for donation of electrons.

Figure 2.1 depicts the reductive degradation of a chlorinated organic compound by catalyzed nZVI. Fe^0 first hydrolyzes water to produce hydrogen and hydroxide anions. The hydroxide anions may react with Fe^{2+} to form iron oxide species or, if released to the surrounding water, raise the pH of the solution [45]. The hydrogen produced may adsorb to the nZVI and, importantly, the catalyst surface as hydrogen ions [66,69]. It may also form molecular hydrogen (H_2), which interacts with the nZVI surface through diffusion [66,69,70]. At the catalyst surface, electrons donated by Fe reduce the contaminant and, in the case of hydrodechlorination, hydrogen replaces the liberated chloride ion [67,69,71]. Over time, growth of the iron oxide layer inhibits electron transfer from the zero-valent core and quenches the catalyst [72,73].

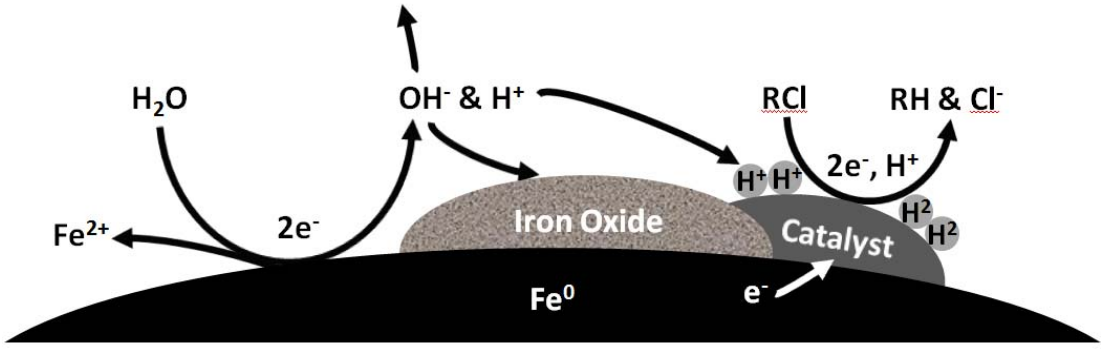

Figure 2.1. Process of reductive dechlorination by catalyzed nZVI.

Given the important role hydrogen plays in the degradation of chlorinated organic compounds, it is no surprise that pH has a dramatic effect on the reactivity of catalyzed nZVI. Across three studies, the ideal pH for degradation ranged from weakly acidic at pH 4 to neutral at pH 7 [60,73,74]. Under weakly acidic conditions, the hydrolysis of water by nZVI occurs faster, rapidly consuming it and producing large amounts of hydrogen [60,73]. Subsequently, greater disassociation of molecular hydrogen and attachment of hydrogen ions, H^+, to the catalyst

surface occurs, speeding contaminant degradation [60,73]. However, if too much hydrogen gas accumulates on the particle surface its presence may actually inhibit degradation by blocking access to the reactive sites [73]. Under slightly basic conditions, the increased presence of hydroxide anions contributes to development of an inhibitive iron oxide layer on the nZVI surface [60,73,74]. Furthermore, basic conditions have been shown to lack sufficient amounts of hydrogen necessary for effective dechlorination activity [73].

Contaminant	Catalyst Type	Catalyst Load, % (w/w)	nZVI Load, g/L	Initial Conc., mg/L	Removal Efficiency		k_{SA}, L/hr/m^2 or (k_m), (L/hr/g)	Chlorinated End Products	Ref.
Tetrachloroethylene (PCE)	Pd	0.10	5.0	20.0	94%,	1.5 hr	1.2E-02	None	68
	Pd	1.0	0.25	30.0	–		2.3E-01	None	71
	Pd	0.10	0.10	15.0	80%,	2 hr	2.4E+00	TCE	58
	Pd	–	20.0	20.0	100%,	0.25 hr	–	None	61
Trichloroethene (TCE)	Pd	0.10	5.0	20.0	100%,	1.5 hr	1.8E-02	None	68
	Pd	0.10	0.10	25.0	100%,	1.5 hr	6.7E-01	DCE, Trace	22
	Pd	–	50.0	20.0	100%,	0.25 hr	1.0E-01	None	1
	Pd	0.10	0.10	50.0	100%,	1 hr	1.6E+00	None	27
	Pd	5.0	5.0	120.0	–		5.4E-03	–	71
	Pd	0.10	0.10	20.0	70%,	1 hr	6.4E-03	–	57
	Pd	0.10	0.10	15.0	80%,	2 hr	2.4E+00	–	58
	Pd	0.10	0.10	50.0	100%,	0.35 hr	2.5E-01	–	24
	Pd	0.05	2.00	17.0	100%,	2.5 hr	–	–	35
	Pd	–	20.0	20.0	100%,	0.25 hr	–	None	61
	Pd	0.05	–	100.0	–		1.3E-01	None	62
	Ni	20.0	2.5	24.0	100%,	3 hr	9.8E-02	None	69
	Ni	25.0	2.5	10.0	100%,	2 hr	5.7E-02	None	91
	Ni	21.4	0.60	80.0	–		(3.1E+00)	–	92
	Ni	6.6	1.0	350.0	100%,	44 hr	–	None	97
	Ni	0.05	–	100.0	–		1.2E-02	None	62
	Pt	–	20.0	20.0	100%,	1 hr	–	None	61
	Cu	0.03	–	100.0	–		2.0E-03	None	62
1,1-Dichloroethene (1,1-DCE)	Pd	0.10	5.0	20.0	92%,	1.5 hr	1.2E-02	None	68
cis-1,2-Dichloroethene (*c*-DCE)	Pd	0.10	5.0	20.0	100%,	1.25 hr	1.8E-02	None	68
	Pd	–	20.0	20.0	100%,	1 hr	–	None	61
trans-1,2-Dichlroethene (*t*-DCE)	Pd	0.10	5.0	20.0	100%,	1.5 hr	1.5E-02	None	68
	Pd	–	100.0	9.7	100%,	0.25 hr	–	None	61
	Ni	–	100.0	9.7	98%,	2 hr	–	None	61
Vinyl Chloride (VC)	Pd	–	20.0	20.0	100%,	3 hr	–	None	61
Hexachloroethane (HCA)	Pd	0.50	5.0	30.0	100%,	1.75 hr	2.0E-02	None	79
Pentachloroethane (PCA)	Pd	0.50	5.0	30.0	~100%,	1.5 hr	2.6E-02	None	79
1,1,2,2-Tetrachloroethane (1,1,2,2-TeCA)	Pd	0.50	5.0	~25.0	~100%,	1.25 hr	8.8E-03	None	79
1,1,1,2-Tetrachloroethane (1,1,1,2-TeCA)	Pd	0.50	5.0	~25.0	~100%,	1.5 hr	2.1E-02	None	79
1,1,1-Trichloroethane (1,1,1-TCA)	Pd	0.50	5.0	~25.0	100%,	7 hr	5.4E-03	None	79
	Pd	0.10	0.10	15.0	50%,	2 hr	4.3E-01	–	58
1,2-Dichloroethane (1,2-DCA)	Pd	0.50	5.0	~25.0	<5%,	24 hr	–	–	79
Carbon Tetrachloride (CT)	Pd	0.10	12.5	15.4	100%,	1 hr	9.0E-03	CF, DCM	78
	Pd	0.20	10.0	100.0	100%,	3 hr	3.6E-03	–	73
	Pd	3.8	1.2	15.4	–		(5.3E+00)	CF	64
	Ni	25.0	2.5	20.0	100%,	1 hr	9.2E-02	CF, DCM	90
	Ni	2.4	1.2	15.4	–		(2.1E+01)	CF	64
	Cu	2.1	1.2	30.8	100%,	0.1 hr	(4.4E+01)	CF, DCM	64
Chloroform (CF)	Pd	0.10	12.5	14.3	92%,	1 hr	6.5E-03	DCM	78
	Pd	0.20	10.0	100.0	100%,	3 hr	2.7E-03	–	73
Dichlromethane (DCM)	Pd	0.10	12.5	6.5	30%,	2 hr	–	–	78
	Pd	0.20	10.0	100.0	~15%,	8 hr	3.5E-05	–	73
Carbon Tetrabromide (CTB)	Ni	20.0	2.5	21.2	100%,	0.5 hr	2.0E-01	BM	95
Bromoform (BF)	Ni	20.0	2.5	21.6	100%,	1 hr	4.9E-02	BM	95
Dibromomethane (DBM)	Ni	20.0	2.5	21.9	100%,	3.5 hr	1.1E-02	BM	95

Table 2.3. Summary of catalyzed nZVI studies that used chlorinated and brominated ethenes, ethanes, or methanes as the target contaminant(s).

Contaminant	Catalyst Type	Catalyst Load, % (w/w)	nZVI Load, g/L	Initial Conc., mg/L	Removal Efficiency	k_{SA}, hr/m^2 or (k_m), (L/hr/g)	Chlorinated End Products	Ref.
Pentachlorophenol (PCP)	Pd	0.05	12.5	5.0	97%, 1.7 hr	(4.0E-01)	–	85
	Ni	20.0	2.5	50.6	100%, 0.33 hr	–	None	74
	Ni	25.0	1.3	50.0	80%, 20 hr	–	CP	98
2,4,6-Trichlorophenol (246TCP)	Pd	0.50	5.0	20.0	94%, 1 hr	2.4E-02	DCP, CP	77
	Ni	0.50	5.0	20.0	56%, 1 hr	–	–	77
	Pt	0.50	5.0	20.0	~18%, 1 hr	–	–	77
	Co	0.50	5.0	20.0	~15%, 1 hr	–	–	77
	Cu	0.50	5.0	20.0	~9%, 1 hr	–	–	77
2,4-Dichlorophenol (24DCP)	Pd	0.50	5.0	20.0	100%, 1 hr	3.4E-02	CP, <6%	77
4-Chlorophenol (4CP)	Pd	0.50	5.0	20.0	100%, 1 hr	1.1E-01	None	77
	Ni	10.0	0.40	80.4	100%, 1 hr	(2.5E+01)	None	93
Polychlorinated Biphenyls (PCBs)	Pd	–	50.0	5.0	100%, 17 hr	–	–	1
	Pd	0.10	1.0	2.5	75%, 100 hr	3.1E-04	Present	22
	Pd	0.25	10.0	0.25	100%, 56 d	(7.5E-04)	2,3-DCB	86
Polybrominated Diphenyl Etheres (PBDEs)	Pd	0.25	10.0	0.25	100%, 2.5-15 d	(~5.5E-02)	Lower PBDEs	86
1,2,3,4-Tetrachlorodibenzo-*p*-dioxin (1,2,3,4-TeCDD)	Pd	0.50	5.0	0.50	~75%, 48 hr	3.0E-04	Lower CDDs	66
	Pd	0.01	20.8	0.35	100, 10 d	1.5E-02	Lower CDDs	65
	Pd	0.02	20.8	0.35	–	1.3E-02	–	65
	Pd	0.04	20.8	0.35	–	1.2E-02	–	65
	Ni	–	20.8	0.35	Non-Reactive	–	–	65
	Cu	–	20.8	0.35	Non-Reactive	–	–	65
1,2,3-Trichlorodibenzo-*p*-dioxin (1,2,3-TriCDD)	Pd	0.50	5.0	0.50	~93%, 48 hr	1.5E-03	Lower CDDs	66
1,2-Dichlorodibenzo-*p*-dioxin (1,2-DiCDD)	Pd	0.50	5.0	–	–	2.7E-03	Mono-CDDs	66
1,2,4-Trichlorobenzene (1,2,4-TCB)	Pd	1.0	1.7	30.8	100%, 1 hr	1.5E-01	None	80
	Pd	0.10	0.71	15.0	100%, 0.75 hr	3.9E-01	12DCB, <5%	81
	Pd	0.10	0.71	20.0	–	2.7E-01	DCBs, MCB	82
1,2-Dichlorobenzene (12DCB)	Pd	0.10	0.71	15.0	100%, 0.5 hr	5.0E-01	None	81
1,3-Dichlorobenzene (13DCB)	Pd	0.10	0.71	15.0	–	5.6E-01	–	81
1,4-Dichlorobenzene (14DCB)	Pd	0.10	0.71	15.0	–	8.9E-01	–	81
Monochlorobenzene (MCB)	Pd	0.10	0.71	15.0	100%, 0.25 hr	1.1E+00	None	81
p-Nitrochlorobenzene (*p*-NCB)	Pd	0.20	0.20	50.0	100%, 0.5 hr	(7.8E+00)	Chloroaniline	60
γ-Hexachlorocyclohexane (Lindane)	Pd	0.20	0.50	5.0	100%, 5 hr	2.0E+00	None	83
	Pd	0.80	0.50	1.0	100%, 0.85 hr	–	–	87
Atrazine	Pd	0.80	0.50	1.0	100%, 0.15 hr	–	–	87
Hexavalent Chromium (Cr(VI))	Pd	0.50	–	–	>85%, 0.17 hr	4.0E-01	–	63
	Cu	0.50	–	–	>85%, 0.17 hr	3.5E-01	–	63
Selenate (SeO_4^{2-})	Ni	–	5.0	106	100%, 1.4 hr	(6.0E+00)	–	89
Nitrate (NO_3^-)	Ni	0.20	10.0	1000	100%, 1 min	–	–	99
	Pt	–	0.50	20.0	75%, 4 hr	2.9E-02	–	103

Table 2.4. Summary of catalyzed nZVI studies that used chlorinated cyclic hydrocarbons, heavy metals, or nitrate as the target contaminant(s).

Multiple Metals.

There are many studies that examine the reactivity of multiple catalysts under the same conditions. These studies are especially useful in elucidating the relative reactivity of different nZVI-catalyst combinations and contaminant-dependent changes in catalyst reactivity [56,57,61-65,75-77]. The first such study with nano-scale particles, by Zhang et al. (1998), primarily investigated the reduction of chlorinated ethenes by Pd catalyzed (Fe/Pd) nZVI [61]. The authors found that at high Fe/Pd loadings of 20 g/L, tetrachloroethylene (PCE), trichloroethylene (TCE), *trans*-dichloroethene (*trans*-DCE), and vinyl chloride (VC) were all completely degraded within 3 hours with no chlorinated byproducts present. In contrast, degradation of TCE by Fe/Pt nZVI took 4 times longer than Fe/Pd nZVI. A test of Fe/Ni nZVI showed that, even at 5 times higher nZVI loading, it took more than twice as long as Fe/Pd nZVI to degrade *trans*-DCE. Another study, by Kim and Carraway (2003), studied the degradation of TCE by Fe/Pd, Fe/Ni, and Fe/Cu nZVI [62]. TCE at a concentration of 100 mg/L was degraded by 25 g/L of Fe/Pd and Fe/Ni nZVI within 1 hour and 13 days, respectively. No chlorinated byproducts were observed. As seen in Table 2.3 (Ref. 62), surface-area-normalized reaction rates for all three catalysts indicate the order of catalyst reactivity is Pd>Ni>Cu. Taken together, these findings suggest that for chlorinated ethenes the order of catalyst reactivity is Pd>Pt>Ni>Cu.

The degradation of carbon tetrachloride (CT), a related chlorinated methane, by Fe/Pd, Fe/Ni, and Fe/Cu nZVI was reported by Chun et al. (2010) [64]. Three nZVI synthesis methods were tested, including hydrogen reduction process (HRP) and solution deposition process (SDP). The authors found that the order of catalyst reactivity depended on the synthesis process. As detailed in Table 2.3 (Ref. 64), for HRP-nZVI, the order of catalyst reactivity was Cu>Ni>Pd. However, for SDP-nZVI (not included in Table 2.3), this order was reversed, agreeing with

previously studies. This discrepancy among HRP-synthesized nZVI was attributed to segregation of the catalyst on the particle surface, leading the catalyst to act as separate, individual particles, which was shown to be less reactive [61]. Both chloroform (CF) and dichloromethane (DCM) were observed as chlorinated byproducts.

Two studies have investigated the degradation recalcitrant cyclic compounds by catalyzed nZVI. The first, reported by Wang et al. (2010) used Fe/Pd, Fe/Ni, and Fe/Cu nZVI to degrade 1,2,3,4-tetrachlorodibenzo-*p*-dioxin (1,2,3,4-TCDD), one of a group of chlorinated dioxins and furans [65]. Interestingly, not only bare nZVI, but also Fe/Ni and Fe/Cu nZVI, were unreactive toward 1,2,3,4-TCDD. Fe/Pd nZVI, however, fully degraded 1,2,3,4-TCDD within 10 days from an initial concentration of 0.35 mg/L. Although 7 chlorinated byproducts were identified, >95% of the parent compound proceeded to a non-chlorinated byproduct. The second study, by Zhou et al. (2010), reported the ability of Pd/Fe, Pt/Fe, Ni/Fe, Cu/Fe, and Co/Fe nZVI to degrade chlorophenols, a widespread industrial chemical and contaminant [77]. A good illustration of the higher reactivity of nano-scale particles, 50 g/L of microscale ZVI doped with Pd degraded only 9.1% of 2,4,6-trichlorophenol (246TCP) in 24 hours, whereas 5 g/L of Fe/Pd nZVI degraded 94% in only 1 hour. As shown in Table 2.4 (Ref. 77), the order of catalyst reactivity for degradation of 246TCP is Pd>Ni>Pt>Co>Cu. Phenol was the major byproduct (80% to 100%) of degradation for the three chlorophenols tested.

Finally, a study by Rivero-Huguet and Marshall (2009) compared the performance of a wide variety of bimetallics, including Pd/Fe and Cu/Fe nZVI, for the remediation of hexavalent chromium (Cr(VI)), a heavy metal toxin widely found at industrial sites [63]. For micro-scale zero-valent iron bimetals, the authors found the order of catalyst reactivity to be Pd>Ag>Ni>Zn>Cu. As seen in Table 2.4 (Ref. 63), for nZVI, Fe/Pd and Fe/Cu had similar

surface-area-normalized reaction rates, with reactivity about twice that of bare nZVI. Effectiveness of nZVI remediation of Cr(VI) was highly dependent on pH, with a shift of pH from 2.0 to 6.0 reducing reactivity by about 50 times.

Palladium Catalyzation.

Of the metallic catalysts tested with nZVI, Pd and Ni are the only two investigated in studies that used only one catalyst. Of these, Pd is certainly the most widely studied and used. As seen in the comparative studies, Pd is clearly the most reactive known catalyst for nZVI. Across the 30 articles reviewed here, Pd is shown to improve nZVI reduction of chlorinated ethenes, ethanes, and methanes; brominated methanes; chlorinated phenols; polychlorinated biphenyls; polybrominated diphenyl ethers; dioxins; chlorinated benzene, chlorinated cyclohexane, and atrazine; hexavalent chromium and selenate; and nitrate [1,5,6,22,24,27,29,35,57,58,60-66,68,71-73,77-87]. Addition of Pd was shown to not improve degradation of perchlorate, however [88].

Amendment of nZVI with even very small amounts of Pd has a dramatic effect on the reactivity of the particles. As seen in Tables 2.3 and 2.4, the majority of studies have used a Pd loading of less than 1.0%. Efficient use of Pd catalyst is important because it is a precious metal, costing over 20,000 USD per kilogram. Eight separate studies have, in part, investigated the optimal loading of Pd on nZVI, with a general consensus that between 0.2% and 1.0% is best [29,57,58,60,73,80,81,87]. The earliest of these, by Zhu et al. (2006), found that for the destruction of 1,2,4-trichlorobenzene (124TCB), a Pd loading of 1.0% was preferred over 0.1% and 0.5%, with a 10-fold increase in reactivity when loading increased from 0.1% to 1.0% [80]. In 2007, the same research group further investigated this increase, again with 124TCB; they observed a linear increase in the pseudo-first order degradation rate following a step-wise

increase in Pd loading from 0.01% to 0.5% [81]. He and Zhao (2008) saw that for the degradation of TCE, addition of 0.05% Pd increased the reactivity by an order of magnitude compared to non-catalyzed nZVI [57]. Further increasing Pd loading to 0.1% improved reactivity by another 30%, with no additional gains at 0.2% loading. Cho and Choi (2010), studying TCE, reported similar findings with removal efficiency peaking at 0.1% and not improving at 0.2% or 0.4% [58]. Joo and Zhao (2008), however, found that for the degradation of lindane, a persistent pesticide, a Pd loading of 0.8% was optimal [87]. Wang et al. (2009) conducted a thorough investigation of Pd loading on nZVI for degradation of CT, CF, and DCM [73]. For all three contaminants, they found that removal efficiency dramatically peaked at 0.2% Pd, followed by a steady decrease as loading was increased all the way to 3.0%. For degradation of nitrochlorobenzene, Dong et al. (2011) reported that step-wise increase of Pd loading from 0.05% to 0.2% resulted in consistent improvement in nZVI reactivity [60]. Finally, Kustov et al. (2011) reported that for the degradation of PCE a loading of 1.0% was preferred, in agreement with Zhu et al. (2006) [29,80].

Fe/Pd nZVI undergoes profound structural changes upon reaction with water, contaminants, and other electron acceptors. The question of catalyst stability and what effect it has on reactivity was raised by Zhu and Lim (2007) after they observed release of Fe into solution over the course of degradation experiments [81]. The structural development of Fe/Pd nZVI in an aqueous environment was thoroughly investigated by Yan et al. (2010) [72]. The authors characterized 1.5% Fe/Pd nZVI as having numerous 2-5 nm islets resting on an amorphous oxide shell above a metallic core. Once reacted with water, Pd migrates to the metallic iron core interface, accompanied by oxidation and outward diffusion of iron species. Within 24 hours, Pd is completely covered by an outer iron-oxide matrix. This view of the

inactivation of Pd is supported by the results of Zhu and Lim (2007). They observed a 4-fold decrease in reactivity by the third cycle of 124TCB degradation, and regeneration of the Fe/Pd nZVI by HCl and $NaBH_4$ exposures failed to return it to its original reactivity [81].

Several factors other than pH, which was previously discussed, were shown to impact degradation of contaminants by Fe/Pd nZVI. Typically, Fe/Pd nZVI is synthesized by coating the surface of bare nZVI with Pd. However, one study found that a simple mixture of distinct, monometallic Fe and Pd nanoparticles had twice the reactivity toward TCE as Pd coated, bimetallic particles [73]. It was hypothesized that TCE is reduced at the Pd nanoparticle surface by hydrogen produced from nZVI hydrolysis of water. Another study, by Shih et al. (2011), reported that the addition of Cu and Ni cations to an Fe/Pd nZVI solution increased the reactivity toward pentachlorophenol [85]. This was explained by the fact that the cations would quickly reduce at the nZVI surface, effectively forming trimetallic nZVI particles. Ni cations had a greater effect on reactivity than Cu cations. In the same study, the addition of 10 mM sulfate reduced Fe/Pd nZVI reactivity by 42%, possibly due to adsorption of sulfate to the surface of the particles and subsequent blocking of reactive sites. Natural organic matter (NOM) and humic acid (HA), common to the natural environment, were likewise shown to reduce Fe/Pd nZVI reactivity. Dong et al. (2011) showed that the addition of 10 mg/L of HA reduced reactivity seven-fold [60]. Zhu et al. (2008) found that addition of 50 mg/L of NOM reduced Fe/Pd nZVI reactivity 9-fold [82]. Unlike the previous two studies however, the authors attributed this not to reactive site blockage but to competition by NOM for diatomic hydrogen.

Nickel Catalyzation.

After Pd, Ni is the most-well studied catalyst. As previously discussed, in comparative studies Ni has shown comparable, though not equal, reactivity to Pd for several classes of

contaminants. Ni has the advantage of being a non-precious metal, costing roughly three orders of magnitude less than Pd for chemical reagents. Across the 20 articles employing Ni-catalyzed nZVI reviewed here, Ni catalyzation is shown to improve degradation or reduction of chlorinated ethenes, chlorinated methanes, brominated methanes, chlorinated phenols, dioxins, monoazo dye, nitrate, and heavy metals [21,62,64,65,69,74,76,77,89-99]. In the case of perchlorate, however, addition of Ni to nZVI inhibited degradation [56]. This was explained by simultaneous catalyzation of the hydrolysis reaction with water, which preferentially consumed nZVI and is consistent with the study of Fe/Pd and Fe/Ag nZVI degradation of perchlorate [88].

The amount of Ni used for nZVI synthesis has a dramatic effect on its ability to catalyze degradation. As can be seen in Tables 2.3 and 2.4, the majority of studies have used a Ni catalyst loading near 20%. In cases where multiple loadings were studied, the most reactive loading is reported. In a study by Tee et al. (2005), nickel composition of nZVI was varied from 0% to 100% [91]. A 120-fold increase in reactivity toward TCE was observed as Ni loading was increased from 0% to 25%, followed by a 60-fold decrease as loading was further increased to 80%. Wu and Ritchie (2006) reported a similar steep rise in reactivity toward TCE, ~30-fold, as Ni loading was increased to 14.3%, followed by a ~3-fold drop as loading was further increased to ~35% [92]. The authors concluded that the optimal Ni loading was somewhere between 14.3% and 21.4%. A study by Zhang et al. (2006) investigating the degradation of pentachlorophenol (PCP) by Fe/Ni found removal efficiency improved from 32% to 98% as Ni loading increased from 0% to 10%, with marginal improvement in reactivity as Ni loading was further increased to 20% [1]. A 2007 study by the same research group reported a 430-fold increase in reactivity of Fe/Ni nZVI toward *p*-chlorophenol as Ni loading was increased from 0% to 10%; higher loadings were not investigated [93]. Finally, in contrast to other studies, Barnes et al. (2010)

found a loading of only 8.5% resulted in optimal TCE degradation, although 15% performed comparably [97].

The majority of nZVI studies synthesize nanoparticles via the aqueous reduction of metallic ions by $NaBH_4$. In the case of Fe/Ni nZVI, many articles report co-precipitation of Fe and Ni; that is, nanoparticles are formed in a solution containing both metallic ion precursors. This method incorporates Ni into the core of the particles, where it likely cannot serve as a catalyst, as well as the surface. In contrast, post-coating of nZVI particles with Ni deposits the catalyst only on the surface. One study investigating the outcomes of these two methods found differences in both size and reactivity [92]. Post-coated particle sizes ranged from 7-11 nm, while co-precipitated particles were 11-24 nm. The larger co-precipitated particles have less relative surface area and would likely not transport as well *in situ*. Furthermore, mass-normalized reactivity of the post-coated particles was 5-fold higher than the co-precipitated Fe/Ni nZVI.

The foremost concern with amending nZVI with Ni is the possible health issues associated with disassociation of Ni from the particles and into groundwater. Chronic exposure to Ni in drinking water may cause decreased body weight and heart and liver damage [100]. The U.S. EPA set the maximum contaminant level (MCL) for Ni at 0.1 mg/L, although this was remanded in 1995 [100]. In 2011, the World Health Organization set a drinking water guideline of 0.07 mg/L for Ni [101]. Full-scale implementation of nZVI involves injection of many kilograms or particles into the subsurface, of which Ni would be a significant mass-fraction. Wu and Ritchie (2006) studied the dissolution of Ni into the batch reactors used for Fe/Ni nZVI degradation of TCE [92]. They observed a gradual increase in Ni concentration over time. Barnes et al. (2010) also observed a rise in aqueous Ni concentration to between 1.8 and 6.8 mg/L, depending on the Ni loading, concurrent with the degradation of TCE [97]. As will be

discussed in the next section, nZVI concentrations injected in field-scale operations commonly exceed 1.0 g/L. Paired with the fact that optimal Fe/Ni nZVI catalyst loading is twice the highest level studied by Barnes et al. (2010), even higher levels of dissolved Ni, well in excess of drinking water guidelines, could be expected during field use.

Field-Scale Use of Stabilized and Catalyzed nZVI

Three field studies using Pd-catalyzed nZVI, two of which also employed a polyelectrolyte stabilizer, have been reported in the literature [5,6,16,45,102]. The earliest of these, by Elliott and Zhang (2001), sought to remediate chlorinated aliphatic hyrdrocarbon (CAH) contamination, predominantly TCE, at an active manufacturing facility in Trenton, NJ [5]. The size of the test site was small, measuring 4.5 m by 3.0 m and 9 m to confining clay and bedrock. TCE concentrations at the site consistently tested between 0.45 and 0.80 mg/L. Fe/Pd nZVI with a Pd loading of 0.33% was used. Initial laboratory tests indicated that amendment of nZVI with Pd decreased the half-life of TCE by a factor of 60. In the field, nZVI was injected in two phases, using a set of recirculating wells and gravity-fed into an injection well, respectively. nZVI injection concentrations ranged from 0.75 to 1.5 g/L, with a total of 1.7 kg injected over two days.

CAH concentrations and site conditions were monitored at the injection well and at three surrounding monitoring wells. Oxidation-reduction potential (ORP) measures the *in situ* electron activity, with negative values indicating a reducing environment conducive to reductive dechlorination. Post-injection, ORP shifted from historically positive values between +150 and +250 mV to strongly reducing conditions (-360 mV) at the injection well and slightly reducing conditions (-20 to -75 mV) at the monitoring wells. pH also increased from a range of 4.6–5.2 to 5.1–7.7. Dissolved oxygen (DO) was completely eliminated, almost certainly by reaction with

nZVI. A pumping test 6 weeks after injection confirmed no significant change in hydraulic conductivity due to nZVI injection. TCE removal efficiency varied both spatially and temporally, ranging from 1.5% to 96.5% over the three weeks following injection. Rebound of TCE concentrations to pre-injection levels was observed over several months, suggesting limited longevity of the nZVI treatment.

The second field study, by Henn and Waddill (2008), remediated a source area on the Naval Air Station in Jacksonville, FL contaminated with a combination of chlorinated ethenes and ethanes [102]. The test site was small, with a 98 m^2 area and 6 m depth to confining clay. Remediation was contracted to Tetra Tech NUS, Inc. and for this reason the formulation of polyelectrolyte-coated Fe/Pd nZVI used remains proprietary. The maximum total concentration of all contaminants was 550 mg/kg in soil and 80 mg/L in groundwater. As in the study by Elliott and Zhang (2001), both gravity-fed direct-injection wells and recirculating wells were used to deliver nZVI to the source area. Recirculating wells produced favorable iron delivery and enhanced mass transfer of sorbed and NAPL phase contaminants to the aqueous phase, where they could be degraded. A total of 150 kg of nZVI was injected over two weeks at concentrations ranging from 2.0 to 4.5 g/L.

Post-injection, ORP reduced from initial levels between +100 and -100 mV to stongly reducing conditions between -200 and -550 mV. DO levels were also significantly reduced. pH remained stable between 6 and 7. Despite an initial pumping test indicating no difference in soil permeability at the time of injection, a subsequent test one year later indicated a 45% reduction in soil permeability. Aqueous removal efficiencies of individual contaminants ranged from 65% to 99%, with some degrading to non-chlorinated end products. Total mass reduction, including sorbed, NAPL, and dissolved phases, was between 16% and 62%, with 23% most likely.

Furthermore, mass flux of contaminants from the source area was reduced. Rebound of aqueous contaminant concentrations was observed within a year, suggesting nZVI longevity of between 6 and 9 months.

Finally, the third field study, by He et al. (2010), sought to remediate a former manufacturing facility contaminated with chlorinated ethenes and polychlorinated biphenyls (PCBs) [6]. The pilot-scale test, employing a combination of CMC stabilizer and Pd catalyst to modify nZVI, was the culmination of a series of studies by He, Zhao, and co-workers optimizing the reactivity and transport of nZVI [22,33,27,57,44]. The test-site was small, measuring 5 m by 3 m, with injection and monitoring wells reaching a depth of 15 m. Monitoring wells were placed 1.5 m (MW-1) and 3.0 m (MW-2) downgradient of the injection well. The concentrations of the primary contaminants, PCE, TCE, *cis*-DCE, VC, and PCB1242, were 1.2-12.0 mg/L, 1.6-23.8 mg/L, 8.5-20.0 mg/L, 1.1-2.2 mg/L, and 6.9-97.4 μg/L, respectively. Direct-injection, first gravity-fed and later under <34 kPa of pressure, was used to deliver two separate loadings of nZVI; delivery under pressure resulted in better transport of nZVI within the aquifer. Nanoparticles were synthesized on-site for maximum reactivity. For the first injection, approximately 570 liters of 0.2 g/L nZVI was delivered. A month later, another 570 liters of 1.0 g/L nZVI was injected. Pd loading for both was 0.1%.

After injection, ORP in MW-1 and MW-2 reduced drastically, to highly negative values (-350 and -180 mV, respectively), but returned to only slightly negative pre-injection values (-50 to -20 mV) within 10 days. Decrease in ORP was matched by a complete, though transient, consumption of DO. nZVI successfully transported to MW-1, with >10% of the original concentration reaching it after the first injection and >80% after the second, but <5% reached MW-2, only 3.0 m away, in both cases. For chlorinated ethenes, nZVI injection resulted in

drastic reductions in aqueous concentrations, between 70% and ~100%, within the first 10 days. However, by day 13 concentrations rebounded significantly. Over the next 20 months, concentrations continued to slowly decline and remained below pre-injection levels. In the case of PCB1242, nZVI injection saw an ~80%, long-term decline in its concentration in MW-2, but no degradation at MW-1. While not suited for long-term control of a plume, the short longevity and high reactivity of stabilized, Fe/Pd nZVI makes it effective for source-zone remediation.

A common observation made across all three studies was that nZVI injection also established conditions conducive to long-term biotic destruction of contaminants. Elliot and Zhang (2001) note that establishing moderately-reducing ORP, raising pH to near neutral, and reducing DO all work to create favorable conditions for the growth of anaerobic, iron-reducing bacteria which may degrade chlorinated organic contaminants. Henn and Waddill (2008) note that favorable ORP conditions persisted at their study site. Biological degradation was observed and the site was transitioned to monitored natural attenuation as the long-term site remedy. Finally, He et al. (2010) also report favorable site conditions and appreciable, persistent biotic degradation of PCE and TCE through the end of their 20 month monitoring period. Furthermore, the authors hypothesize that the CMC used to stabilize the nZVI and molecular hydrogen produced by nZVI hydrolysis of water act as a carbon source and preferred electron donor, respectively, for microorganisms that degrade chlorinated organic contaminants.

Ongoing Research Needs

Before nZVI can become a widely accepted remediation tool the cost of implementation must be lowered or its utility must be improved, likely both. nZVI is synthesized by energy and reagent intensive processes, which makes it relatively expensive compared to micro-scale particles and industrial byproducts such as iron filings. Estimates as recent as 2011 put the cost

of nZVI between 50 and 200 USD per kg [2,3]. To be cost-competitive with other remediation techniques, the price will need to drop to between 10 and 25 USD per kg [2,3]. Prospective improvements in utility include increased reactivity, transportability, NAPL targeting, and the successful implementation of higher concentrations of stabilized nZVI *in situ*. Given the rapid development of nZVI in the past 15 years, these advancements seem feasible within the next decade.

However, to overcome these challenges, a greater degree of coordination and experimental planning is needed. In their 2011 review, Crane and Scott point out the need for a standardized nZVI testing framework in both academia and industry. Tables 2.3 and 2.4, included here, further advance this point. Surface area normalized pseudo-first order decay rates (k_{SA}), a supposedly universal method of comparing nZVI reactivity, commonly vary by more than three orders-of-magnitude for a given target contaminant. In some cases, this expresses genuine differences in nZVI formulation, but most often not. Neither can this variability be attributed to differences in specific surface area alone, which are typically less than one order-of-magnitude for stabilized nZVI. The culprit is variability in testing parameters: nZVI synthesis method, post-synthesis handling and storage, nZVI loading, catalyst loading, and initial contaminant concentration. Lack of control for these parameters across the literature makes comparison of study results difficult, if not impossible. Furthermore, many studies fail to report one or more of these fundamental parameters. Of the studies reviewed here, a quarter fail to provide rate constant data (i.e. k_{SA}, k_m, or k_{obs}). Others do not report chlorinated byproduct generation, leaving the question of whether nZVI reduces overall toxicity of a sample unanswered. As an alternative to large-scale standardization of testing procedures, a greater

number of comparative studies (i.e. those which include a wide range of catalysts, stabilizers, etc.) could further elucidate the relative performance of different nZVI formulations.

Although polyelectrolyte stabilizers clearly improve nZVI transport in laboratory settings, the relative performance of different types and molecular weights of polyelectrolyte stabilizers is unclear and often varies between studies. This is also true in terms of polyelectrolyte stabilized nZVI reactivity; few studies include multiple polyelectrolyte types and molecular weights. Also, the use of copolymers, specially engineered polymer combinations, remains largely unexplored. However, the most pressing question for polyelectrolyte stabilized nZVI is whether or not concentrations relevant to effective remediation can be successfully transported *in situ* at flowrates, ionic strength, and hydraulic conductivity heterogeneities that are representative of subsurface conditions.

As previously discussed, comparative studies of catalysts are limited. No study compares all proposed catalysts together. Relative catalyst performance may also be contaminant-dependent, confounding comparison between the comparative studies that do exist. Furthermore, as evidenced by the Pd and Ni catalyst studies, the optimal catalyst loading varies between metals. Comparisons of many catalysts at only one loading may under-represent the true potential of an individual catalyst. Although Pd and Ni have rightly received the majority of research attention, other effective catalysts may have been overlooked. Specifically, Ag was shown to outperform Ni and provide comparable reactivity to Pd, with the benefit of being much less expensive than Pd [63]. Finally, it remains to be answered whether injecting nZVI catalyzed by metals which are either precious or raise health concerns is a wise practice from an economic or environmental viewpoint. The question of catalyst leaching, specifically Ni leaching, into groundwater should be conclusively answered before its wide-scale implementation.

Furthermore, trade-offs may exist between the increased reactivity afforded by catalyzation and longevity of nZVI *in situ*.

Field-scale studies of nZVI are few, and many possibilities for future research exist. Ultimately, field studies are needed to discover how nZVI can be successfully transported to reach and mix with target contaminants *in situ*. Many laboratory studies report impressive contaminant degradation results, but only at nZVI loadings well in excess of what was successfully used in field scale tests. In contrast, recent studies reporting impressive gains in nZVI reactivity by catalyzing or stabilizing the particles have yet to be scaled to nZVI loadings above 1.0 g/L. This disparity between laboratory findings and practical field-scale use of nZVI should be bridged with research focused on synthesizing nZVI that takes advantage of stabilization and catalyzation at higher nZVI loadings on the order of 5 to 20 g/L. Finally, given the important role long-term natural attenuation can play in management of a contaminated site, the promotion of contaminant-reducing microorganisms by nZVI should be further investigated.

Literature Cited

[1] C.B. Wang and W.X. Zhang, *Synthesizing nanoscale iron particles for rapid and complete dechlorination of TCE and PCBs*, Environ. Sci. Technol. 31 (1997), pp. 2154-2156.

[2] R.A. Crane and T.B. Scott, *Nanoscale zero-valent iron: Future prospects for an emerging water treatment technology,* preprint (2011), accepted for publication, to appear in J. Hazard. Mater., doi:10.1016/j.jhazmat.2011.11.073.

[3] X. Li, D.W. Elliott, and W. Zhang, *Zero-valent iron nanoparticles for abatement of environmental pollutants: Materials and engineering aspects*, Crit. Rev. Solid State Mater. Sci. 31 (2006), pp. 111-122.

[4] E.K Nyer and D.B. Vance, *Nano-scale iron for dehalogenation*, Ground Water Monit. Rem. 21 (2001), pp. 41-46.

[5] D.W. Elliott and W.X. Zhang, *Field assessment of nanoscale bimetallic particles for groundwater treatment*, Environ. Sci. Technol. 35 (2001), pp. 4922-4926.

[6] F. He, D. Zhao, and C. Paul, *Field assessment of carboxymethyl cellulose stabilized iron nanoparticles for in situ destruction of chlorinated solvents in source zones*, Water Res. 44 (2010), pp. 2360-2370.

[7] P.G. Tratnyek and R.L. Johnson, *Nanotechnologies for environmental cleanup*, Nano Today 1 (2006), pp. 44-48.

[8] A.D. Henderson and A.H. Demond, *Long-term performance of zero-valent iron permeable reactive barriers: A critical review*, Environ. Eng. Sci. 24 (2007), pp. 401-423.

[9] C.L. Geiger and K.M. Carvalho-Knighton (ed.), *Environmental Applications of Nanoscale and Microscale Reactive Metal Particles*, ACS Symposium Series 1027, American Chemical Society, Washington, DC, 2009.

[10] W. Zhang, *Nanoscale iron particles for environmental remediation: An overview*, J. Nanopart. Res. 5 (2003), pp. 323-332.

[11] A.B. Cundy, L. Hopkinson, and R.L.D. Whitby, *Use of iron-based technologies in contaminated land and groundwater remediation: A review*. Sci. Total Environ. 400 (2008), pp. 42-51.

[12] S.M. Cook, *Assessing the use and application of zero-valent iron nanoparticle technology for remediation at contaminated sites*, Report, U.S. EPA, Office of Superfund and Technology Innovation, Washington, DC, 2009.

[13] Q. Xinhong and F. Zhanqiang, *Degradation of Halogenated Organic Compounds by Modified Nano Zero-Valent Iron*, Prog. Chem. 22 (2010), pp. 291-297.

[14] L. Li, M. Fan, R.C. Brown, J.H. Van Leeuwen, J. Wang, W. Wang, Y. Song, and P. Zhang, *Synthesis, properties, and environmental applications of nanoscale iron-based materials: A review*, Crit. Rev. Env. Sci. Technol. 36 (2006), pp. 405-431.

[15] R. Glazier, R. Venkatakrishnan, F. Gheorghiu, L. Walata, R. Nash, and W.X. Zhang, *Nanotechnology takes roots*, Civil Eng. 73 (2003), pp. 64-69.

[16] A. Gavaskar, L. Tatar, W. Condit, *Cost and performance report, nanoscale zero-valent iron technologies for source remediation*, Contract Rep. CR-05-007-ENV, Naval Facilities Engineering Command, Port Hueneme, California, 2005.

[17] W.X. Zhang and D.W. Elliott, *Applications of iron nanoparticles for groundwater remediation*, Remediation 16 (2006), pp. 7-21.

[18] S. Comba, A.D. Molfetta, and R. Sethi, *A comparison between field applications of nano-, micro-, and millimetric zero-valent iron for the remediation of contaminated aquifers*, Water, Air, Soil Pollut. 215 (2011), pp. 595-607.

[19] A.R. Petosa, D.P. Jaisi, I.R. Quevedo, M. Elimelech, and N. Tufenkji, *Aggregation and deposition of engineered nanomaterials in aquatic environments: Role of physiochemical interactions*, Environ. Sci. Technol. 44 (2010), pp. 6532-6549.

[20] T. Phenrat, N. Saleh, K. Sirk, H.J. Kim, R.D. Tilton, and G.V. Lowry, *Stabilization of aqueous nanoscale zerovalent iron dispersions by anionic polyelectrolytes: Adsorbed anionic polyelectrolyte layer properties and their effect on aggregation and sedimentation*, J. Nanopart. Res. 10 (2008), pp. 795-814.

[21] B. Schrick, B.W. Hydutsky, J.L. Blough, and T.E. Mallouk, *Delivery Vehicles for Zerovalent Metal Nanoparticles in Soil and Groundwater*, Chem. Mater. 16 (2004), pp. 2187-2193.

[22] F. He and D. Zhao, *Preparation and characterization of a new class of starch-stabilized bimetallic nanoparticles for degradation of chlorinated hydrocarbons in water*, Environ. Sci. Technol. 39 (2005), pp. 3314-3320.

[23] C.M. Cirtiu, T. Raychoudhury, S. Ghoshal, and A. Moores, *Systematic comparison of the size, surface characteristics and colloidal stability of zero valent iron nanoparticles pre- and post-grafted with common polymers*, Colloids Surf., A 390 (2011), pp. 95-104.

[24] N. Sakulchaicharoen, D.M. O'Carroll, and J.E. Herrera, *Enhanced stability and dechlorination activity of pre-synthesis stabilized nanoscale FePd particles*, J. Contam. Hydrol. 118 (2010), pp. 117-127.

[25] S.M. Ponder, J.G. Darab, and T.E. Mallouk, *Remediation of Cr(VI) and Pb(II) aqueous solutions using supported, nanoscale zero-valent iron*, Environ. Sci. Technol. 34 (2000), pp. 2564-2569.

[26] S.M. Ponder, J.G. Darab, J. Bucher, D. Caulder, I. Craig, L. Davis, N. Edelstein, W. Lukens, H. Nitsche, L. Rao, D.K. Shuh, and T.E. Mallouk, *Surface chemistry and electrochemistry of supported zerovalent iron nanoparticles in the remediation of aqueous metal contaminants*, Chem. Mater. 13 (2001), pp. 479-486.

[27] F. He, D. Zhao, J. Liu, and C.B. Roberts, *Stabilization of Fe-Pd nanoparticles with sodium carboxymethyl cellulose for enhanced transport and dechlorination of trichloroethylene in soil and groundwater*, Ind. Eng. Chem. Res. 46 (2007), pp. 29-34.

[28] P. Jiemvarangkul, W.X. Zhang, and H.L. Lien, *Enhanced transport of polyelectrolyte stabilized nanoscale zero-valent iron (nZVI) in porous media*, Chem. Eng. J. 170 (2011), pp. 482-491.

[29] L.M. Kustov, E.D. Finashina, E.V. Shuvalova, O.P. Tkachenko, and O.A. Kirichenko, *Pd-Fe nanoparticles stabilized by chitosan derivatives for perchloroethene dechlorination*, Environ. Int. 37 (2011), pp. 1044-1052.

[30] A.V. Dobrynin and M. Rubinstein, *Theory of polyelectrolytes in solutions and at surfaces*, Prog. Polym. Sci. 30 (2005), pp. 1049-1118.

[31] H.J. Kim, T. Phenrat, R.D. Tilton, and G.V. Lowry, *Fe^0 nanoparticles remain mobile in porous media after aging due to slow desorption of polymeric surface modifiers*, Environ. Sci. Techno. 43 (2009), pp. 3824-3830.

[32] Y.H. Lin, H.H. Tseng, M.Y. Wey, and M.D. Lin, *Characteristics of two types of stabilized nano zero-valent iron and transport in porous media*, Sci. Total Environ. 408 (2010), pp. 2260-2267.

[33] F. He and D. Zhao, *Manipulating the size and dispersability of zerovalent iron nanoparticles by use of carboxymethyl cellulose stabilizers*, Environ. Sci. Technol. 41 (2007), pp. 6216-6221.

[34] T. Phenrat, Y. Liu, R.D. Tilton, and G.V. Lowry, *Adsorbed polyelectrolyte coatings decrease Fe^0 nanoparticle reactivity with TCE in water: Conceptual model and mechanisms*, Environ. Sci. Technol. 43 (2009), pp. 1507-1514.

[35] Y.H. Lin, H.H. Tseng, M.Y. Wey, and M.D. Lin, *Characteristics, morphology, and stabilization mechanism of PAA250K-stabilized bimetal nanoparticles*, Colloids Surf., A 349 (2009), pp. 137-144.

[36] S.Comba and R. Sethi, *Stabilization of highly concentrated suspensions of iron nanoparticles using shear-thinning gels of xanthan gum*, Water Res. 43 (2009), pp. 3717-3726.

[37] E.D. Vecchia, M. Luna, and R. Sethi, *Transport in porous media of highly concentrated iron micro- and nanoparticles in the presence of xanthan gum*, Environ. Sci. Technol. 43 (2009), pp. 8942-8947.

[38] R.G. Shimmin, A.B. Schoch, and P.V. Braun, *Polymer size and concentration effects on the size of gold nanoparticles capped by polymeric thiols*, Langmuir 20 (2004), pp. 5613-5620.

[39] T. Raychoudhury, G. Naja, and S. Ghoshal, *Assessment of transport of two polyelectrolyte-stabilized zero-valent iron nanoparticles in porous media*, J. Contam. Hydrol. 118 (2010), pp. 143-151.

[40] S.R. Kanel, R.R. Goswami, T.P. Clement, M.O. Barnett, and D. Zhao, *Two dimensional transport of surface stabilized zero-valent iron nanoparticles in porous media*, Environ. Sci. Technol. 42 (2008), pp. 896-900.

[41] T. Phenrat, A. Cihan, H.J. Kim, M. Mital, T. Illangasekare, and G.V. Lowry, *Transport and deposition of polymer-modified Fe^0 nanoparticles in 2-D heterogeneous porous media: Effects of particle concentration, Fe^0 content, and coatings*, Environ. Sci. Technol. 44 (2010), pp. 9086-9093.

[42] T. Phenrat, F. Fagerlund, T. Illangasekare, G.V. Lowry, and R.D. Tilton, *Polymer-modified Fe0 nanoparticles target entrapped NAPL in two dimensional porous media: Effect of particle concentration, NAPL saturation, and injection strategy*, Environ. Sci. Technol. 45 (2011), pp. 6102-6109.

[43] T. Phenrat, H.J. Kim, F. Fagerlund, T. Illangasekare, and G.V. Lowry, *Empirical correlations to estimate agglomerate size and deposition during injection of a polyelectrolyte-modified Fe^0 nanoparticle at high particle concentration in saturated sand*, J. Contam. Hydrol. 118 (2010) 152-164.

[44] F. He, M. Zhang, T. Qian, and D. Zhao, *Transport of carboxymethyl cellulose stabilized iron nanoparticles in porous media: Column experiments and modeling*, J. Colloid Interface Sci. 334 (2009), pp. 96-102.

[45] J. Quinn, D. Elliott, S. O'Hara, A. Billow, *Use of nanoscale iron and bimetallic particles for environmental remediation: A review of field-scale applications*, C.L. Geiger and K.M. Carvalho-Knighton, eds., American Chemical Society, Washington, D.C., 2009, pp. 263-283.

[46] T. Phenrat, N. Saleh, K. Sirk, R.D. Tilton, and G.V. Lowry, *Aggregation and sedimentation of aqueous nanoscale zerovalent iron dispersions*, Environ. Sci. Technol. 41 (2007), pp. 284-290.

[47] E.H. Jones, D.A. Reynolds, A.L. Wood, and D.G. Thomas, *Use of electrophoresis for transporting nano-iron in porous media*, Groundwater 49 (2011), pp. 172-183.

[48] T. Phenrat, H.J. Kim, F. Fagerlund, T. Illangasekare, R.D. Tilton, and G.V. Lowry, *Particle size distribution, concentration, and magnetic attraction affect transport of polymer-modified Fe^0 nanoparticles in sand columns*, Environ. Sci. Technol. 43 (2009), pp. 5079-5085.

[49] N. Saleh, H.J. Kim, T. Phenrat, K. Matyjaszewski, R.D. Tilton, and G.V. Lowry, *Ionic strength and composition affect the mobility of surface-modified Fe^0 nanoparticles in water-saturated sand columns*, Environ. Sci. Technol. 42 (2008), pp. 3349-3355.

[50] K.M. Sirk, N.B. Saleh, T. Phenrat, H.J. Kim, B. Dufour, J. OK, P.L. Golas, K. Matyjaszewski, G.V. Lowry, and R.D. Tilton, *Effect of adsorbed polyelectrolytes on nanoscale zero valent iron particle attachment to soil surface models*, Environ. Sci. Technol. 43 (2009), pp. 3803-3808.

[51] N. Saleh, K. Sirk, Y. Liu, T. Phenrat, B. Dufour, K. Matyjaszewski, R.D. Tilton, and G.V. Lowry, *Surface modifications enhance nanoiron transport and NAPL targeting in saturated porous media*, Environ. Eng. Sci. 24 (2007), pp. 45-57.

[52] N. Saleh, T. Phenrat, K. Sirk, B. Dufour, J. Ok, T. Sarbu, K. Matyjaszewski, R.D. Tilton, and G.V. Lowry, *Adsorbed triblock copolymers deliver reactive iron nanoparticles to the oil/water interface*, Nano Lett. 5 (2005), pp. 2489-2494.

[53] Y.P. Sun, X.Q. Li, W.X. Zhang, and H.P. Wang, *A method for the preparation of stable dispersion of zero-valent iron nanoparticles*, Colloids Surf., A 308 (2007), pp. 60-66.

[54] A. Tiraferri, K.L. Chen, R. Sethi, and M. Elimelech, *Reduced aggregation and sedimentation of zero-valent iron nanoparticles in the presence of guar gum*, J. Colloid Interface Sci. 324 (2008), pp. 71-79.

[55] F.S. Freyria, B. Bonelli, R. Sethi, M. Armandi, E. Belluso, and E. Garrone, *Reactions of acid orange 7 with iron nanoparticles in aqueous solutions*, J. Phys. Chem. 115 (2011), pp. 24143-24152.

[56] Z. Xiong, D. Zhao, and G. Pan, *Rapid and complete destruction of perchlorate in water and ion-exchange brine using stabilized zero-valent iron nanoparticles*, Water Res. 41 (2007), pp. 3497-3505.

[57] F. He and D. Zhao, *Hydrodechlorination of trichloroethene using stabilized Fe-Pd nanoparticles: Reaction mechanism and effects of stabilizers, catalysts and reaction conditions*, Appl. Catal., B 84 (2008), pp. 533-540.

[58] Y. Cho and S.I. Choi, *Degradation of PCE, TCE, and 1,1,1-TCA by nanosized FePd bimetallic particles under various experimental conditions*, Chemosphere 81 (2010), pp. 940-945.

[59] Q. Wang, H. Qian, Y. Yang, Z. Zhang, C. Naman, and X. Xu, *Reduction of hexavalent chromium by carboxymethyl cellulose-stabilized zero-valent iron nanoparticles*, J. Contam. Hydrol. 114 (2010), pp. 35-42.

[60] T. Dong, H. Luo, Y. Wang, B. Hu, and H. Chen, *Stabilization of Fe-Pd bimetallic nanoparticles with sodium carboxymethyl cellulose for catalytic reduction of para-nitrochlorobenzene in water*, Desalination 271 (2011), pp. 11-19.

[61] W.X. Zhang, C.B. Wang, and H.L. Lien, *Treatment of chlorinated organic contaminants with nanoscale bimetallic particles*, Catal. Today 40 (1998), pp. 387-395.

[62] Y.H. Kim and E.R. Carraway, *Reductive dechlorination of TCE by zero valent bimetals*, Environ. Technol. 24 (2003), pp. 69-75.

[63] M. Rivero-Huguet and W.D. Marshall, *Reduction of hexavalent chromium mediated by micro- and nano-sized mixed metallic particles*, J. Hazard. Mater. 169 (2009), pp. 1081-1087.

[64] C.L. Chun, D.R. Baer, D.W. Matson, J.E. Amonette, and R.L. Penn, *Characterization and reactivity of iron nanoparticles prepared with added Cu, Pd, and Ni*, Environ. Sci. Technol. 44 (2010), pp. 5079-5085.

[65] Z. Wang, W. Huang, P. Peng, and D.E. Fennell, *Rapid transformation of 1,2,3,4-TCDD by Pd/Fe catalysts*, Chemosphere 78 (2010), 147-151.

[66] J.H. Kim, P.G. Tratnyek, and Y.S. Chang, *Rapid dechlorination of polychlorinated dibenzo-p-dioxins by bimetallic and nanosized zerovalent iron*, Environ. Sci. Technol. 42 (2008), pp. 4106-4112.

[67] T.T. Lim and B.W. Zhu, *Practical applications of bimetallic nanoiron particles for reductive deahlogenation of haloorganics: Prospects and challenges*, C.L. Geiger and K.M. Carvalho-Knighton, eds., American Chemical Society, Washington, D.C., 2009, pp. 245-261.

[68] H.L. Lien and W.X. Zhang, *Nanoscale iron particles for complete reduction of chlorinated ethenes*, Colloids Surf., A 191 (2001), pp. 97-105.

[69] B. Schrick, J.L. Blough, A.D. Jones, and T.E. Mallouk, *Hydrodechlorination of trichloroethylene to hydrocarbons using bimetallic nickel-iron nanoparticles*, Chem. Mater. 14 (2002), pp. 5140-5147.

[70] G.V. Lowry and M. Reinhard, *Pd-catalyzed TCE dechlorination in water: Effect of $[H_2](aq)$ and H_2-utilizing competitive solutes on the TCE dechlorination rate and product distribution*, Environ. Sci. Technol. 35 (2001), pp. 696-702.

[71] H.L. Lien and W.X. Zhang, *Nanoscale Pd/Fe bimetallic particles: Catalytic effects of palladium on hydrodechlorination*, Appl. Catal., B 77 (2007), pp. 110-116.

[72] W. Yan, A.A. Herzing, X.Q. Li, C.J. Kiely, and W.X. Zhang, *Structural evolution of Pd-doped nanoscale zero-valent iron (nZVI) in aqueous media and implications for particle aging and reactivity*, Environ. Sci. Technol. 44 (2010), pp. 4288-4294.

[73] X. Wang, C. Chen, Y. Chang, and H. Liu, *Dechlorination of chlorinated methanes by Pd/Fe bimetallic nanoparticles*, J. Hazard. Mater. 161 (2009), pp. 815-823.

[74] W. Zhang, W. Quan, J. Wang, Z. Zhang, and S. Chen, *Rapid and complete dechlorination of PCP in aqueous solution using Ni-Fe nanoparticles under assistance of ultrasound*, Chemosphere 65 (2006), pp. 58-64.

[75] C.J. Lin, S.L. Lo, and Y.H. Liou, *Dechlorinatino of trichloroethylene in aqueous solution by noble metal-modified iron*, J. Hazard. Mater. B116 (2004), pp. 219-228.

[76] Y.H. Tee, L. Bachas, D. Bhattacharyya, *Degradation of trichloroethylene by iron-based bimetallic nanoparticles*, J. Phys. Chem., C 113 (2009), pp. 9454-9464.

[77] T. Zhou, Y. Li, and T.T. Lim, *Catalytic hydrodechlorination of chlorophenols by Pd/Fe nanoparticles: Comparisons with other bimetallic systems, kinetics, and mechanism*, Sep. Purif. Technol. 76 (2010), pp. 206-214.

[78] H.L. Lien and W.X. Zhang, *Transformation of chlorinated methanes by nanoscale iron particles*, J. Environ. Engr. 125 (1999), pp. 1042-1047.

[79] H.L. Lien and W.X. Zhang, *Hydrodechlorination of chlorinated ethanes by nanoscale Pd/Fe bimetallic particles*, J. Environ. Eng. 131 (2005), pp. 4-10.

[80] B.W. Zhu, T.T. Lim, and J. Feng, *Reductive dechlorination of 1,2,4-trichlorobenzene with palladized nanoscale Fe^0 particles supported on chitosan and silica*, Chemosphere 65 (2006), pp. 1137-1145.

[81] B.W. Zhu and T.T. Lim, *Catalytic reduction of chlorobenzenes with Pd/Fe nanoparticles: Reactive sites, catalyst stability, particle aging, and regeneration*, Environ. Sci. Technol. 41 (2007), pp. 7523-7529.

[82] B.W. Zhu, T.T. Lim, and J. Feng, *Influences of ampiphiles on dechlorination of a trichlorobenzene by nanoscale Pd/Fe: Adsorption, reaction kinetics, and interfacial interactions*, Environ. Sci. Technol. 42 (2008), pp. 4513-4519.

[83] V. Nagpal, A.D. Bokare, R.C. Chikate, C.V. Rode, and K.M. Paknikar, *Reductive dechlorination of γ-hexachlorocyclohexane using Fe-Pd bimetallic nanoparticles*, J. Hazard. Mater. 175 (2010), pp. 680-687.

[84] M. Zhang, F. He, D. Zhao, and X. Hao, *Degradation of soil-sorbed trichloroethylene by stabilized zero valent iron nanoparticles: Effects of sorption, surfactants, and natural organic matter*, Water Res. 45 (2011), pp. 2401-2414.

[85] Y.H. Shih, M.Y. Chen, and Y.F. Su, *Pentachlorophenol reduction by Pd/Fe bimetallic nanoparticles: Effects of copper, nickel, and ferric cations*, Appl. Catal., B 105 (2011), pp. 24-29.

[86] Y. Zhuang, S. Ahn, A.L. Seyfferth, Y. Masue-Slowey, S. Fendorf, and R.G. Luthy, *Dehalogenation of polybrominated diphenyl ethers and polychlorinated biphenyl by bimetallic, impregnated, and nanoscale zerovalent iron*, Environ. Sci. Technol. 45 (2011), pp. 4896-4903.

[87] S.H. Joo and D. Zhao, *Destruction of lindane and atrazine using stabilized iron nanoparticles under aerobic and anaerobic conditions: Effects of catalyst and stabilizer*, Chemosphere 70 (2008), pp. 418-425.

[88] J. Cao, D. Elliott, and W.X. Zhang, *Perchlorate reduction by nanoscale iron nanoparticles*, J. Nanopart. Res. 7 (2005), pp. 499-506.

[89] K. Mondal, G. Jegadeesan, and S.B. Lalvani, *Removal of selenate by Fe and NiFe nanosized particles*, Ind. Eng. Chem. Res. 43 (2004), pp. 4922-4934.

[90] J. Feng and T.T. Lim, *Pathways and kinetics of carbon tetrachloride and chloroform reductions by nano-scale Fe and Fe/Ni particles: Comparison with commercial micro-scale Fe and Zn*, Chemosphere 59 (2005), pp. 1267-1277.

[91] Y.H. Tee, E. Grulke, and D. Bhattacharyya, *Role of Ni/Fe nanoparticle composition on the degradation of trichloroethylene from water*, Ind. Eng. Chem. Res. 44 (2005), pp. 7062-7070.

[92] L. Wu and S.M.C. Ritchie, *Removal of trichloroethylene from water by cellulose acetate supported bimetallic Ni/Fe nanoparticles*, Chemosphere 63 (2006), pp. 285-292.

[93] W.H. Zhang, X. Quan, and Z.Y. Zhang, *Catalytic reductive dechlorination of p-chlorophenol in water using Ni/Fe nanoscale particles*, J. Environ. Sci. 19 (2007), pp. 362-366.

[94] A.D. Bokare, R.C. Chikate, C.V. Rode, and K.M. Paknikar, *Effect of surface chemistry of Fe-Ni nanoparticles on mechanistic pathways of azo dye degradation*, Environ. Sci. Technol. 41 (2007), pp. 7437-7443.

[95] T.T. Lim, J. Feng, and B.W. Zhu, *Kinetic and mechanistic examinations of reductive transformation pathways of brominated methanes with nano-scale Fe and Ni/Fe particles*, Water Res. 41 (2007), pp. 875-883.

[96] R.J. Barnes, O. Riba, M.N. Gardner, A.C. Singer, S.A. Jackman, and I.P. Thompson, *Inhibition of biological TCE and sulphate reduction in the presence of iron nanoparticles*, Chemosphere 80 (2010), pp. 554-562.

[97] R.J. Barnes, O. Riba, M.N. Gardner, T.B. Scott, S.A. Jackman, and I.P. Thompson, *Optimization of nano-scale nickel/iron particles for the reduction of high concentration chlorinated aliphatic hydrocarbons*, Chemosphere 79 (2010), pp. 448-454.

[98] R. Cheng, W. Zhou, J.L. Wang, D. Qi, L. Guo, W.X. Zhang, and Y. Qian, *Dechlorination of pentachlorophenol using nanoscale Fe/Ni particles: Role of nano-Ni and its size effect*, J. Hazard. Mater. 180 (2010), pp. 79-85.

[99] A. Ryu, S.W. Jeong, A. Jang, and H. Choi, *Reduction of highly concentrated nitrate using nanoscale zero-valent iron: Effects of aggregation and catalyst on reactivity*, Appl. Catal., B 105 (2011), pp. 128-135.

[100] U.S. Enivonrmental Protection Agency, *Technical factsheet on: Nickel*. Available at http://www.epa.gov/ogwdw/pdfs/factsheets/ioc/tech/nickel.pdf.

[101] World Health Organization, *Guidelines for drinking-water quality, 4th Ed*, Geneva, Switzerland, 2011. Available at http://whqlibdoc.who.int/publications/2011/9789241548151_eng.pdf.

[102] K.W. Henn and D.W. Waddill, *Utilization of nanoscale zero-valent iron for source remediation–A case study*, Remediation. J. 16 (2006), pp. 57-77.

[103] S.S. Chen, H.D. Hsu, and C.W. Li, *A New Method to Produce Nanoscale Iron for Nitrate Removal*, J. Nanopart. Res. 6 (2004), pp. 639-647.

[104] B.W. Hydutsky, E.J. Mack, B.B. Beckerman, J.M. Skluzacek, and T.E. Mallouk, *Optimization of nano- and microiron transport through sand columns using polyelectrolyte mixtures*, Environ. Sci. Technol. 41 (2007), pp. 6418-6424.

[105] A. Tiraferri and R. Sethi, *Enhanced transport of zerovalent iron nanoparticles in saturated porous media by guar gum*, J. Nanopart. Res. 11 (2009), pp. 635-645.

[106] Z.M. Xiu, K.B. Gregory, G.V. Lowry, and P.J.J. Alvarez, *Effect of bare and coated nanoscale zerovalent iron on tceA and vcrA gene expression in Dehalococcoides spp.*, Environ. Sci. Technol. 44 (2010), pp. 7647-7651.

III. Scholarly Article: Research Article

To be submitted to *Environmental Science & Technology*

Optimization of CMC-Stabilized, Pd-Catalyzed nZVI for the Degradation of Chlorinated Organic Water Contaminants

Abstract

New methods which improve nZVI reactivity and transport characteristics, including polyelectrolyte stabilization and bimetal catalyzation, are necessary to develop nZVI as an economically viable technology for the remediation of contaminated groundwater. Here, the borohydride reduction synthesis method, carboxymethyl cellulose (CMC) stabilizer concentration, and Pd catalyst loading were optimized for degradation of chlorinated methanes and ethenes, which are among the most common groundwater contaminants. Increasing the ratio of $NaBH_4$ reductant to ferrous iron precursor from the stoichiometric amount of 2:1 to 6:1 improved nZVI degradation of carbon tetrachloride (CT) by 72%. Increasing CMC concentration from 0.5 g/L to 8.0 g/L further improved reactivity by 452%. This increase in reactivity was paired with a decrease in particle agglomeration and mean particle diameter, from 29.3 to 4.6 nm, as determined by transmission electron microscopy. Finally, amending nZVI with 3.3% (w/w) Pd catalyst improved reactivity another 375% while reducing formation of chlorinated byproducts. Also, the degradation pathways of CT and chloroform (CF) by nZVI reduction are further elucidated. The formation of significant amounts of tetrachloroethene (PCE) during CT degradation is reported for the first time.

Introduction

Nanoscale zero-valent iron is a rapidly developing, highly promising new material that can be applied for the remediation of groundwater contaminants, including a wide variety of chlorinated and non-chlorinated organics, heavy metals, perchlorate, and nitrate [1,2]. Of these contaminants, chlorinated methanes and ethenes, such as carbon tetrachloride (CT), chloroform (CF), tetrachloroethene (PCE), and trichloroethene (TCE), were identified in 2006 as among the most prevalent in U.S. aquifers [3]. Their wide use as solvents, refrigerants, and chemical precursors has resulted in their ubiquity at contaminated industrial sites. Despite the growing attention garnered by nZVI as a potential remediation technology in the last decade, the technology continues to face several challenges, including its relatively high cost of synthesis, its disappointing transport *in situ*, and the formation of toxic byproducts during nZVI remediation of chlorinated organics. A recent estimate suggests nZVI cost must drop by about 10 fold to become competitive with existing remediation methods [1]. Alternatively, improving the utility of nZVI may make it a more viable, mainstream remediation option.

Three approaches for overcoming the challenges facing nZVI include: (1) improving nZVI synthesis methods to enhance reactivity, (2) improving nZVI reactivity and mobility by adding stabilizers, and (3) improving nZVI reactivity while minimizing toxic byproduct formation by amending nZVI with a catalyst.

Perhaps the greatest challenge to implementing nZVI in subsurface remediation is the rapid agglomeration of bare nZVI particles due to attractive van der Waals and magnetic forces [4]. Agglomeration decreases the available reactive surface area of nZVI particles and larger aggregates are not readily transported in porous media [5]. Beginning in 2004, researchers began applying polyelectrolyte stabilizer coatings to nZVI, which are conclusively shown to decrease aggregation, produce smaller particles, and improve nanoparticle transport [6]. Smaller diameter

particles have relatively more surface area, thereby boosting reactivity. Polyelectrolyte stabilizers achieve this by attaching to the nZVI surface and establishing electrosteric repulsion between individual particles and subsurface media [4,7]. Polyelectolyte coatings are an attractive solution because of their low cost, wide availability, ease of implementation, and lack of toxicity.

The ability of catalysts to improve contaminant degradation was established well before the development of nano-scale ZVI. Many different metals have been used to catalyze nZVI, including Co, Pt, Pd, Ag, Cu, Ni, and Zn [1]. Of these, Pd is clearly the most effective catalyst across a wide range of contaminants [8,9]. However, Pd is also a precious metal, costing upwards of 20,000 USD per kilogram. When Pd is added to the nZVI surface, a galvanic cell is established between the metals; Fe becomes a sacrificial anode, transferring electrons to and thereby protecting the Pd cathode [1]. In the presence of atomic hydrogen formed by the hydrolysis of water, Pd-catalyzed hydrodechlorination of chlorinated methanes and ethenes results in faster degradation and fewer chlorinated byproducts [10,11].

Experimental Procedures

Chemicals.

The following chemicals were used as received: iron sulfate ($FeSO_4 \cdot 7H_2O$, MP Biomedicals, Solon, OH); sodium borohydride ($NaBH_4$, Acros, New Jersey); sodium carboxymethyl cellulose (CMC, M_r=90 000, D.S.=0.7, Sigma-Aldrich, St. Louis, MO); potassium hexachloropalladate (K_2PdCl_6, 99%, Sigma Aldrich, St. Louis, MO); carbon tetrachloride (ACS Grade, Fisher Scientific, Pittsburgh, PA); chloroform (ACS Grade, Fisher Scientific, Pittsburgh, PA); dichloromethane (DCM, ACS Grade, Fischer Scientific, Pittsburgh, PA); tetrachloroethene (HPLC Grade, Aldrich, Milwaukee, WI); trichloroethene (ACS Grade, Acros, New Jersey); TAPSO buffer (99+%, Sigma-Aldrich, St. Louis, MO); sodium hydroxide

(NaOH, 97+%, EMD Chemicals, Gibbstown, NJ); and Milli-Q ultrapure water (Millipore, Molsheim, France).

Preparation of Nanoparticles.

Pd catalyzed nZVI (Pd-nZVI) particles were synthesized using a variation of the $NaBH_4$ reduction method proposed by He and Zhao (2005) [7]. Nanoparticles were synthesized in a glovebox under an anaerobic atmosphere; all stock solutions were purged with nitrogen for 20 minutes to eliminate dissolved oxygen. Particles were synthesized at room temperature (21 °C). To begin synthesis, 10 mM $FeSO_4 \cdot 7H_2O$ was added to 20 g/L CMC stock solution in 160 mL serum bottles. nZVI loading was either 0.01 g/L or 0.10 g/L, depending on the experiment. Final CMC concentration varied from 0.5 to 9.0 g/L. After 15 minutes wait time, 50 mM $NaBH_4$ was added rapidly via pipette to reduce Fe ions to zero-valent nanoparticles. For experiments including palladium, 0.1 mM K_2PdCl_6 was added via pipette following addition of $NaBH_4$. Pd is reduced at the nZVI surface according to Equation 1:

$$Pd^{2+} + Fe^0 \rightarrow Pd^0 + Fe^{2+} \quad (1)$$

Bottles were then swirled gently by hand for 3 seconds to improve mixing. Next, TAPSO buffer adjusted to pH 7 was added at a final concentration of 7.81 mM. Finally, enough Milli-Q water was added to make a final solution volume of 96 mL. Bottles were then sealed with teflon-coated butyl rubber septa.

Degradation Experiments.

Batch experiments were conducted in 160 mL serum bottles with 96 mL of solution and 64 mL of headspace. All experiments were done in triplicate and nZVI was reacted with the contaminant within 20 minutes of synthesis. Control experiments indicated that the synthesized nZVI is unstable in buffered, pH 7 water, with significant loss of reactivity within one hour. To

initiate the degradation experiment, enough stock solution was added to give an initial contaminant concentration between 0.25 and 1.8 mg/L, depending on the experiment. Immediately after addition of the contaminant, the bottles were vortexed (Fisher Vortex Genie 2, Fisher Scientific) for 20 seconds at setting 8 to achieve thorough mixing. Bottles were then placed on a rotator at 75 rpm at room temperature (21 °C). Control experiments confirmed that the presence of CMC had no effect on CT and CF partitioning to headspace. Experiments to control for degradation of CT by $NaBH_4$ alone showed no degradation at relevant concentrations.

Analytical Methods.

For degradation experiments, bottle headspace was sampled every 15 minutes using a 50 µL gastight syringe (Hamilton Co., Reno, NV). Headspace samples were analyzed using an Agilent 7890A GC equipped with a µECD and, for later experiments, a FID. For detailed GC column and method information please reference the Supporting Information.

Dynamic light scattering (DLS) size measurements were done with a Malvern Zetasizer Nano ZS system. Single samples were prepared and measured in triplicate. The intensity-weighted, z-average diameter was used to quantify particle size. The viscosities of CMC solutions varying in concentration from 0.5 to 9 g/L were measured using a Gilmont falling ball viscometer (Size No. 1, Cole-Palmer, Vernon Hills, IL) and used to correct for viscosity effects on DLS measurement (see Supporting Information). Because the hydrodynamic diameter of non-agglomerated nZVI particles has been demonstrated to increase appreciably within the first hour of synthesis, nZVI for DLS analysis was synthesized immediately before measurement [4]. Samples were prepared and measured at room temperature (21 °C).

Transmission electron microscope (TEM) size measurements were done with a Hitachi H-7600 TEM equipped with a tungsten filament at an accelerating voltage of 120 kV. nZVI

samples were prepared by depositing a drop of solution on a 400 mesh, carbon-coated grid which was then dried for 24 hours under an anaerobic atmosphere. Particle diameter histograms were developed by hand-measurement of TEM images ($n \geq 493$ for each condition).

Results and Discussion

Kinetic Modeling.

Rate of contaminant degradation within the batch reactors was used as an indicator of nZVI reactivity. All degradation experiment data were fit with a pseudo-first order rate model, given by Equation 2,

$$-\frac{dC}{dt} = k_{obs}C = k_m \rho_m C \quad (2)$$

where k_{obs} (1/hr) is the observed rate constant, C (μg/L) is the contaminant concentration at time t (hr), k_m (L/g/hr) is the mass-normalized rate constant, and ρ_m (g/L) is the nZVI mass loading. In the case of CF degradation, where bi-modal kinetics were observed, the first data point was omitted from modeling (see Supporting Information). The initial rapid decrease in CF concentration which was observed is hypothesized to be due to sorption to nZVI surfaces.

Note that in this study, the commonly applied surface-area-normalized rate constant, k_{SA}, was not used. As discussed elsewhere, comparing nZVI on a surface-area-normalized basis may prove unreliable [12]. Furthermore, because both k_{SA} and specific surface area, from which k_{SA} is derived, are unique to a particular nZVI sample, a better metric of comparison is the mass-normalized reaction constant, k_m, which combines the two values. Normalizing on a mass basis is also helpful because it relates reactivity directly to the cost of nZVI synthesis materials, a driving factor of design.

For all CT degradation experiments, R^2 values quantifying goodness-of-fit to the pseudo-first order model were higher than 0.985, with most above 0.990. In most cases, the model was

fit to four or more data points, with a minimum of three points used in cases of rapid degradation. For CF and PCE degradation, bi-modal kinetics and slow headspace partitioning, respectively, resulted in poorer model fits. However, in most cases R^2 values were still above 0.900. See the Supporting Information for specific values and data. All error bars represent one standard deviation.

For conventional zero-valent iron, it has been shown that reaction rate is a function of initial contaminant concentration, suggesting that pseudo-1st order kinetics inadequately model contaminant degradation [13]. This is apparently due to saturation of surface reaction sites. However, for nZVI, it was shown that reaction rate is not a function of initial contaminant concentration below 0.12 mM, likely owing to the greater surface area of nano-scale particles compared to conventional ZVI [12,14,15]. For all experiments reported here, initial contaminant concentrations were well below 0.12 mM.

Effect of BH_4^- : Fe^{2+} Molar Ratio.

Commercial synthesis of nZVI by technology leaders Golder Associates Inc. and Toda Kogyo Ltd. is accomplished by ball milling of micro-scale particles and hydrogen reduction of iron oxide nanoparticles, respectively [1,16]. However, the most commonly used nZVI synthesis method among laboratory and smaller field-scale studies is the borohydride (BH_4^-) reduction method [17,18,19]. BH_4^- reduction of Fe ions follows one of two net chemical equations, depending on whether the Fe ions are ferric or ferrous [20, 21]:

$$Fe(H_2O)_6^{3+} + 3BH_4^- + 3H_2O \rightarrow Fe^0\downarrow + 3B(OH)_3 + 10.5H_2 \quad (3)$$

$$Fe(H_2O)_6^{2+} + 2BH_4^- \rightarrow Fe^0\downarrow + 2B(OH)_3 + 7H_2 \quad (4)$$

Since the remediation of chlorinated organic water contaminants by BH_4^- reduced nZVI was first proposed in 1997, the majority of researchers have used stoichiometric ratios of BH_4^- to Fe ions

[7,11,12,17,19,22-28]. However, a few have noted that excess BH_4^- is necessary for rapid and uniform synthesis of nZVI [29-31]. Two other reactions compete for BH_4^- in the aqueous system [20,21]:

$$BH_4^- + 2H_2O = BO_2^- + 4H_2\uparrow \quad (5)$$

$$BH_4^- + H_2O \rightarrow B\downarrow + OH^- + 2.5H_2 \quad (6)$$

The extent to which the hydrolysis reactions described by equations 5 and 6 compete with the iron reduction reactions described by equations 3 and 4 depends on the experimental conditions [20,21]. One study indicates that the usual ratio of BH_4^- consumption by reaction 4 compared to reaction 6 is 1.0 to 1.5 [20]. In another study, it was found that BH_4^- reduces Fe ions most efficiently when aqueous $Fe^{2+/3+}$ solution is added quickly to solid $NaBH_4$ [21]. This is consistent with control experiments that were performed which showed that delaying reaction of freshly prepared $NaBH_4$ solution with $FeSO_4$ solution by 15 minutes resulted in significantly less reactive nZVI.

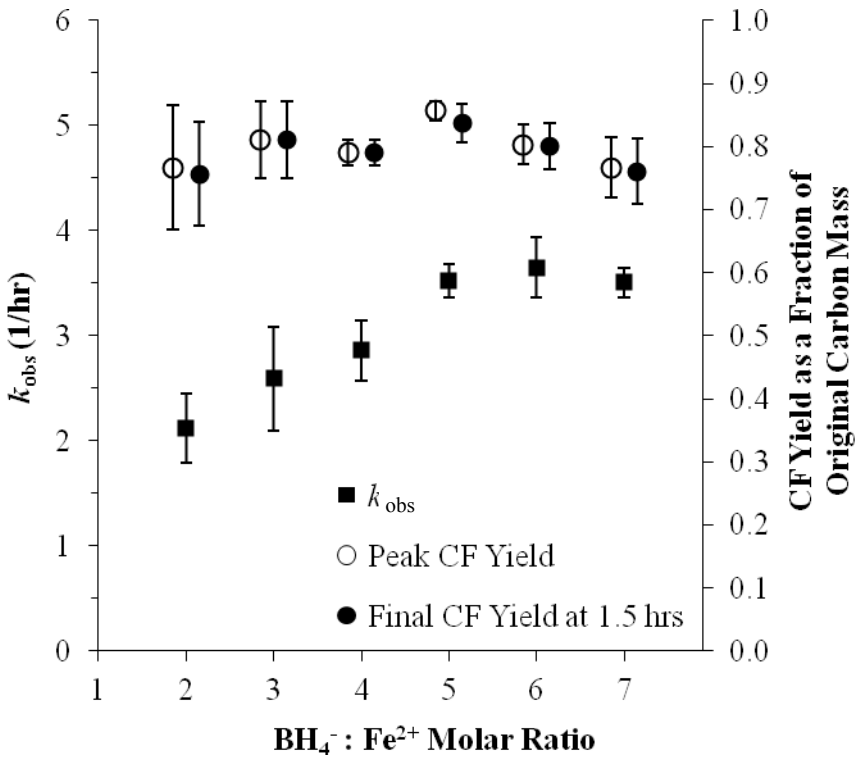

Figure 3.1. Degradation of CT by nZVI synthesized at varying BH_4^- : Fe^{2+} molar ratios. k_{obs} is the observed pseudo-first order rate constant. [nZVI] = 0.01 g/L, [C0] = 0.25 mg/L, [CMC] = 2 g/L, pH = 7, and the sampling period lasted 1.50 hrs.

Taken together, the competition for BH_4^- in the aqueous system suggests that using stoichiometric amounts of BH_4^- to reduce $Fe^{2+/3+}$ to nZVI may be insufficient to accomplish complete reduction. Figure 3.1 shows the pseudo-first order degradation rate constants, k_{obs}, for CT over a range of BH_4^- : Fe^{2+} molar ratios. Increasing the BH_4^- : Fe^{2+} ratio from the stoichiometric ratio of 2:1 to 6:1 increased nZVI reactivity, characterized by the CT degradation rate, by 72%. Initially, increasing BH_4^- loading resulted in a linear increase in reactivity with a slope of 0.45/hr (R^2=0.973). This is consistent with the hypothesis that additional BH_4^- results in more complete reduction of Fe^{2+}. Further increasing the ratio from 5:1 to 7:1 resulted in no appreciable change in reactivity, likely because Fe^{2+} was completely reduced to Fe^0 and small amounts of excess aqueous BH_4^- had little to no effect on CT degradation. Both peak CF yield,

the maximum amount observed during the experiment, and final CF yield, the amount present at the end of the experiment, remained relatively unchanged. The difference between peak and final yields represents the degradation of CF to other byproducts after the peak yield occurred. A BH_4^- : Fe^{2+} molar ratio of 6:1 was chosen for use in all subsequent experiments. The scalability of this finding remains untested; it is unclear whether the same ratio is optimal at higher nZVI loadings and, subsequently, higher reagent concentrations.

Effect of CMC Concentration on Reactivity.

Of the many polyelectrolytes used to stabilize nZVI, CMC has received the most attention. Across several comparative studies, CMC of varying molecular weights has outperformed other stabilizers by producing nanoparticles with smaller size, higher reactivity, and better transport characteristics [4,24,32-34]. Also, as with several other stabilizers, CMC is a food-grade additive, and therefore safe and relatively inexpensive. Although CMC was used in no fewer than 19 previous studies, optimization of CMC loading has not been adequately investigated [11,25,33,35]. While polyelectrolyte coatings increase the reactive surface area of nZVI by decreasing particle size and interparticle aggregation, they also decrease reactivity by blocking the reactive nZVI surfaces [36]. Thus, optimizing CMC loading is important because excess polyelectrolyte can have the net effect of reducing reactivity [11].

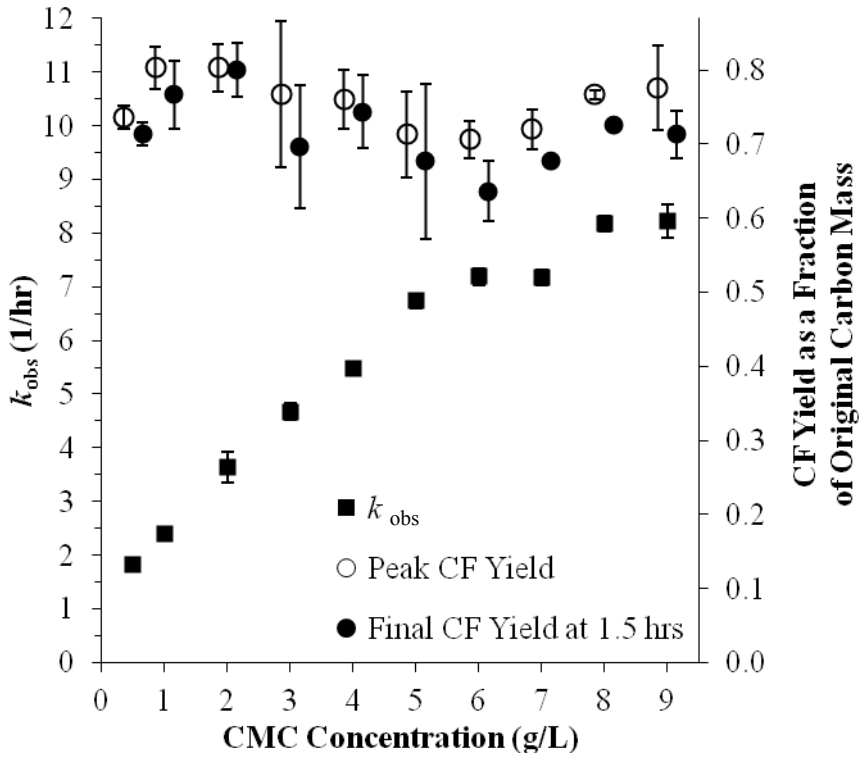

Figure 3.2. Degradation of CT by nZVI synthesized at varying CMC concentrations. k_{obs} is the observed pseudo-first order rate constant. [nZVI] = 0.01 g/L, [C_0] = 0.25 mg/L, BH_4^- : Fe^{2+} molar ratio = 6:1, pH = 7, and the sampling period lasted 1.5 hrs.

To thoroughly investigate the effect of CMC stabilizer on nZVI reactivity, CMC concentration was varied from 0.5 g/L to 9.0 g/L over a series of degradation experiments. As shown in Figure 3.2, the addition of CMC stabilizer significantly improved nZVI reactivity toward CT, by as much as 452% between 0.5 and 8.0 g/L. Between CMC loadings of 0.5 and 5.0 g/L, a linear response in reactivity with a slope of 1.07/hr was observed (R^2=0.996). Beyond 8.0 g/L CMC loading, a plateau in reactivity was observed, which may be attributable to two factors: (1) higher CMC concentrations may have no further effect on particle size or stability, or (2) continued improvements in particle size or stability may be negated by the reaction-inhibiting effect of the CMC surface coating [36]. Surface-mediated reaction likely remains the rate-limiting step in degradation because, as will be shown, the addition of a surface-bound catalyst further increases reactivity [10]. Increasing CMC loading did not have a significant effect on CF

byproduct production or degradation; poor degradation of CF is attributed to the near-complete consumption of nZVI within the first 1.5 hours. In this study, 8.0 g/L was chosen as an optimal CMC loading and used for all further experiments, at both 0.01 g/L and 0.10 g/L nZVI loading.

Although optimal CMC loading was reported relative to nZVI loading in the past, there is evidence that the absolute CMC concentration, regardless of nZVI loading, is a better predictor of performance [11,25]. It was previously observed that failure of polyelectrolytes to prevent nanoparticle aggregation is not caused by insufficient amounts of stabilizer, but rather the slow rate of particle coating at low stabilizer concentrations [37]. Furthermore, during particle synthesis polyelectrolytes mediate the formation of more numerous, smaller particles, an effect dependent on absolute polyelectrolyte concentration [25,26,38]. In this study, 8 g/L CMC was found to be optimal at 0.01 g/L nZVI loading. At an nZVI loading of 0.10 g/L, He and Zhao (2007, 2008) determined that 4.0 g/L and 2.0 g/L CMC loading gave the smallest and the most reactive nZVI particles, respectively [11,25]. Finally, at 1.0 g/L nZVI loading, Cirtiu et al. (2011) found that 5.0 g/L CMC loading clearly outperformed 2.5 g/L and 1.0 g/L in terms of particle size, producing particles less than 10 nm in diameter [33]. Variability in the optimal CMC loading between studies is limited to a factor of four despite two order-of-magnitude differences in nZVI loading.

Physical Characterization of CMC Stabilized nZVI.

Both DLS particle sizing and TEM imaging were used to further investigate the effect of CMC stabilizer concentration on nZVI particle size and aggregation. For DLS measurements, CMC concentration was varied between 0.5 and 9.0 g/L, matching concentrations used for degradation experiments. Measured z-average particle diameters varied between 121 and 241 nm, with no clear trend present (see Supporting Information).

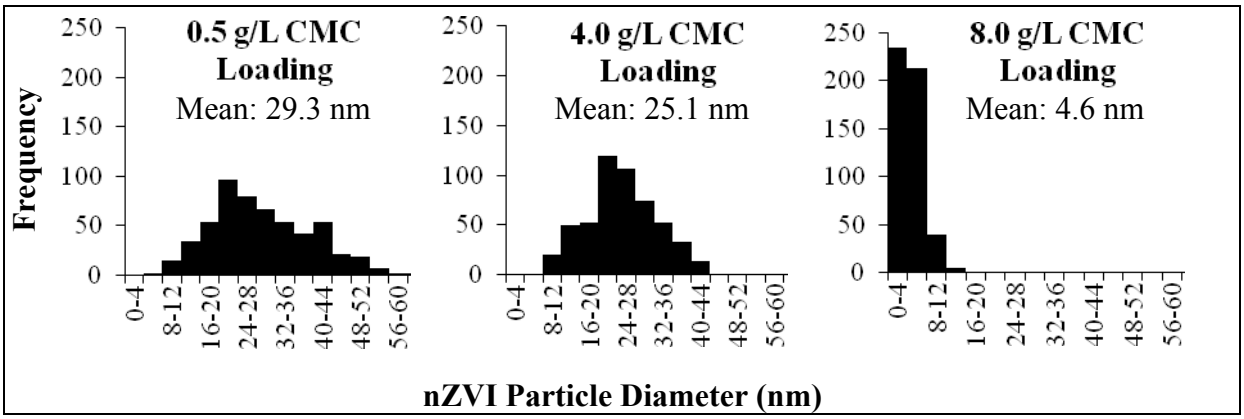

Figure 3.3. TEM particle size histograms of nZVI synthesized at varying CMC loadings. [nZVI] = 0.01 g/L, BH_4^- : Fe^{2+} molar ratio = 6:1.

In contrast to DLS measurement, TEM imaging lends the advantage of directly observing the size and morphology of nanoparticles. However, representativeness of the images may be affected in two important ways: (1) necessary drying of the sample may alter particle sizes and the degree of agglomeration and (2) only a small fraction of the sample is imaged and measured. If the chosen images are not representative of the sample as a whole, sizing estimates may be biased [26]. Figure 3.3 compares the particle diameter histograms for nZVI samples prepared at varying CMC concentrations. At 0.5 g/L CMC, nZVI particles are relatively polydisperse, ranging from as small as 6 nm to as large as 62 nm. The particles are also highly aggregated, with individual particles overlapping each other in images, suggesting interparticle attachment (see Supporting Information for sample images). Increasing the CMC concentration to 4.0 g/L results in only a modest reduction in mean particle diameter. Although the majority of particles remain aggregated, greater separations between individual particles exist, suggesting the presence of electrosteric repulsion afforded by the CMC stabilizer [25,26]. These small-scale physical separations may, by increasing the reactive surface area, be responsible for the improved nZVI reactivity in the absence of an appreciable reduction in mean particle diameter. Further increasing CMC concentration to 8.0 g/L results in a drastic reduction in size and change

in morphology. The particle size distribution is much more monodisperse and the majority of particles are less than 8 nm in diameter, with far less aggregation present. These drastic reductions in particle diameter and agglomeration further account for the increase in nZVI reactivity observed as CMC concentration is increased to 8.0 g/L.

The TEM sizing data are consistent with previously reported TEM imaging of stabilized nZVI, where particles between 2.4 and 98.5 nm in diameter were observed [4,11,22-26,35,39]. The disparity between DLS and TEM sizing of the nZVI samples may be explained in part by differences between the two measurement techniques. DLS measures the intensity-weighted average hydrodynamic diameter of a collection of hydrated particles. Attachment of CMC molecules to the surfaces of nZVI particles may have increased their hydrodynamic diameters. Also, sample polydispersity will bias the z-average diameter towards larger particle sizes. Number-weighted mean diameters for the same data were on average 31% smaller. In contrast, TEM imaging provides a number-weighted average diameter of dehydrated particles and omits any surface-attached CMC from measurement. Similar disparities between DLS and TEM sizing have been reported elsewhere, although to a lesser extent [25,26].

Effect of Pd Catalyst Amendment.

As shown in Figure 3.4, addition of Pd catalyst enhanced the reactivity of nZVI toward CT by as much as 375%. Pd-nZVI completely degraded CT and partially degraded CF within the 1.6 hr sampling periods. At Pd loadings below 1.0% (w/w), no difference in reactivity was observed, nor was there a significant change in CF and PCE byproduct yield or degradation. However, increasing Pd loading to 3.3% drastically increased reactivity, by as much as 375%, while decreasing CF yield. Although PCE production increased, above 2.3% none persisted at the end of sampling. Further increasing Pd loading to 5.0% had no significant effect on reactivity

or byproduct yield. The plateau in reactivity at higher Pd loadings may be due to a shift from a catalytically-limited reaction to a reaction limited by (1) diffusion of contaminant to the nZVI surface, (2) electron transfer from the Pd-nZVI, or (3) hydrogen production [10,40].

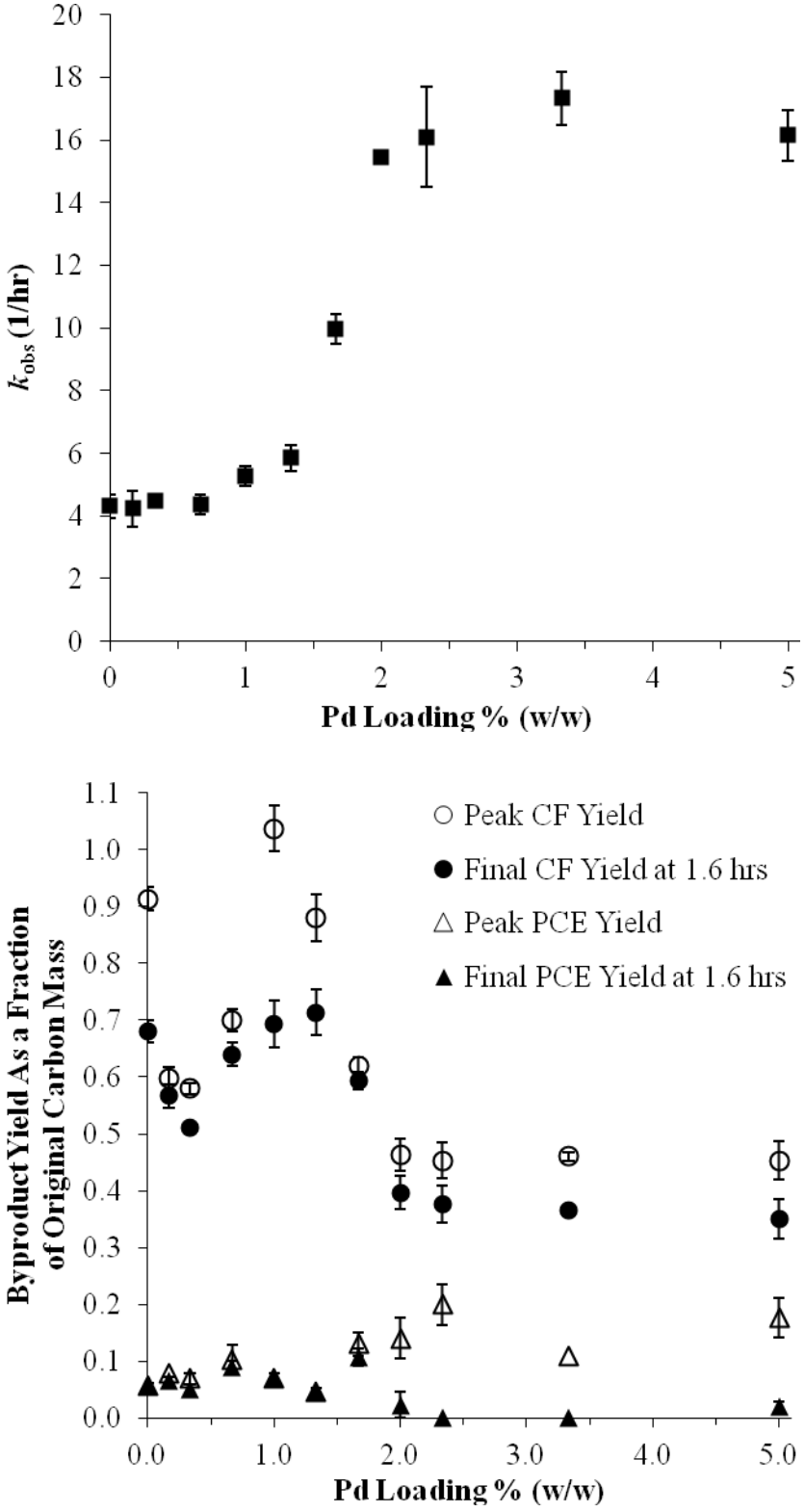

Figure 3.4. Degradation of CT at varying Pd loadings, (a) CT degradation rate, and (b) byproduct formation and subsequent degradation. k_{obs} is the observed pseudo-first order

rate constant. [nZVI] = 0.01 g/L, [C_0] = 0.88 mg/L, [CMC] = 8 g/L, BH_4^- : Fe^{2+} molar ratio = 6:1, pH = 7, and the sampling period lasted 1.6 hrs.

Field-scale implementation of nZVI typically uses nZVI concentrations between 0.2 and 4.5 g/L, well above the 0.01 g/L loading initially studied here [2,18,19]. To further investigate the scalability of the findings, Pd loading was again varied at an nZVI loading of 0.10 g/L. CF was used as a target contaminant instead of CT because it is more recalcitrant, allowing for better observation of kinetics. As shown in Figure 3.5, the addition of Pd improved the removal efficiency of CF by as much as 6 fold compared to non-catalyzed nZVI. Reactivity toward CF, as expressed by the degradation rate constant, also improved by 385% as loading was increased to 6.6% (see Supporting Information). The 338% increase in degradation rate between 0.0% and 3.3% Pd loading agrees well with the results of CT degradation at lower nZVI loading, suggesting that optimized Pd loadings are scalable. Although increasing Pd loading to 4.0% and 6.6% further improved CF degradation, it also resulted in higher DCM byproduct yields. Given this and the results from CT degradation experiments, 3.3% was chosen as an optimal Pd loading and used in subsequent degradation experiments. Trace amounts of ethane byproduct were also observed under all experimental conditions. The mass-normalized decay rate constant, k_m, for CF was 1.62E+01 L/g/hr.

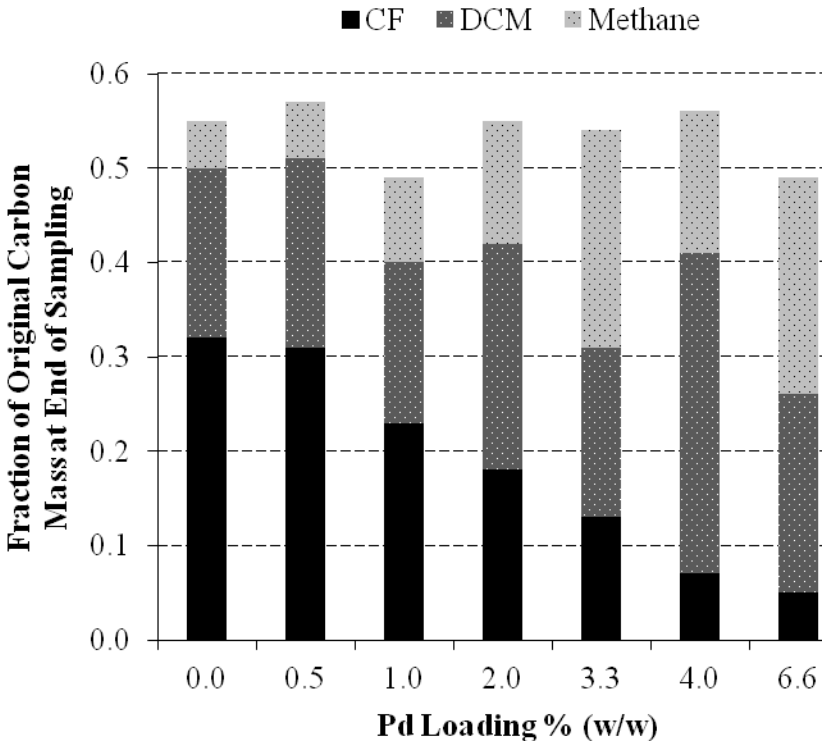

Figure 3.5. Degradation of CF at varying Pd loadings. [nZVI] = 0.1 g/L, [C_0] = 1.7 mg/L, [CMC] = 8 g/L, BH_4^- : Fe^{2+} molar ratio = 6:1, pH = 7, and the sampling period lasted 1.6 hrs.

Three studies have previously investigated the use of Pd-nZVI for degradation of chlorinated methanes, including CT, CF, and DCM [29,41,42]. In each case, the presence of Pd significantly improved degradation. Two further studies sought to optimize Pd loading [41,42]. In contrast to the results presented here, Wang et al. (2009) observed dramatic improvement in removal efficiencies of CT, CF, and DCM as Pd loading increased to 0.2%, followed by a gradual decrease in reactivity as it was further increased to as high as 3.0% [42]. The decrease in efficiency above 0.2% was attributed to hindrance of reactive surface sites, although higher Pd loadings may also hasten side hydrolysis reactions and the formation of passivating oxide layers [43]. However, Chun et al. (2010) reported that for CT degradation, a Pd loading of 3.8% outperformed loadings of 0.84% and 2.10% by 190% and 155%, respectively [41]. This agrees

well with Figures 3.4 and 3.5. Differences in the optimal Pd loading between studies may be the result of different nZVI synthesis methods [41]. They may also reflect inefficiencies in the Pd doping process, and an opportunity to more efficiently use this precious metal.

The optimized nZVI system, at 8 g/L CMC and 3.3% Pd loading, has a mass-normalized decay rate constant, k_m, of 1.73E+03 L/g/hr for CT, which is much more reactive than previously reported preparations. Compared to non-catalyzed nZVI, it is 55 to 93,000 times more reactive on a mass-normalized basis. Compared to other Pd-nZVI systems, it is 328 to 9,350 times more reactive. A detailed comparison to past studies may be found in the Supporting Information. It is important to note that, although these increases in performance seem impressive, they cannot be solely attributed to the CMC-stabilization and Pd-catalyzation of the nZVI. Many differences also exist between nanoparticle synthesis and handling, iron loading, and pH, all of which play an important role in determining reactivity [1,44].

Chlorinated Methane Degradation Pathways.

A major concern associated with reductive degradation of chlorinated methanes is the production of still-toxic byproducts. As successive dehalogenation of chlorinated methanes occurs, less chlorinated byproducts degrade even more slowly, with degradation rates of CT>CF>>DCM [12,29,41,45-47]. Two studies have proposed similar degradation pathways for the dehalogenation of CT and CF by zero-valent iron [12,47]. The first step involves reductive elimination of one chlorine to produce a trichloromethyl radical, after which the pathways branch. If hydrogenation occurs to replace the chlorine, CF is formed, which may further degrade to DCM [12,47]. In this study, CF was a major byproduct of CT degradation under all conditions, accounting for as much as 81% of original carbon mass. DCM was also observed as a byproduct of both CT and CF degradation, accounting for as much as 9% and 34% of original

carbon mass, respectively. The majority of studies report DCM as a final product; however, it is possible that DCM will further reduce to methane in the presence of a catalyst or biotic activity [12,29,41,47]. Experiments with DCM as the target contaminant indicate it degrades very slowly or not at all in the presence of CMC-stabilized Pd-nZVI (see Supporting Information). Methane formed during degradation is therefore the result of alternative pathways. For chlorinated methane degradation experiments, not all of the original carbon mass could be accounted for by CT, CF, DCM, PCE, and methane. The remaining 15% to 63% was likely degraded to carbon monoxide, formic acid, and long-chain aliphatic hydrocarbons not detected by the analytical methods used here [12,47].

If, rather than being hydrogenated, the trichloromethyl radical again undergoes reductive dechlorination, dichlorocarbene will form [12,47]. Normally, the degradation products of this pathway include relatively non-toxic formic acid, carbon monoxide, hydrochloric acid, and methane [47]. However, PCE, a carcinogenic chlorinated ethene, was also observed to form under all CT degradation conditions. PCE production was only reported in one other study of CT degradation by nZVI, and it occurred at trace concentrations near the detection limit of the researchers' GC/MS [47]. As shown in Figure 3.4b, the production of significant amounts of PCE, accounting for as much as 20% of original carbon, indicates dimerization of single-carbon species to double-bonded, two-carbon ethene species along CT degradation pathways. Dimerzation of trichloromethyl and dichloromethyl radicals was previously proposed [47]. Dimerization of dichlorocarbene molecules may also occur [12]. The presence of trace amounts of ethane byproduct during CF degradation suggests that dimerization may also occur along CF degradation pathways. However, the small amounts of ethane observed here suggest that for Pd-

nZVI the dimerization of dichloromethyl radicals, as proposed by Feng and Lim (2005), or dichlorocarbene molecules is a minor pathway [47].

Chlorinated Ethene Degradation.

To further investigate the effect of Pd catalyzation on nZVI performance, the optimized nZVI system was also tested with two widely studied chlorinated ethenes, PCE and TCE. As shown in Figure 3.6, Pd-nZVI was much more reactive toward both contaminants compared to non-catalyzed nZVI. For PCE, although the difference in reactivity could not be accurately quantified due to a poor model fit to the non-catalyzed data, removal efficiency improved several times, yielding a mass-normalized decay rate constant of 1.32E+02 L/g/hr. This is more than 4 times higher than a previously reported rate for PCE degradation by CMC stabilized Pd-nZVI, where a lower CMC concentration and Pd loading was used [22]. TCE byproduct formation was minimal at less than 3%. Greater PCE degradation by Pd-nZVI was partially accounted for by increased ethane yield.

For TCE, the addition of Pd improved reactivity by 486%, yielding a mass-normalized decay rate constant of 1.40E+03 L/g/hr. This is between 19 and 127 times higher than previously reported rates for TCE degradation by CMC stabilized Pd-nZVI, where lower CMC concentrations and Pd loadings were used [11,22,26]. However, differences in initial contaminant concentration, nZVI loading, and pH exist between the studies. No chlorinated byproducts were formed and 100% of the original carbon mass was accounted for as relatively non-toxic ethane and ethene gas. Detailed mass balance graphs may be found in the Supporting Information.

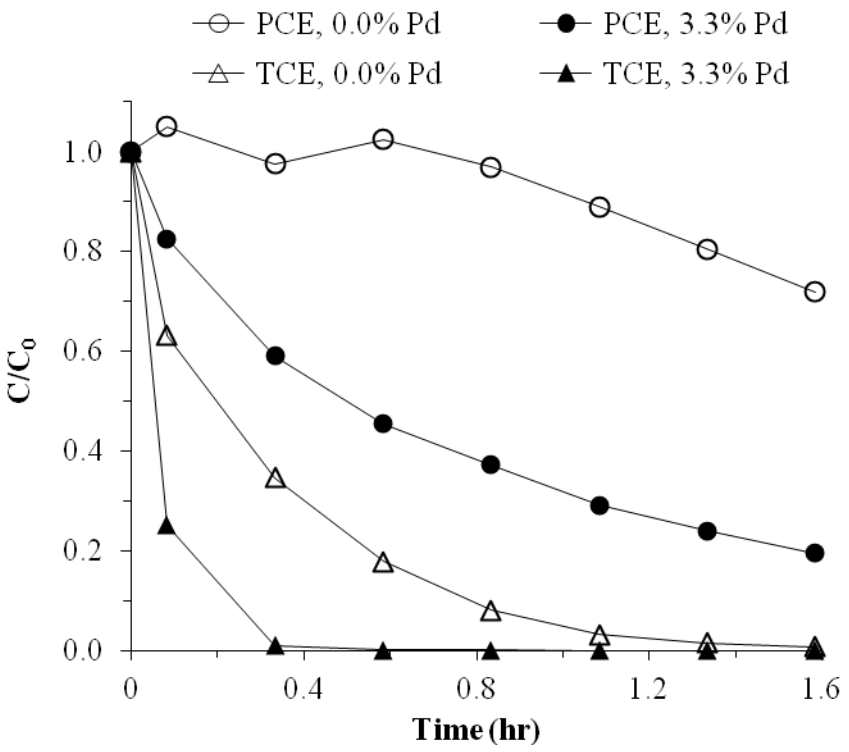

Figure 3.6. Degradation of PCE & TCE w/ and w/o Pd. [nZVI] = 0.1 g/L, [$C_{0,PCE}$] = 1.8 mg/L, [$C_{0,TCE}$] = 1.5 mg/L, [CMC] = 8 g/L, and BH_4^- : Fe^{2+} molar ratio = 6:1, pH = 7. Lines are intended to guide the eye and do not represent model fits.

Similar improvements in the degradation of PCE and TCE by Pd catalyzation were previously reported [10,11,17,22,48]. For PCE, addition of Pd to non-stabilized nZVI improved degradation by about 8 times [48]. Although CMC-stabilized Pd-nZVI was previously tested with PCE, this is the first time the difference between it and non-catalyzed CMC-nZVI has been explicitly demonstrated [22]. Past reports of chlorinated byproduct formation during Pd-nZVI degradation of PCE are mixed. One study reported TCE yields as high as 15% while others saw none [10,22,48]. For TCE, additions of Pd between 0.1% and 1.0% increased reactivity between 4 and 70 times. Previous studies also found that no chlorinated byproducts, such as dichloroethene (DCE) and vinyl chloride (VC), persist in the presence of Pd-nZVI [17,22,48].

Implications for In Situ Remediation.

Based on the current state of the technology, nZVI appears to be too expensive for mainstream use as a remediation tool [1,49]. Increasing the reactivity of nZVI toward chlorinated contaminants and improving its transport characteristics makes it a more viable, cost-effective option for remediation of contaminated groundwater. As shown, increased reactivity can be achieved by adjusting the quantities of $NaBH_4$ reductant, CMC stabilizer, and Pd catalyst during nZVI synthesis. CMC stabilization also significantly reduces interparticle aggregation and particle size. Pd catalyst amendment minimizes the generation of more recalcitrant, still-toxic chlorinated byproducts during degradation, a factor essential to the utility of nZVI. As Pd-nZVI is developed for large-scale field use, it is important to understand the trade-offs between improved performance and catalyst cost.

Acknowledgements

We appreciate the Air Force Institute of Technology Faculty Research Council for their generous funding of research. We also recognize the Naval Facilities Engineering Service Center for their sponsorship of research. We thank Elizabeth Maurer of the Air Force's 711th Human Performance Wing for her help performing DLS analysis. Also, thanks go to Barbara Miller of the University of Dayton's Nanoscale Engineering Science & Technology (NEST) laboratory for conducting TEM imaging.

Supporting Information Available

The Supporting Information contains mass balances, model fitting, and quantitative summaries for each degradation experiment presented here. It also includes GC analysis details,

CMC viscosity measurements, and comparisons to previously reported CT degradation rates.

This information is available free of charge via the Internet at http://pubs.acs.org.

Literature Cited

[1] Crane, R.A.; Scott, T.B. Nanoscale zero-valent iron: Future prospects for an emerging water treatment technology. *J. Hazard. Mater.* [Online early access]. DOI: 10.1016/j.jhazmat.2011.11.073. Published online: Nov 28, 2011. http://www.sciencedirect.com/science/article/pii/S0304389411014531 (accessed Feb 6, 2012) (accepted manuscript, article in press).

[2] Quinn, J.; et al. Use of nanoscale iron and bimetallic particles for environmental remediation: A review of field-scale applications. In *Environmental Applications of Nanoscale and Microscale Reactive Metal Particles*; Geiger, C. L., Carvalho-Knighton, K. M., Eds.; American Chemical Society: Washington DC 2009; pp 263.

[3] *The Quality of Our Nation's Waters: Volatile Organic Compounds in the Nation's Ground Water and Drinking-Water Supply Wells*; Circular 1292; United States Geological Survey: Reston, VA, 2006; pubs.usgs.gov/circ/circ1292.

[4] Phenrat, T.; Saleh, N; Sirk, K.; Kim, H.; Tilton, R.; Lowry, G. Stabilization of aqueous nanoscale zerovalent iron dispersions by anionic polyelectrolytes: Adsorbed anionic polyelectrolyte layer properties and their effect on aggregation and sedimentation. *J. Nanopart. Res.* **2008**, 10, 795-814.

[5] Petosa, A.R.; Jaisi, D.P.; Quevedo, I.R.; Elimelech, M.; Tufenkji, N. Aggregation and deposition of engineered nanomaterials in aquatic environments: Role of physiochemical interactions. *Environ. Sci. Technol.* **2010**, 44, 6532-6549.

[6] Schrick, B.; Hydutsky, B.W.; Blough, J.L.; Mallouk, T.E. Delivery vehicles for zerovalent metal nanoparticles in soil and groundwater. *Chem. Mater.* **2004**, 16, 2187-2193.

[7] He, F.; Zhao, D. Preparation and characterization of a new class of starch-stabilized bimetallic nanoparticles for degradation of chlorinated hydrocarbons in water. *Environ. Sci. Technol.* **2005**, 39, 3314-3320.

[8] Rivero-Huguet, M.; Marshall, W.D. Reduction of hexavalent chromium mediated by micro- and nano-sized mixed metallic particles. *J. Hazard. Mater.* **2009**, 169, 1081-1087.

[9] Zhou, T.; Li, Y.; Lim, T.T. Catalytic hydrodechlorination of chlorophenols by Pd/Fe nanoparticles: Comparisons with other bimetallic systems, kinetics and mechanism. *Sep. Purif. Technol.* **2010**, 76, 206-214.

[10] Lien, H.L.; Zhang, W.X. Nanoscale Pd/Fe bimetallic particles: Catalytic effects of palladium on hydrodechlorination. *Appl. Catal., B.* **2007**, 77, 110-116.

[11] He, F.; Zhao, D. Hydrodechlorination of trichloroethene using stabilized Fe-Pd nanoparticles: Reaction mechanism and effects of stabilizers, catalysts, and reaction conditions. *Appl. Catal, B.* **2008**, 84, 533-540.

[12] Song, H.; Carraway, E.R. Reduction of chlorinated methanes by nano-sized zero-valent iron—kinetics, pathways, and effect of reaction conditions. *Environ. Eng. Sci.* **2006**, 23, 272-284.

[13] Arnold, W. W.; Roberts, L. Pathways and kinetics of chlorinated ethylene and chlorinated acetylene reaction with Fe(0) particles. *Environ. Sci. Technol*. **2000**, 34, 1794-1805.

[14] Song, H.; Carraway, E.R. Reduction of chlorinated ethanes by nanosized zero-valent iron: Kinetics, pathways, and effects of reaction conditions. *Environ. Sci. Technol.* **2005**, 39, 6237-6245.

[15] Liu, Y.; Phenrat, T.; Lowry, G.V. Effect of TCE concentration and dissolved groundwater solutes on nZVI-promoted TCE dechlorination and H_2 evolution. *Environ. Sci. Technol.* **2007**, 41, 7881-7887.

[16] Borda, M. J.; et al. Status of nZVI technology: lessons learned from North American and international implementations. In *Environmental Applications of Nanoscale and Microscale Reactive Metal Particles*; Geiger, C. L., Carvalho-Knighton, K. M., Eds.; American Chemical Society: Washington DC 2009; pp 219.

[17] Wang, C.B.; Zhang, W.X. Synthesizing Nanoscale Iron particles for rapid and complete dechlorination of TCE and PCBs. *Environ. Sci. Technol.* **1997**, 31, 2154-2156.

[18] Elliott, D. W.; Zhang, W. Field assessment of nanoscale bimetallic particles for groundwater treatment. *Environ. Sci. Technol.* **2001**, 35, 4922-4926.

[19] He, F.; Zhao, D.; Paul, C. Field assessment of carboxymethyl cellulose stabilized iron nanoparticles for in situ destruction of chlorinated solvents in source zones. *Water Res.* **2010**, 44, 2360-2370.

[20] Shen, J.; Li, Z.; Yan, Q.; Chen, Y. Reactions of bivalent metal ions with borohydride in aqueous solution for the preparation of ultrafine amorphous alloy particles. *J. Phys. Chem*. **1993**, 97, 8504-8511.

[21] Glavee, G.N.; Klabunde, K.J.; Sorensen, C.M.; Hadjipanayis, G.C. Chemistry of borohydride reduction of iron(II) and iron(III) ions in aqueous and nonaqueous media—formation of nanoscale Fe, FeB, and Fe_2B powders. *Inorg. Chem*. **1995**, 34, 28-35.

[22] Cho, Y.; Choi, S.; Degradation of PCE, TCE, and 1,1,1-TCA by nanosized FePd bimetallic particles under various experimental conditions. *Chemospere*. **2010**, 81, 940-945.

[23] Dong, T.; Luo, H.; Wang, Y.; Hu, B.; Chen, H. Stabilization of Fe-Pd bimetallic nanoparticles with sodium carboxymethyl cellulose for catalytic reduction of para-nitrochlorobenzene in water. *Desalination*. **2011**, 271, 11-19.

[24] Sakulchaicharoen, N.; O'Carroll, D.M.; Herrera, J.E. Enhanced stability and dechlorination activity of pre-synthesis stabilized nanoscale FePd particles. *J. Contam. Hydrol*. **2010**, 118, 117-127.

[25] He, F.; Zhao, D. Manipulating the size and dispersibility of zerovalent iron nanoparticles by use of carboxymethyl cellulose stabilizers. *Environ. Sci. Technol.* **2007**, 41, 6216-6221.

[26] He, F.; Zhao, D.; Liu, J.; Roberts, C.B. Stabilization of Fe-Pd nanoparticles with sodium carboxymethyl cellulose for enhanced transport and dechlorination of trichloroethylene in soil and groundwater. *Ind. Eng. Chem. Res.* **2007**, 46, 29-34.

[27] He, F.; Zhang, M.; Qian, T.; Zhao, D. Transport of carboxymethyl cellulose stabilized iron nanoparticles in porous media: Column experiments and modeling. *J. Colloid. Interface Sci.* **2009**, 334, 96-102.

[28] Zhang, M.; He, F.; Zhao, D.; Hao, X. Degradation of soil-sorbed trichloroethylene by stabilized zero valent iron nanoparticles: Effects of sorption, surfactants, and natural organic matter. *Water Res.* **2011**, 45, 2401-2414.

[29] Lien, H.L; Zhang, W. Transformation of chlorinated methanes by nanoscale iron particles. *J. Environ. Eng.* **1999**, 125, 1042-1047.

[30] Lien, H.L.; Zhang, W.X. Transformation of chlorinated methanes by nanoscale iron particles. *J. Environ. Eng.* **1999**, 125, 1042-1047.

[31] Lien, H.L.; Zhang, W.X. Hydrodechlorination of chlorinated ethanes by nanoscale Pd/Fe bimetallic particles. *J. Environ. Eng.* **2005**, 131, 4-10.

[32] Raychoudhury, T.; Naja, G.; Ghoshal, S. Assessment of transport of two polyelectrolyte-stabilized zero-valent iron nanoparicles in porous media. *J. Contam. Hydrol.* **2010**, 118, 143-151.

[33] Cirtiu, C.M.; Raychoudhury, T.; Ghoshal, S.; Moores, A. Systematic comparison of the size, surface characteristics and colloidal stability of zero valent iron nanoparticles pre- and post-grafted with common polymers. *Colloids Surf., A.* **2011**, 390, 95-104.

[34] Xiong, Z.; Zhao, D.; Pan, G. Rapid and complete destruction of perchlorate in water and ion-exchange brine using stabilized zero-valent iron nanoparticles. *Water Res.* **2007**, 41, 3497-3505.

[35] Wang, Q.; Qian, H.; Yang, Y.; Zhang, Z.; Naman, C.; Xu, X. Reduction of hexavalent chromium by carboxymethyl cellulose-stabilized zero-valent iron nanoparticles. *J. Contam. Hydrol.* **2010**, 114, 35-42.

[36] Phenrat, T.; Liu, Y.; Tilton, R.D.; Lowry, G.V. Adsorbed polyelectrolyte coatings decrease Fe^0 nanoparticle reactivity with TCE in water: Conceptual model and mechanisms. *Environ. Sci. Technol.* **2009**, 43, 1507-1514.

[37] Ditsch, A.; Laibinis, P.E.; Wang, D.I.C.; Hatton, T.A. Controlled clustering and enhanced stability of polymer-coated magnetic nanoparticles. *Langmuir.* **2005**, 21, 6006-6018.

[38] Shimmin, R.G.; Schoch, A.B.; Braun, P.V. Polymer size and concentration effects on the size of gold nanoparticles capped by polymeric thiols. *Langmuir.* **2004**, 20, 5613-5620.

[39] Sun, Y.P.; Li, X.Q.; Zhang, W.X.; Wang, H.P. A method for the preparation of stable dispersion of zero-valent iron nanoparticles. *Colloids Surf., A.* **2007**, 308, 60-66.

[40] Li, T.; Farrell, J. Electrochemical investigation of the rate-limiting mechanisms for trichloroethylene and carbon tetrachloride reduction at iron surfaces. *Environ. Sci. Technol.* **2001**, 35, 3560-3565.

[41] Chun, C.L.; Baer, D.R.; Matson, D.W.; Amonette, J.E.; Penn, R.L. Characterization and reactivity of iron nanoparticles prepared with added Cu, Pd, and Ni. *Environ. Sci. Technol.* **2010**, 44, 5079-5085.

[42] Wang, X.; Chen, C.; Chang, Y.; Huiling, L. Dechlorination of chlorinated methanes by Pd/Fe bimetallic nanoparticles. *J. Hazard. Mater.* **2009**, 161, 815-823.

[43] Yan, W.; Herzing, X.Q.; Kiely, C.J.; Zhang, W.X. Structural evolution of Pd-doped nanoscale zero-valent iron (nZVI) in aqueous media and implications for particle aging and reactivity. *Environ. Sci. Technol.* **2010**, 44, 4288-4294.

[44] Sarathy, V.; Tratnyek, P.G.; Nurmi, J.T.; Baer, D.R.; Amonette, J.E.; Chun, C.L.; Penn, R.L.; Reardon, E.J. Aging of iron nanoparticles in aqueous solution: Effects on structure and reactivity. *J. Phys. Chem. C*. **2008**, 112, 2286-2293.

[45] Matheson, L.J.; Tratnyek, P.G. Reductive dehalogenation of chlorinated methanes by iron metal. *Environ. Sci. Technol.* **1994**, 28, 2045-2053.

[46] Warren, K.D.; Arnold, R.G.; Bishop, T.L.; Lindholm, L.C.; Betterton, E.A. Kinetics and mechanisms of reductive dehalogenation of carbon tetrachloride using zero-valence metals. *J. Hazard. Mater.* **1995**, 41, 217-227.

[47] Feng, J.; Lim, T.T. Pathways and kinetics of carbon tetrachloride and chloroform reductions by nano-scale Fe and Fe/Ni particles: Comparison with commercial micro-scale Fe and Zn. *Chemosphere*. **2005**, 59, 1267-1277.

[48] Zhang, W.; Wang, C.B.; Lien, H.L. Treatment of chlorinated organic contaminants with nanoscale bimetallic particles. *Catal. Today.* **1998**, 40, 387-395.

[49] Li, X.; Elliott, D.W.; Zhang, W. Zero-valent iron nanoparticles for abatement of environmental pollutants: Materials and engineering aspects. *CRC Cr. Rev. Sol. State.* **2006**, 31, 111-122.

[50] Nurmi, J.T.; Tratnyek, P.G.; Sarathy, V.; Baer, D.R.; Amonette, J.E.; Pecher, K.; Wang, C.; Linehan, J.C.; Matson, D.W.; Penn, R.L.; Driessen, M.D. Characterization and properties of metallic iron nanoparticles: Spectroscopy, electrochemistry, and kinetics. *Environ. Sci. Technol.* **2005**, 39, 1221-1230.

[51] Zhang, X.; Deng, B.; Guo, J.; Wang, Y.; Yeqing, L. Ligand-assisted degradation of carbon tetrachloride by microscale zero-valent iron. *J. Environ. Manage.* **2011**, 92, 1328-1333.

IV. Conclusion

Chapter Overview

This concluding chapter discusses the research findings within the context of the research questions outlined in Chapter I, Introduction. The two scholarly articles communicate the most important findings of the critical literature review and laboratory research. However, restrictions on article length and content prohibit the inclusion of a more broad discussion of the findings. Here, one set of results not included in the research article is discussed, the research is briefly reviewed, and its significance is stated. Opportunities for future research, both those directly related to the research presented here and, more-broadly, those critical to the future development of nZVI technology, are discussed.

Effect of Increasing nZVI Loading on CF Degradation and Byproducts

An additional set of experiments was conducted to investigate the effect of increasing nZVI loading on CF degradation and byproduct formation at a fixed CMC concentration and Pd loading of 8.0 g/L and 3.3%, respectively (see Appendix B). As nZVI loading was increased from 0.01 to 0.10 g/L, the observed degradation rate increased as well. However, further increasing the nZVI loading to 0.20 g/L decreased both the observed and mass-normalized degradation rate. This result may be indicative of failure of the CMC stabilizer to prevent aggregation at higher nZVI loadings. However, this explanation is in disagreement with the previously stated hypothesis that absolute CMC concentration, not the ratio of CMC to nZVI, is a better indicator of stabilizer

performance and the observation by Cirtiu et al. (2011) that 5 g/L of CMC could stabilize as much as 1.0 g/L nZVI (see Chapter III). As discussed in Chapter II, an alternative explanation may be that CMC chelation of the higher Fe^{2+} concentrations used to synthesize nZVI at 0.2 g/L resulted in the formation of larger particles with relatively less reactive surface area.

Review of Findings

The four research questions presented in the introduction sought to clarify and investigate 1.) aspects of the nZVI synthesis process that might be optimized, 2.) how stabilizers might be optimized to improve reactivity while decreasing particle size and interparticle aggregation, 3.) how catalyst use might be optimized to improve reactivity and decrease the formation of toxic chlorinated organic byproducts, and 4.) the pathways and kinetics of chlorinated organic contaminant degradation by stabilized, catalyzed nZVI.

1.) nZVI synthesis process optimization for increased reactivity:

A review of the literature identified the borohydride-reduction method as the most commonly used nZVI synthesis method among laboratory and small-scale field studies. During initial efforts to synthesize nZVI using this method, it was observed that precipitation of the nanoparticles was slow to occur and often inconsistent between samples. Paired with the observations of other researchers that excess amounts of borohydride reductant hastened nZVI precipitation, the hypothesis that stoichiometric amounts of borohydride may be insufficient to completely reduce nZVI was proposed. Experimental results indicate that increasing the ratio of borohydride to ferrous iron

precursor from 2:1 to 6:1 increases reactivity by 72%. The failure of stoichiometric amounts of borohydride to completely reduce ferrous iron to nZVI was attributed to competing hydrolysis reactions.

2.) Stabilizer optimization for increased reactivity and improved transport:

A review of the literature indicates that polyelectrolyte stabilization of nZVI is clearly a highly successful and cost-effective way of improving nZVI reactivity, decreasing nanoparticle size and aggregation, and improving subsurface transport. Of the many polyelectrolytes used, CMC proved to be the most promising choice by most measures. Both through quantification of degradation kinetics and TEM imaging of the nanoparticles, it was demonstrated that addition of 8.0 g/L CMC to 0.01 g/L nZVI outperforms lower CMC loadings. Increasing CMC concentration from 0.5 to 8.0 g/L increased reactivity by 452%. CMC coatings were observed to establish interparticle electrosteric repulsion, drastically reducing aggregation. Furthermore, a comparison of the optimal CMC loading to previously reported values suggests that absolute CMC concentration, not CMC amount relative to nZVI loading, is a better predictor of stabilizer performance. This is accounted for by the role of polyelectrolytes in coordinating the formation of smaller, more numerous particles during initial synthesis.

3.) Catalyst optimization for increased reactivity and reduction of chlorinated byproduct formation:

A review of the literature indicates that Pd is clearly the most effective catalyst to be paired with nZVI, improving the degradation of a wide range of contaminants. While amendment of Pd to nZVI generally reduces the production of toxic byproducts, in many cases their presence is still reported. Based on the literature, it is clear that the formation

of hydrogen and its subsequent role in the hydrodechlorination of chlorinated organic contaminants is an important aspect of Pd-catalyzed nZVI degradation. Degradation experiments indicate that a Pd loading of 3.3% (w/w) is optimal, increasing reactivity by 375% while decreasing chlorinated byproduct formation. These findings contrast with the majority of previously reported studies, which indicate that optimal Pd loading is between 0.2% and 1.0%, although one other study also found that a Pd loading above 3.0% was optimal [1:5081].

4.) Chemical pathways and rates of degradation:

In most cases, contaminant degradation was well-modeled by pseudo-first order kinetics. Exceptions to this were CF and PCE, which exhibited sorption and slow partitioning to the reactor headspace, respectively. However, for CF, portions of these degradation curves could still be fit with the pseudo-first order model to quantify reactivity. Also, for each parent compound, degradation byproducts detectable by our analytical methods were reported, but detailed chemical degradation pathways were only presented for CT and CF. Significant portions of CT degraded to CF, DCM, and methane. PCE was, for the first time, also observed as a significant byproduct of CT degradation. The hypothesized pathway for PCE formation was dimerization of trichloromethyl radicals, dichloromethyl radicals, or dichlorocarbene intermediaries [3:1276; 8:281]. Trace amounts of ethane byproduct were also observed during CF degradation experiments. The small amount of ethane formed suggests that the dichloromethyl radical dimerization pathway proposed by Feng and Lim (2005) is only a minor pathway for degradation of CF by Pd-nZVI [3:1276]. During experiments with PCE as the parent contaminant, significant amounts of ethane and ethene formed, with minor amounts of

TCE present. 1,1,2-TCA was also formed during PCE degradation in the presence of Pd catalyzed nZVI, but not when PCE was degraded by non-catalyzed nZVI. During experiments with TCE as the parent contaminant, only ethane and ethene were formed, which accounted for 100% of the original contaminant mass.

Significance of Research

Because of widespread groundwater contamination at DOD sites and, more broadly, industrial and commercial sites across the U.S. and the world, there is a great need for more effective, less costly remediation options. nZVI holds promise to be one such tool. Broadly, it was shown that optimization of the nZVI synthesis process, stabilizer concentration, and catalyst loading can increase nZVI reactivity by many times. Relative to the 72% gain in reactivity achieved during synthesis optimization, the cost of additional borohydride is minimal, suggesting this may be one cost-effective way of producing more reactive nZVI. The 452% increase in reactivity observed during CMC concentration optimization indicates that this low-cost stabilizer is certainly worthwhile. For Pd loading optimization, the need to use relatively high amounts of Pd, at least 1.0% and as high as 3.3%, to achieve better degradation may make Pd catalyzation cost-prohibitive due to the high cost of Pd.

Future Research

Many opportunities for future research are identified in the critical review of literature; still others are raised by the findings of the research presented here. Generally, the most important areas for the future development of nZVI technology are:

- Transport of stabilized nZVI at realistic groundwater flowrates and nZVI loadings capable of significant contaminant remediation (i.e. > 1.0 g/L)
- The scalability of stabilizer and catalyst use to these higher nZVI loadings
- More thorough, controlled comparison of possible catalysts
- The toxicological effects of nZVI and its catalysts (i.e. nickel)
- Use of engineered copolymers to stabilize nZVI
- Schemes for nZVI targeting of NAPLs
- Promotion of *in situ* biodegradation following nZVI injection

Several questions specific to the research presented herein also remain unanswered. Although increasing the borohydride to ferrous iron precursor ratio to 6:1 increased nZVI reactivity considerably, it is unclear whether this result is scalable or if, at higher nZVI loadings, a lower ratio would be sufficient. It was suggested, as part of the optimal CMC concentration investigation, that absolute concentration is a better predictor of stabilizer performance than amount of CMC relative to nZVI loading. This remains untested, but would have implications for the scaling of CMC stabilizer use to nZVI loadings above 1.0 g/L. Finally, the reason for the disparity between optimal Pd loadings determined in this research and in the literature is unclear. Comparisons across different contaminants could rule out or confirm a contaminant-dependent effect, which would have important implications for the application of Pd-nZVI *in situ*. Also, detailed investigation of the Pd doping methodology and its effect on nanoparticle morphology and catalyst distribution might reveal more efficient ways to use this precious metal.

Summary

This thesis identified the most promising opportunities for improving nZVI utility and further investigated the optimization of nZVI synthesis, CMC polyelectrolyte stabilizer use, and Pd catalyst amendment. The purpose of this research was to identify and demonstrate cost-effective ways to increase nZVI reactivity while decreasing particle size and improving stability. The research methodology consisted of bench-scale contaminant degradation experiments under varying conditions, paired with physical characterization of nZVI samples by DLS analysis and TEM imaging. The critical literature review outlines the state-of-the-art while identifying research shortfalls and possible opportunities for future research. The research article illustrates the drastic improvements in nZVI utility attained by synthesis optimization, particle stabilization, and catalyzation. These largely cost-effective measures further develop nZVI toward being a viable remediation option with the potential for widespread implementation. Continued development of this technology may help protect human health and the environment while reducing remediation costs to the DOD and others.

Appendix A. Supporting Information to Accompany Research Article Submission

Analytical Methods: Detailed GC Column and Method Information

For experiments varying $NaBH_4$: Fe^{2+} molar ratio, CMC concentration, and Pd loading, injector and detector (μECD) temperatures were set at 250 °C and 300 °C, respectively. A 50:1 split was used with a helium carrier gas flowrate of 1 mL/min and a nitrogen makeup gas flowrate of 60 mL/min. For experiments varying $NaBH_4$: Fe^{2+} molar ratio and CMC concentration experiments, the GC was equipped with an HP-5MS capillary column (30 m long and 0.25 mm ID, Agilent Tech., Santa Clara, CA) and the oven temperature was fixed at 80 °C. For experiments varying Pd loading, the capillary column was updated to an Rxi®-624Sil MS (30 m long and 0.25 mm ID, Restek Co., Bellefonte, PA) and the oven temperature was fixed at 100 °C for better separation of daughter-product peaks. For all later experiments, which include gas (methane, ethane, and ethylene) analysis, a split was added to the injector, with the μECD still paired with the Rxi®-624Sil MS column and a FID paired with a GS-Gaspro column (15m long, 0.25 mm ID, J&W Scientific, Folsom, CA). For these later experiments a new method was used; injector and front detector (FID) temperatures were set at 250 °C. Back detector (μECD) temperature was set to 300 °C. A 50:1 split was used with a helium carrier gas flowrate of 1.8 mL/min and a nitrogen makeup gas flowrate of 60 mL/min on the μECD and 25 mL/min on the FID.

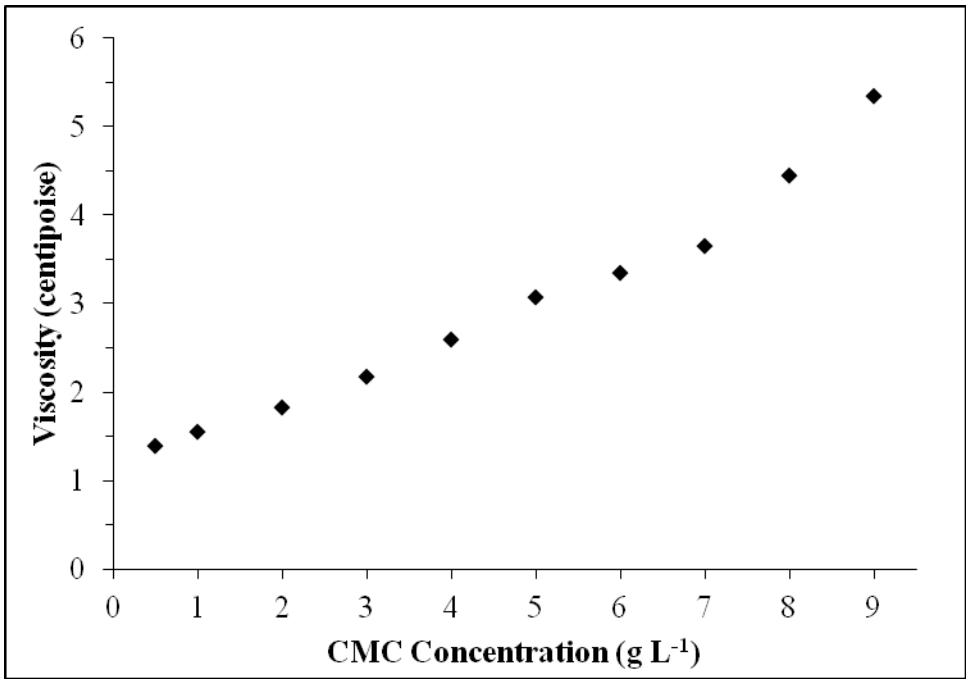

Figure A.1. CMC solution viscosity measurements.

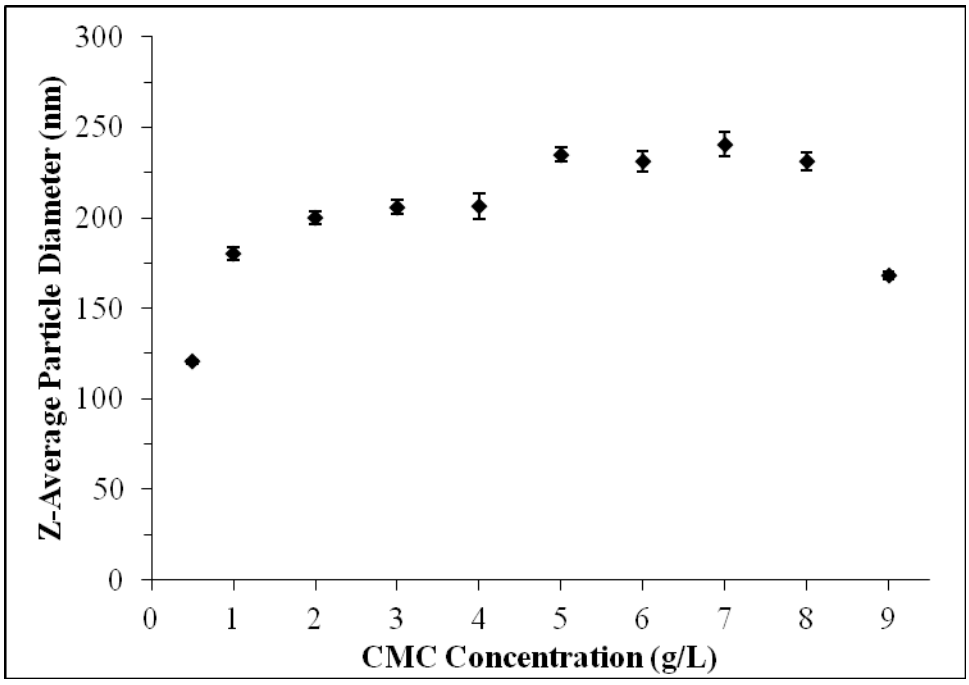

Figure A.2. DLS sizing data for nZVI at varying CMC loadings.

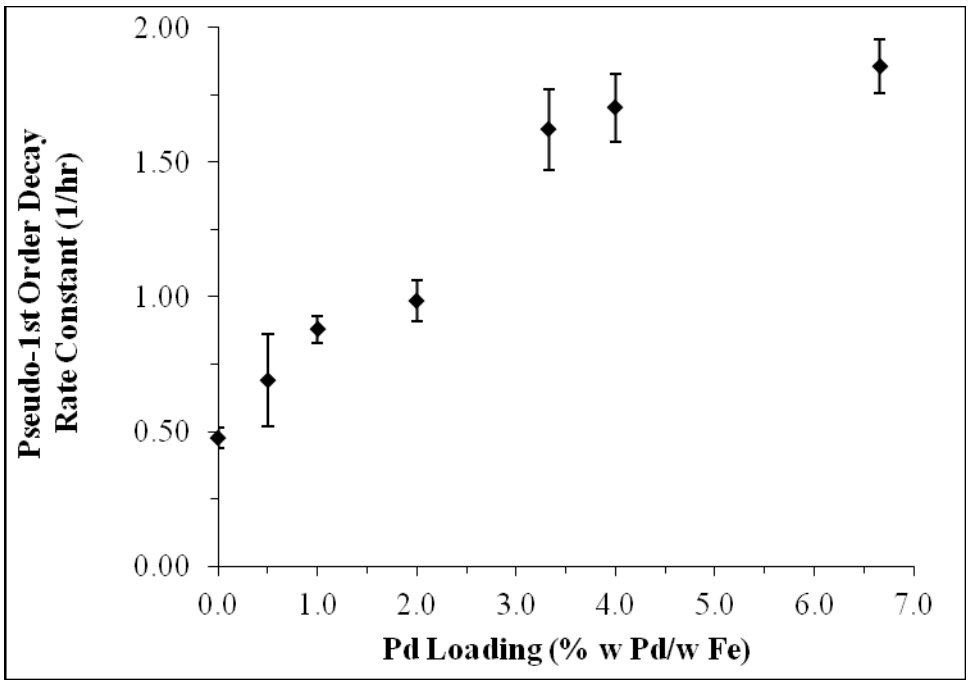

Figure A.3. Pd loading effect on nZVI reactivity toward CF.

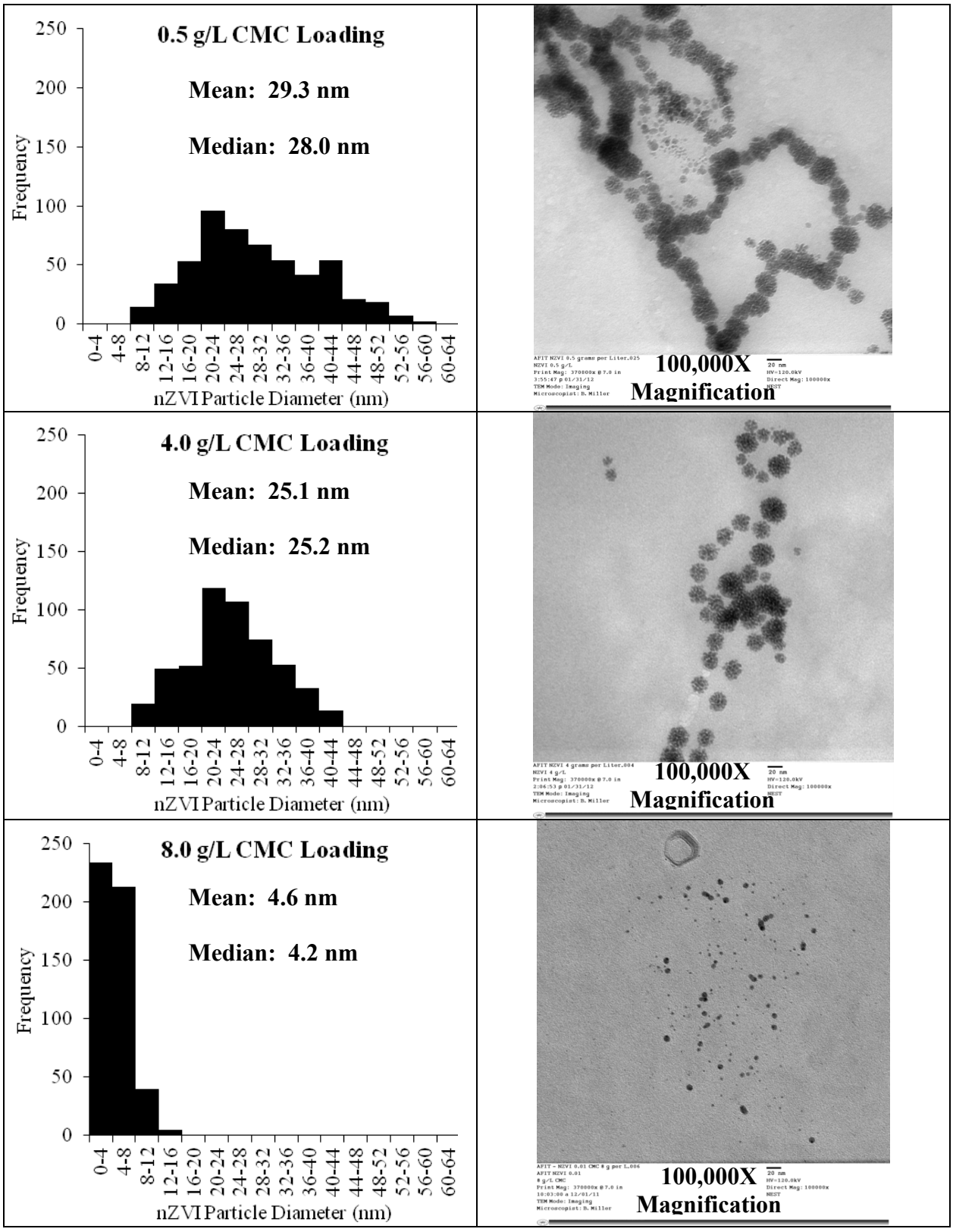

Figure A.4. Individual TEM sizing histograms and representative images.

Authors		Lien and Zhang [29]	Lien and Zhang [29]	Nurmi et al. [50]	Nurmi et al. [50]
Publication Year		1999	1999	2005	2005
Journal		J. Environ. Eng.	J. Environ. Eng.	Environ. Sci. Technol.	Environ. Sci. Technol.
Iron Synthesis	Iron Ionic State	Fe^{3+}	Fe^{3+}	Fe^{3+}	Fe^{3+}
	$NaBH_4$: Fe Mol. Ratio	5.55 : 1	5.55 : 1	5.55 : 1	5.55 : 1
Iron Loading	[g/L]	12.50	12.50	0.15	0.30
pH		Unbuffered	Unbuffered	Variable	Variable
Surface Modifier		None	None	None	None
Catalyst	Catalyst Type	None	Pd	None	None
	Loading [% w/w]		0.1%		
CT Loading	[mM]	0.100	0.103	0.004	0.004
Spec. Surface Area	[m^2/g]	35.00	35.00	33.50	33.50
k_{SA}	[L/h/m^2]	5.31E-04	9.00E-03	–	–
$k_{m, Fe}$	[L/g/hr]	1.86E-02	3.15E-01	1.8E+00 to 1.14E+01	1.8E+00 to 1.14E+01
k_{obs}	[1/h]	2.32E-01	3.94E+00	–	–
CF Yield	% Original Carbon	60%	10%	35-95%	35-95%
PCE Yield	% Original Carbon	–	~3% Ethane	–	–

Table A.1. Degradation of CT by nZVI literature review tables (1 of 4).

Authors		Song and Carraway [12]	Song and Carraway [12]	Sarathy et al. [44]	Sarathy et al. [44]
Publication Year		2006	2006	2008	2008
Journal		Environ. Eng. Sci.	Environ. Eng. Sci.	J. Phys. Chem.	J. Phys. Chem.
Iron Synthesis	Iron Ionic State	Fe^{3+}	Fe^{3+}	Commercial Powder	Commercial powder
	$NaBH_4$: Fe Mol. Ratio	3 : 1	3 : 1		
Iron Loading	[g/L]	0.16	0.16	0.83	1.25
pH		7.5	Unbuffered	Unbuffered	Unbuffered
Surface Modifier		None	None	None	None
Catalyst	Catalyst Type	None	None	None	None
	Loading [% w/w]				
CT Loading	[mM]	0.200	0.200	0.004	0.004
Spec. Surface Area	[m^2/g]	27.90	27.90	29.00	5.20
k_{SA}	[L/h/m^2]	1.12E+00	4.84E-01	–	–
$k_{m,\,Fe}$	[L/g/hr]	3.14E+01	1.35E+01	1.00E-01 to 4.00E+00	1.00E-01 to 4.00E+00
k_{obs}	[1/h]	5.02E+00	2.16E+00	–	–
CF Yield	% Original Carbon	70%	–	25-62%	25-62%
PCE Yield	% Original Carbon	–	–	–	–

Table A.1. Degradation of CT by nZVI literature review tables (2 of 4).

Authors		Feng and Lim [47]	Feng and Lim [47]	Feng and Lim [47]	Chun et al. [41]	Chun et al. [41]
Publication Year		2005	2005	2005	2010	2010
Journal		Chemo-sphere	Chemo-sphere	Chemo-sphere	Environ. Sci. Technol.	Environ. Sci. Technol.
Iron Synthesis	Iron Ionic State	Fe^{2+}	Fe^{2+}	Commercial Powder	Hydrogen Reduction	Hydrogen Reduction
	$NaBH_4$: Fe Mol. Ratio	2.80 : 1	3.59 : 1			
Iron Loading	[g/L]	2.50	2.50	125.00	1.21	1.21
pH		Unbuffered	Unbuffered	Unbuffered	7.5	7.5
Surface Modifier		None	None	None	None	None
Catalyst	Catalyst Type	Ni	None	None	None	Pd
	Loading [% w/w]	25.0%				3.8%
CT Loading	[mM]	0.130	0.130	0.130	0.100	0.100
Spec. Surface Area	[m^2/g]	39.17	26.45	1.32	–	–
k_{SA}	[$L/h/m^2$]	9.22E-02	5.99E-02	6.97E-03	–	–
$k_{m, Fe}$	[L/g/hr]	3.61E+00	1.58E+00	9.20E-03	2.17E+00	5.28E+00
k_{obs}	[1/h]	9.03E+00	3.96E+00	1.15E+00	2.62E+00	6.39E+00
CF Yield	% Original Carbon	5%	80%	5%	36%	25%
PCE Yield	% Original Carbon	Trace	Trace	Trace	–	–

Table A.1. Degradation of CT by nZVI literature review tables (3 of 4).

Authors		Wang et al. [42]	Zhang et al. [51]	Zhang et al. [51]	**This Study**	**This Study**
Publication Year		2009	2011	2011	–	–
Journal		J. Hazard. Mater.	J. Environ. Manage.	J. Environ. Manage.	–	–
Iron Synthesis	Iron Ionic State	Fe^{3+}	Microscale Powder	Microscale Powder	**Fe^{2+}**	**Fe^{2+}**
	$NaBH_4$: Fe Mol. Ratio	Not Given			**6 : 1**	**6 : 1**
Iron Loading	[g/L]	10.00	5.00	5.00	**0.01**	**0.01**
pH		7, Unbuff.	3.5,Unbuff.	3.5, Unbuff.	**7.0**	**7.0**
Surface Modifier		None	None	EDTA	**CMC, 8 g/L**	**CMC, 8 g/L**
Catalyst	Catalyst Type	Pd	None	None	**None**	**Pd**
	Loading [% w/w]	0.2%				**3.3%**
CT Loading	[mM]	0.650	0.130	0.130	**0.010**	**0.010**
Spec. Surface Area	[m^2/g]	51.40	0.22	0.22	–	–
k_{SA}	[$L/h/m^2$]	3.60E-03	–	–	–	–
$k_{m, Fe}$	[L/g/hr]	1.85E-01	4.34E-03	1.69E-01	**4.31E+02**	**1.73E+03**
k_{obs}	[1/h]	1.85E+00	2.17E-02	8.43E-01	**4.31E+00**	**1.73E+01**
CF Yield	% Original Carbon	–	–	–	**68%**	**59%**
PCE Yield	% Original Carbon	–	–	–	**6% at Max, 0% Final**	**18% at Max, 0% Final**

Table A.1. Degradation of CT by nZVI literature review tables (4 of 4).

Table A.2. $NaBH_4$: Fe^{2+} molar ratio experiments, 0.01 g/L nZVI loading, CT (1 of 3).

Group #1: Varying $NaBH_4$: $FeSO_4$ Molar Ratio				k_{obs}	$k_{average}$	k_m	Std.	Fraction Original Carbon Mass at End of Sampling						
Experimental Conditions		#	Condition	(1/hr)	(1/hr)	(L/g/hr)	Dev.	CT	CF	PCE	Methane	Ethane	Ethene	Total
$NaBH_4$: $FeSO_4$	Variable	1	2 : 1 $NaBH_4$: $FeSO_4$ Ratio	2.49	2.12	2.1E+02	0.33	0.04	0.76	No Data	No Data	No Data	No Data	**0.80**
				2.04										
nZVI Loading	0.01 g/L			1.84										
		2	3 : 1 $NaBH_4$: $FeSO_4$ Ratio	3.16	2.59	2.6E+02	0.49	0.02	0.81	No Data	No Data	No Data	No Data	**0.83**
pH	7			2.31										
				2.30										
TAPSO	7.81 mM	3	4 : 1 $NaBH_4$: $FeSO_4$ Ratio	3.04	2.86	2.9E+02	0.29	0.01	0.79	No Data	No Data	No Data	No Data	**0.80**
				3.01										
CMC	2 g/L			2.53										
		4	5 : 1 $NaBH_4$: $FeSO_4$ Ratio	3.47	3.53	3.5E+02	0.16	0.01	0.84	No Data	No Data	No Data	No Data	**0.85**
Pd Loading	None			3.71										
				3.41										
CAH of Study	CT	5	6 : 1 $NaBH_4$: $FeSO_4$ Ratio	3.89	3.65	3.6E+02	0.29	0.00	0.80	No Data	No Data	No Data	No Data	**0.80**
				3.73										
[Contaminant]	250 ppb			3.33										
		6	7 : 1 $NaBH_4$: $FeSO_4$ Ratio	3.67	3.51	3.5E+02	0.14	0.01	0.76	No Data	No Data	No Data	No Data	**0.77**
				3.44										
				3.41										

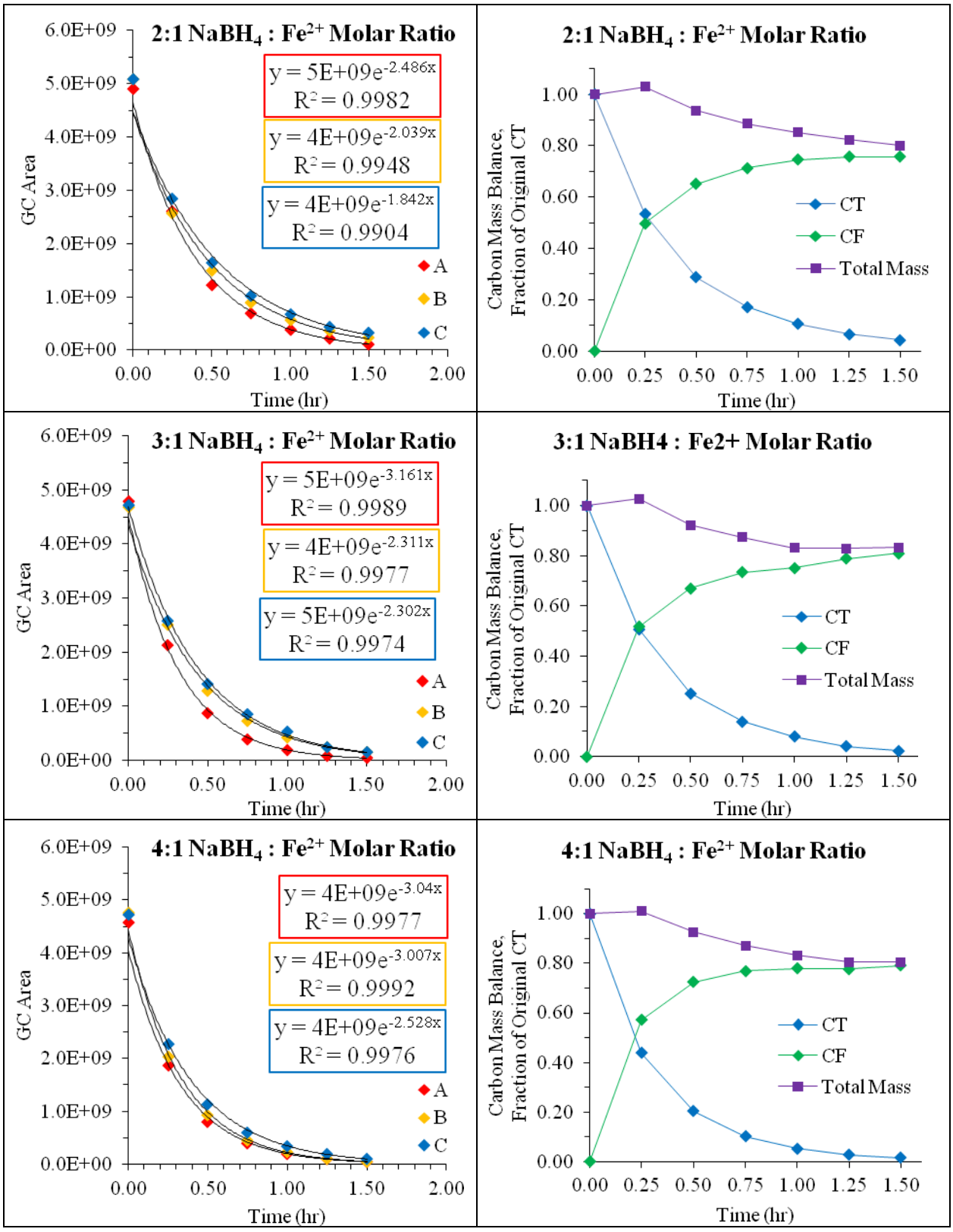

Table A.2. $NaBH_4$: Fe^{2+} molar ratio experiments, 0.01 g/L nZVI loading, CT (2 of 3).

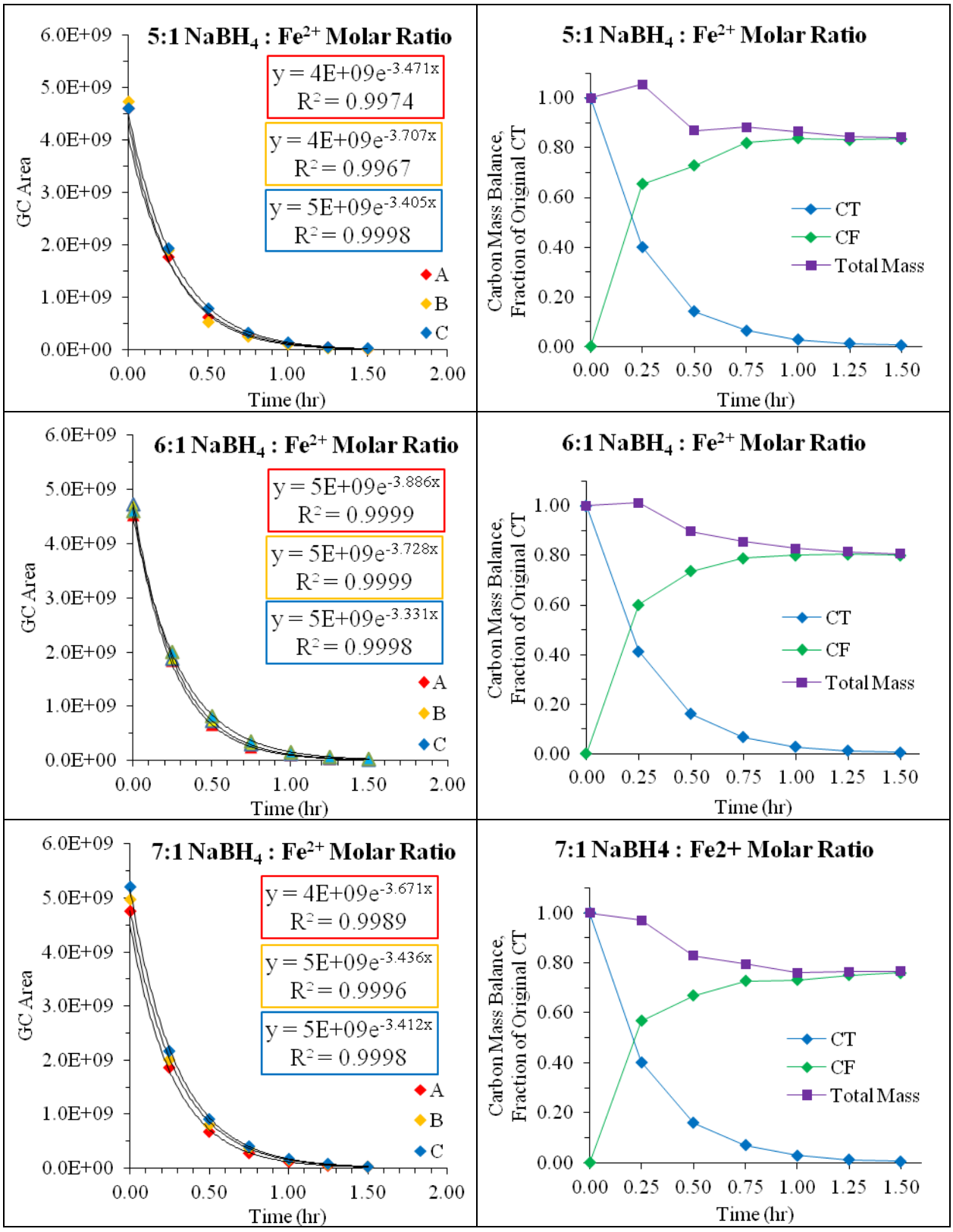

Table A.2. $NaBH_4$: Fe^{2+} molar ratio experiments, 0.01 g/L nZVI loading, CT (3 of 3).

Table A.3. CMC concentration experiments, 0.01 g/L nZVI loading, CT (1 of 5).

Group #2: Varying CMC Concentration				k_{obs}	$k_{average}$	k_m	Std.	Fraction Original Carbon Mass at End of Sampling						
Experimental Conditions		#	Condition	(1/hr)	(1/hr)	(L/g/hr)	Dev.	CT	CF	PCE	Methane	Ethane	Ethene	Total
$NaBH_4$: $FeSO_4$	6 : 1	7	0.5 g/L CMC	1.83	1.82	1.8E+02	0.08	0.06	0.71	No Data	No Data	No Data	No Data	**0.77**
				1.90										
nZVI Loading	0.01 g/L			1.73										
pH	7	8	1.0 g/L CMC	2.51	2.39	2.4E+02	0.11	0.03	0.77	0.04	No Data	No Data	No Data	**0.83**
				2.40										
TAPSO	7.81 mM			2.28										
		5	2.0 g/L CMC	3.89	3.65	3.6E+02	0.29	0.00	0.80	No Data	No Data	No Data	No Data	**0.80**
CMC	Variable			3.73										
				3.33										
Pd Loading	None	9	3.0 g/L CMC	4.83	4.67	4.7E+02	0.15	0.00	0.70	0.02	No Data	No Data	No Data	**0.72**
				4.65										
CAH of Study	CT			4.53										
		10	4.0 g/L CMC	5.52	5.47	5.5E+02	0.04	0.00	0.74	0.02	No Data	No Data	No Data	**0.76**
[Contaminant]	250 ppb			5.47										
				5.43										
		11	5.0 g/L CMC	6.64	6.73	6.7E+02	0.14	0.00	0.68	0.01	No Data	No Data	No Data	**0.69**
				6.67										
				6.89										
		12	6.0 g/L CMC	7.01	7.19	7.2E+02	0.16	0.00	0.64	0.01	No Data	No Data	No Data	**0.65**
				7.33										
				7.21										
		13	7.0 g/L CMC	7.02	7.18	7.2E+02	0.14	0.00	0.68	0.00	No Data	No Data	No Data	**0.68**
				7.27										
				7.25										
		14	8.0 g/L CMC	8.04	8.17	8.2E+02	0.14	0.00	0.73	0.01	No Data	No Data	No Data	**0.74**
				8.31										
				8.16										
		15	9.0 g/L CMC	7.87	8.23	8.2E+02	0.31	0.00	0.71	0.01	No Data	No Data	No Data	**0.72**
				8.41										
				8.41										

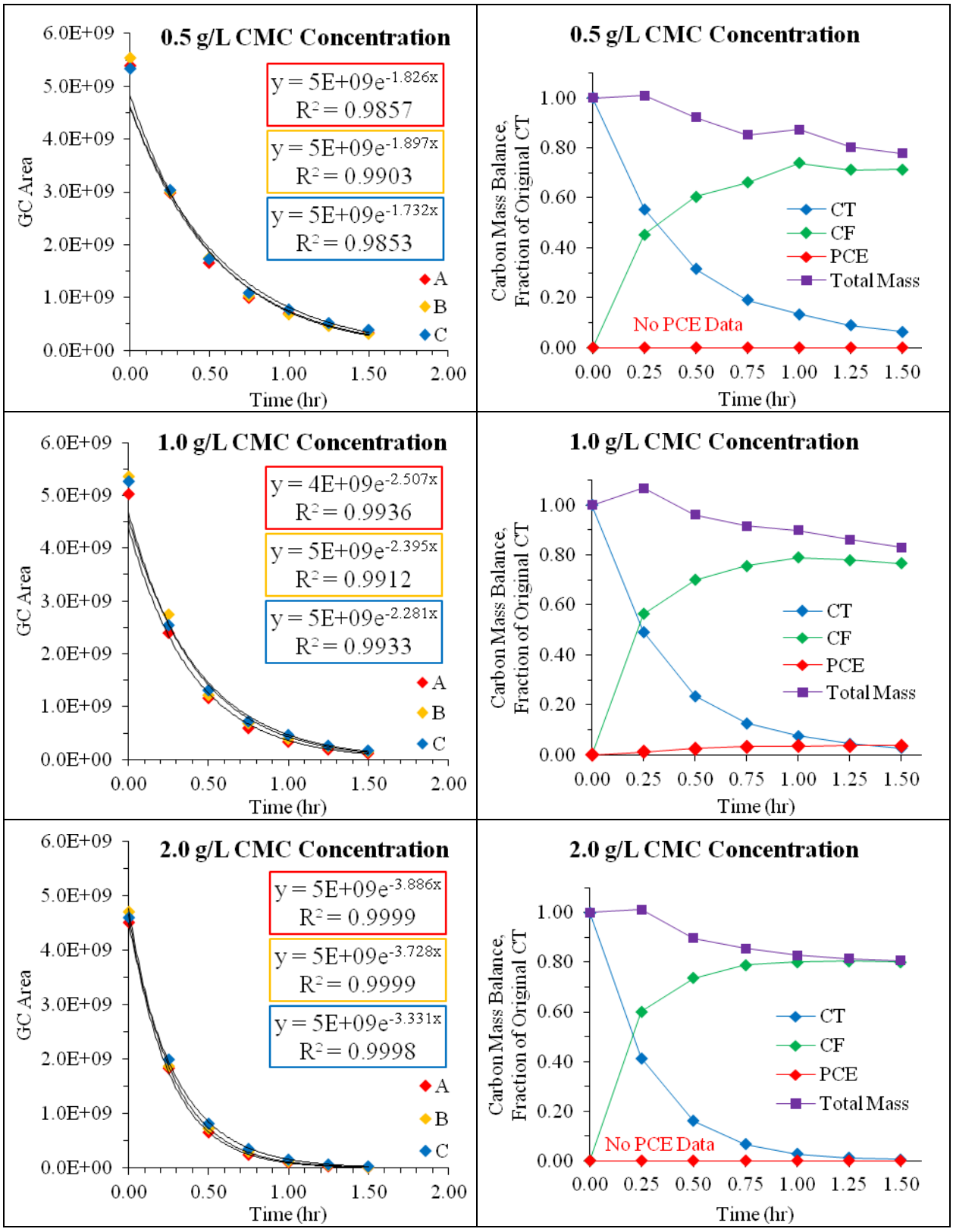

Table A.3. CMC concentration experiments, 0.01 g/L nZVI loading, CT (2 of 5).

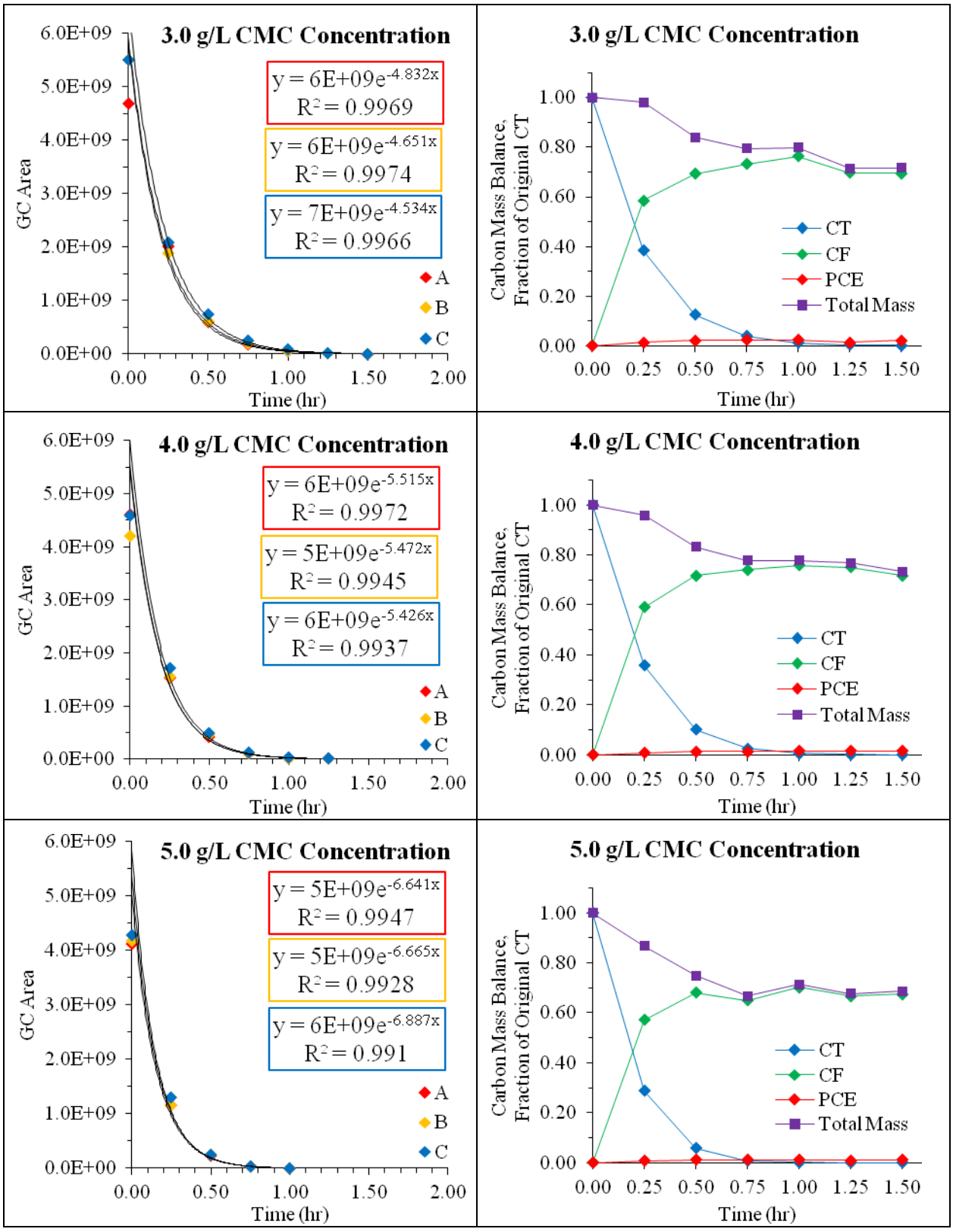

Table A.3. CMC concentration experiments, 0.01 g/L nZVI loading, CT (3 of 5).

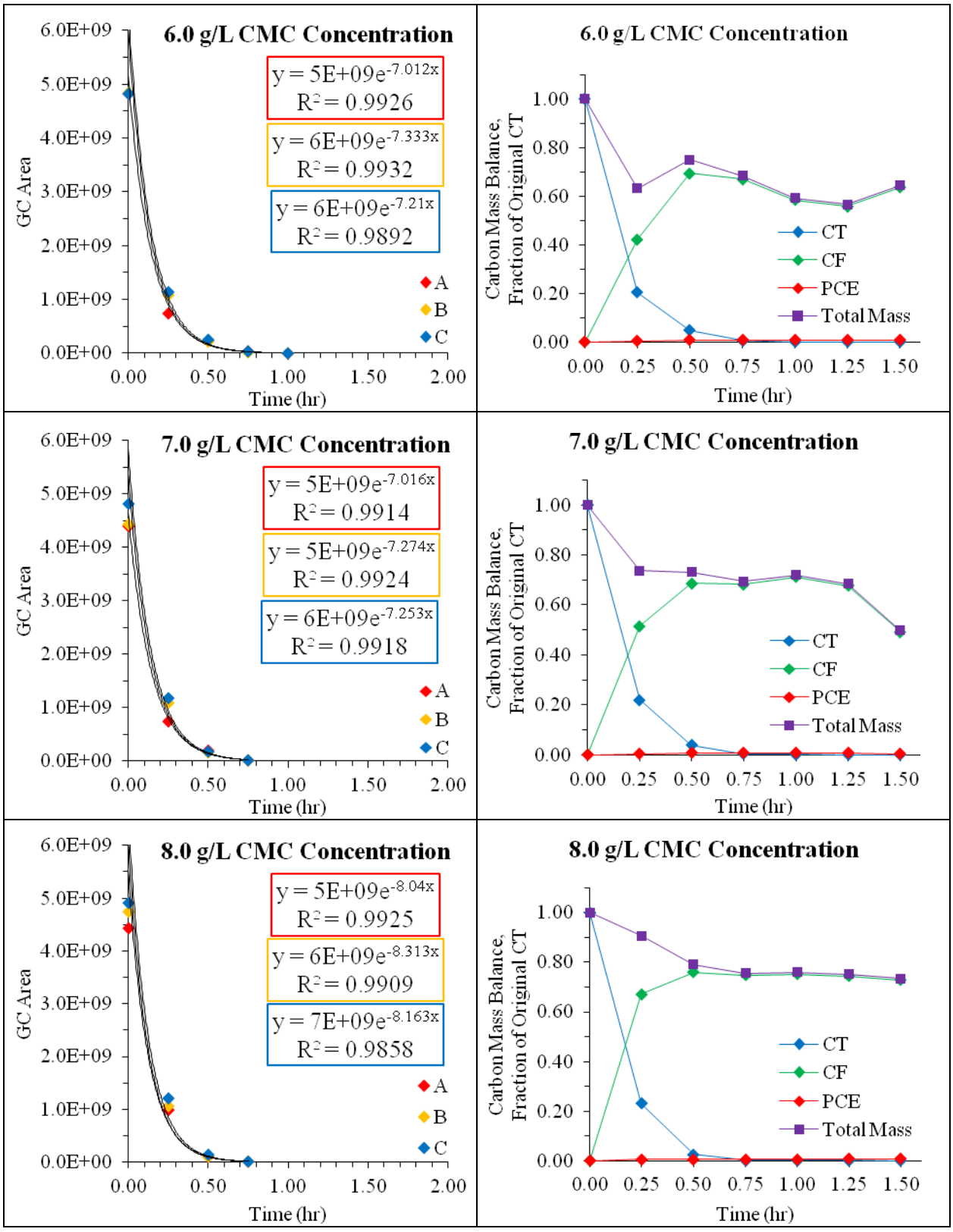

Table A.3. CMC concentration experiments, 0.01 g/L nZVI loading, CT (4 of 5).

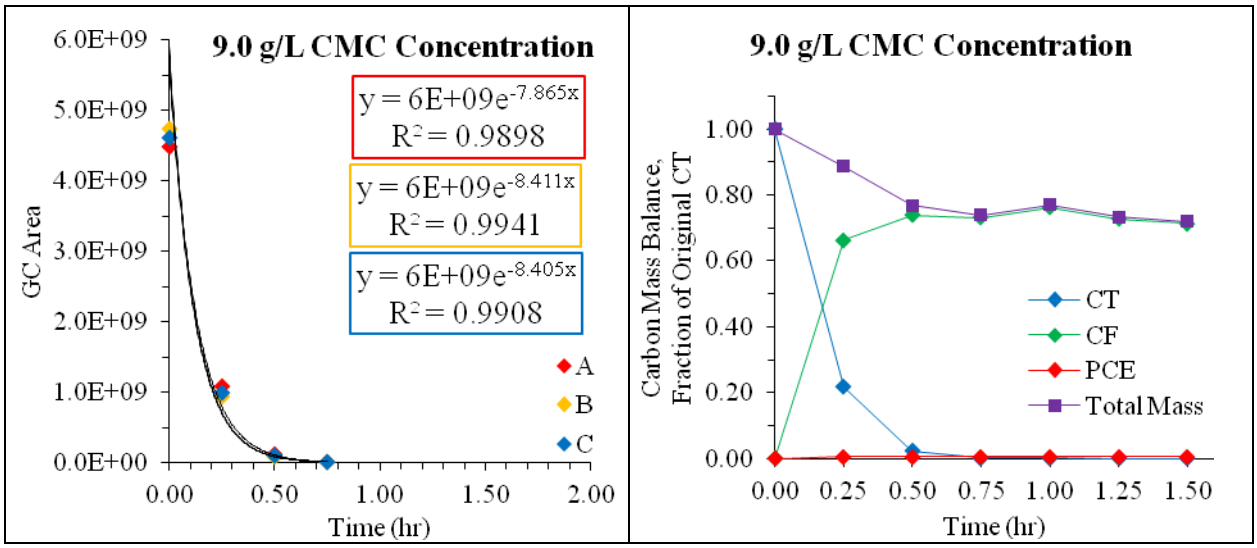

Table A.3. CMC concentration experiments, 0.01 g/L nZVI loading, CT (5 of 5).

Table A.4. Pd loading experiments, 0.01 g/L nZVI loading, CT (1 of 5).

Group #3: Varying Pd Loading				k_{obs}	$k_{average}$	k_m	Std.	Fraction Original Carbon Mass at End of Sampling						
Experimental Conditions		#	Condition	(1/hr)	(1/hr)	(L/g/hr)	Dev.	CT	CF	PCE	Methane	Ethane	Ethene	Total
$NaBH_4$: $FeSO_4$	6 : 1	16	0.00 %w/w Pd Loading	4.572	4.31	4.3E+02	0.38	0.00	0.68	0.06	No Data	No Data	No Data	**0.74**
				4.487										
nZVI Loading	0.01 g/L			3.879										
		17	0.17 %w/w Pd Loading	4.660	4.23	4.2E+02	0.57	0.00	0.57	0.07	No Data	No Data	No Data	**0.63**
pH	7			4.447										
				3.585										
TAPSO	7.81 mM	18	0.33 %w/w Pd Loading	4.572	4.47	4.5E+02	0.20	0.00	0.51	0.05	No Data	No Data	No Data	**0.56**
				4.591										
CMC	8 g/L			4.244										
		19	0.66 %w/w Pd Loading	4.642	4.37	4.4E+02	0.32	0.00	0.64	0.09	No Data	No Data	No Data	**0.73**
Pd Loading	Variable			4.432										
				4.022										
CAH of Study	CT	20	1.00 %w/w Pd Loading	5.418	5.28	5.3E+02	0.32	0.00	0.69	0.07	No Data	No Data	No Data	**0.76**
				5.513										
[Contaminant]	1125 ppb			4.921										
		21	1.33 %w/w Pd Loading	6.168	5.86	5.9E+02	0.42	0.00	0.71	0.05	No Data	No Data	No Data	**0.76**
				6.028										
				5.389										
		22	1.66 %w/w Pd Loading	9.594	9.96	1.0E+03	0.48	0.00	0.59	0.11	No Data	No Data	No Data	**0.70**
				10.500										
				9.773										
		23	2.00 %w/w Pd Loading	15.45	15.46	1.5E+03	0.08	0.00	0.40	0.02	No Data	No Data	No Data	**0.42**
				15.39										
				15.55										
		24	2.33 %w/w Pd Loading	14.95	16.10	1.6E+03	1.61	0.00	0.38	0.00	No Data	No Data	No Data	**0.38**
				17.94										
				15.42										
		25	3.33 %w/w Pd Loading	16.73	17.34	1.7E+03	0.86	0.00	0.37	0.00	No Data	No Data	No Data	**0.37**
				–										
				17.94										
		26	5.00 %w/w Pd Loading	15.38	16.15	1.6E+03	0.81	0.00	0.35	0.02	No Data	No Data	No Data	**0.37**
				16.99										
				16.07										

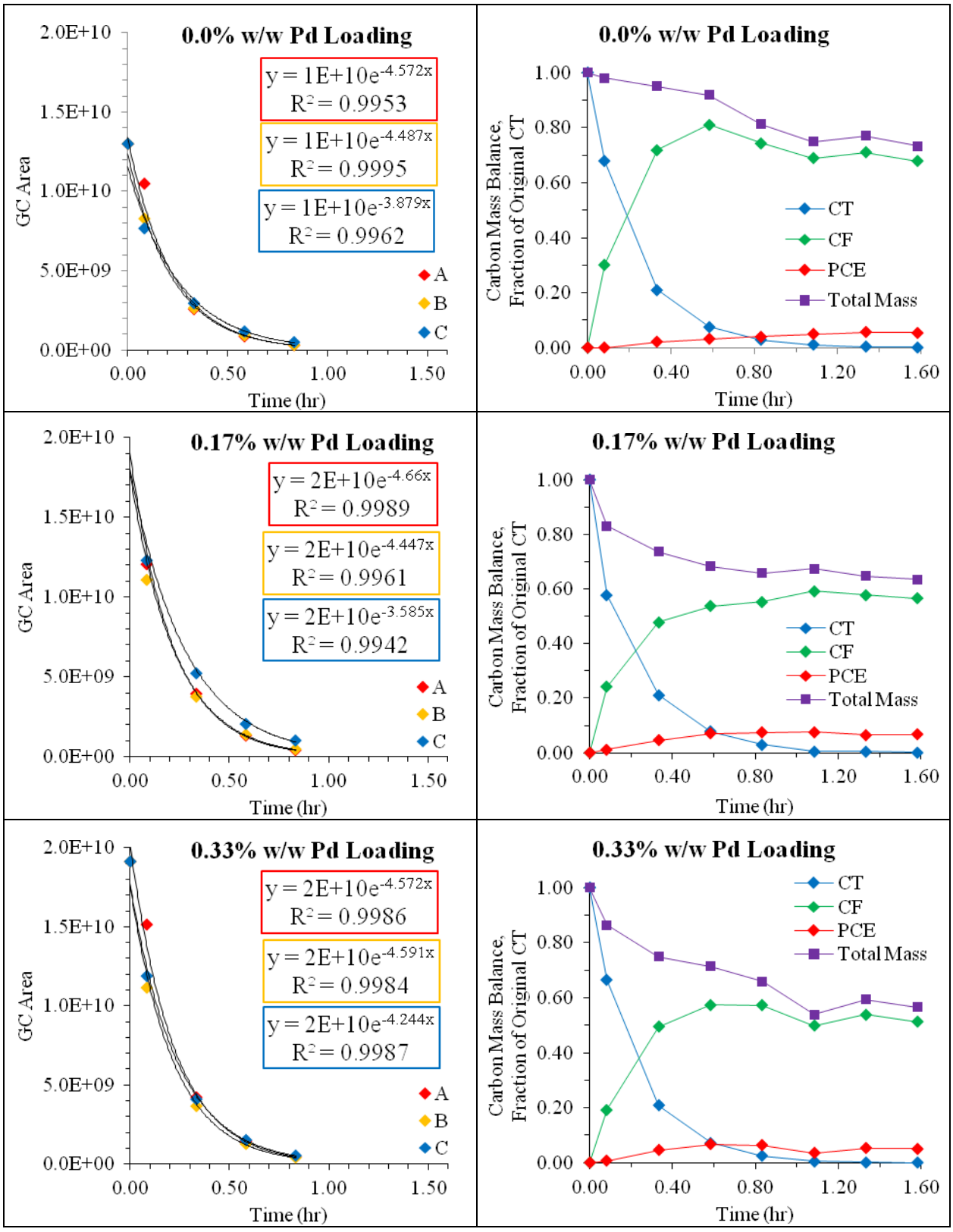

Table A.4. Pd loading experiments, 0.01 g/L nZVI loading, CT (2 of 5).

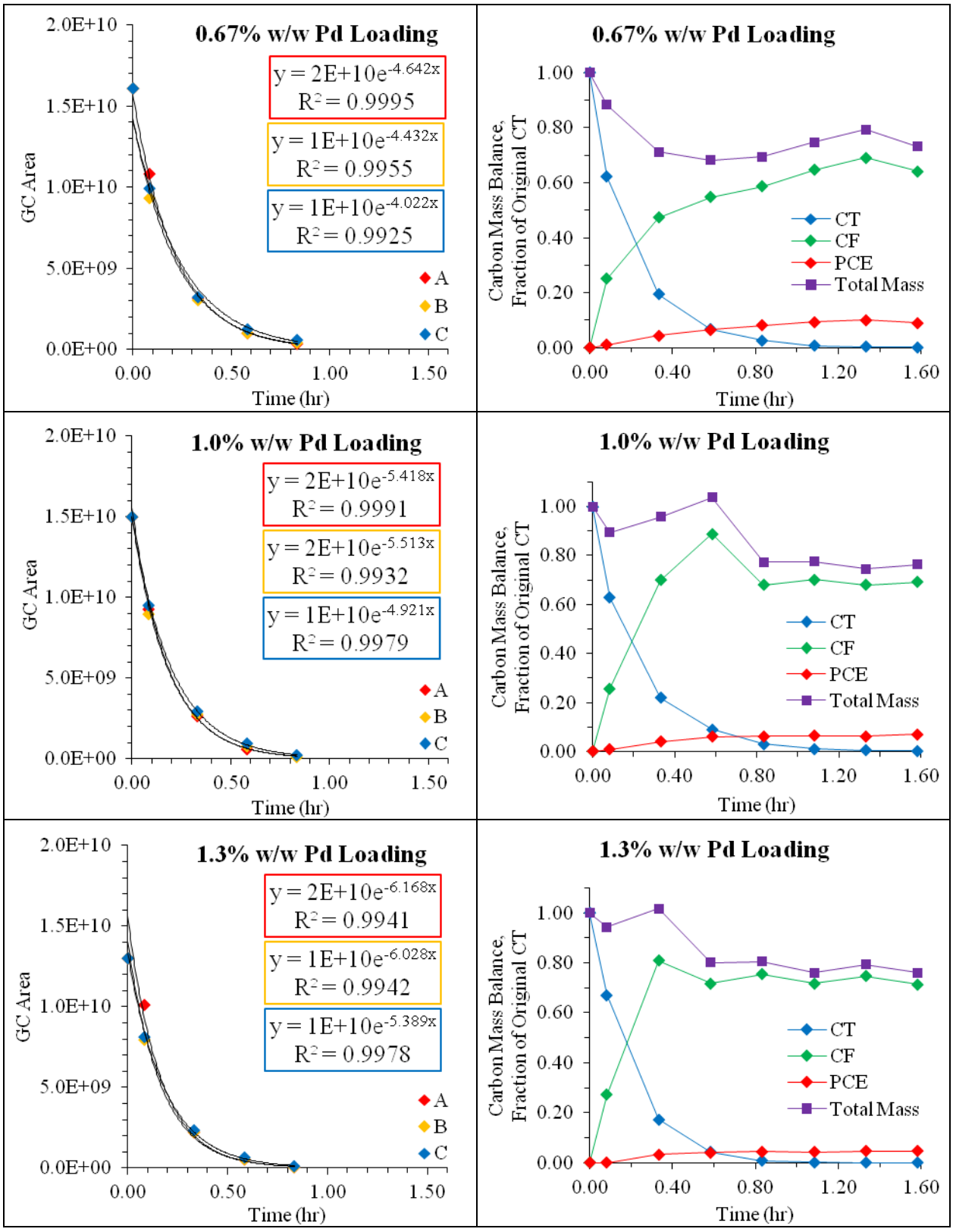

Table A.4. Pd loading experiments, 0.01 g/L nZVI loading, CT (3 of 5).

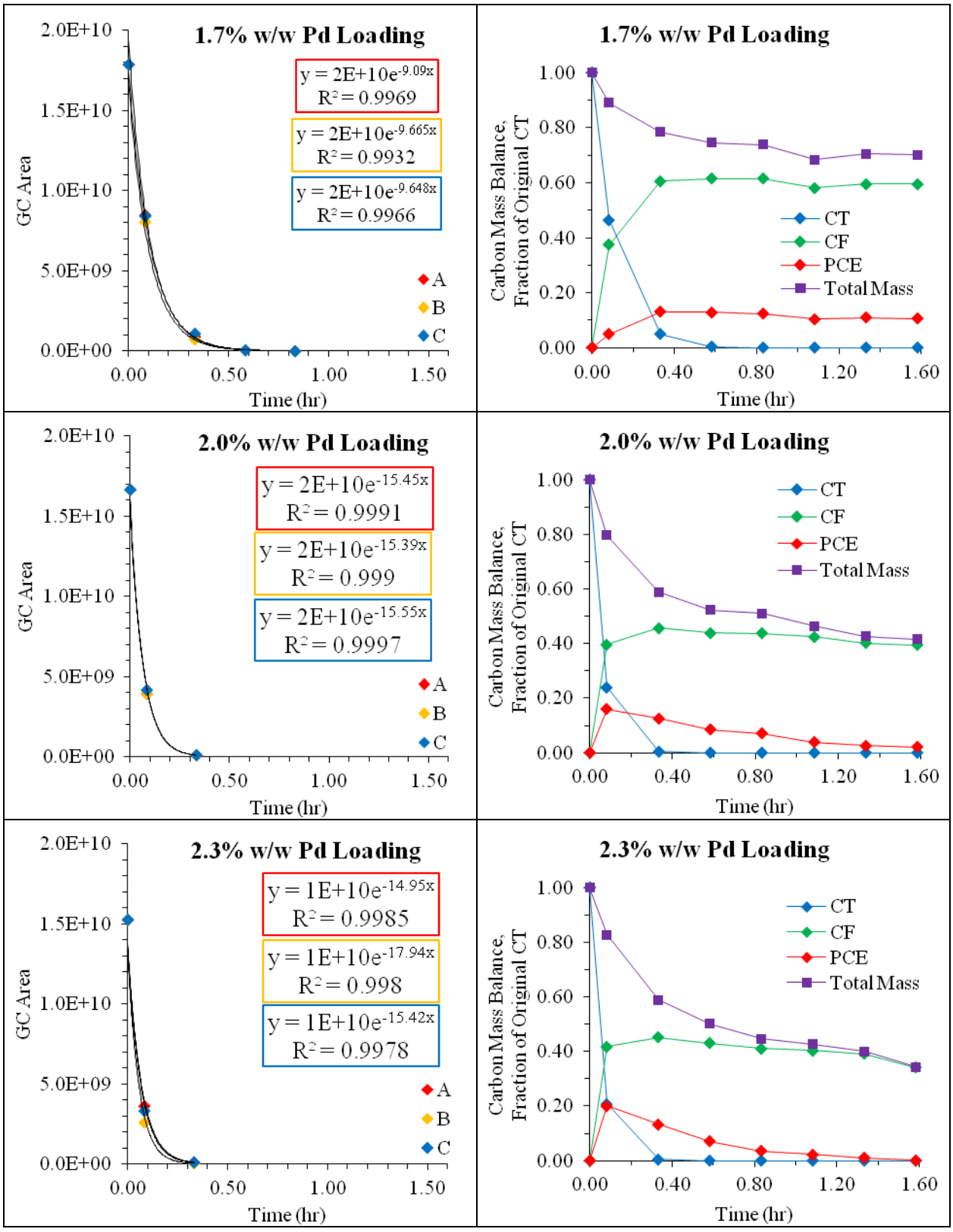

Table A.4. Pd loading experiments, 0.01 g/L nZVI loading, CT (4 of 5).

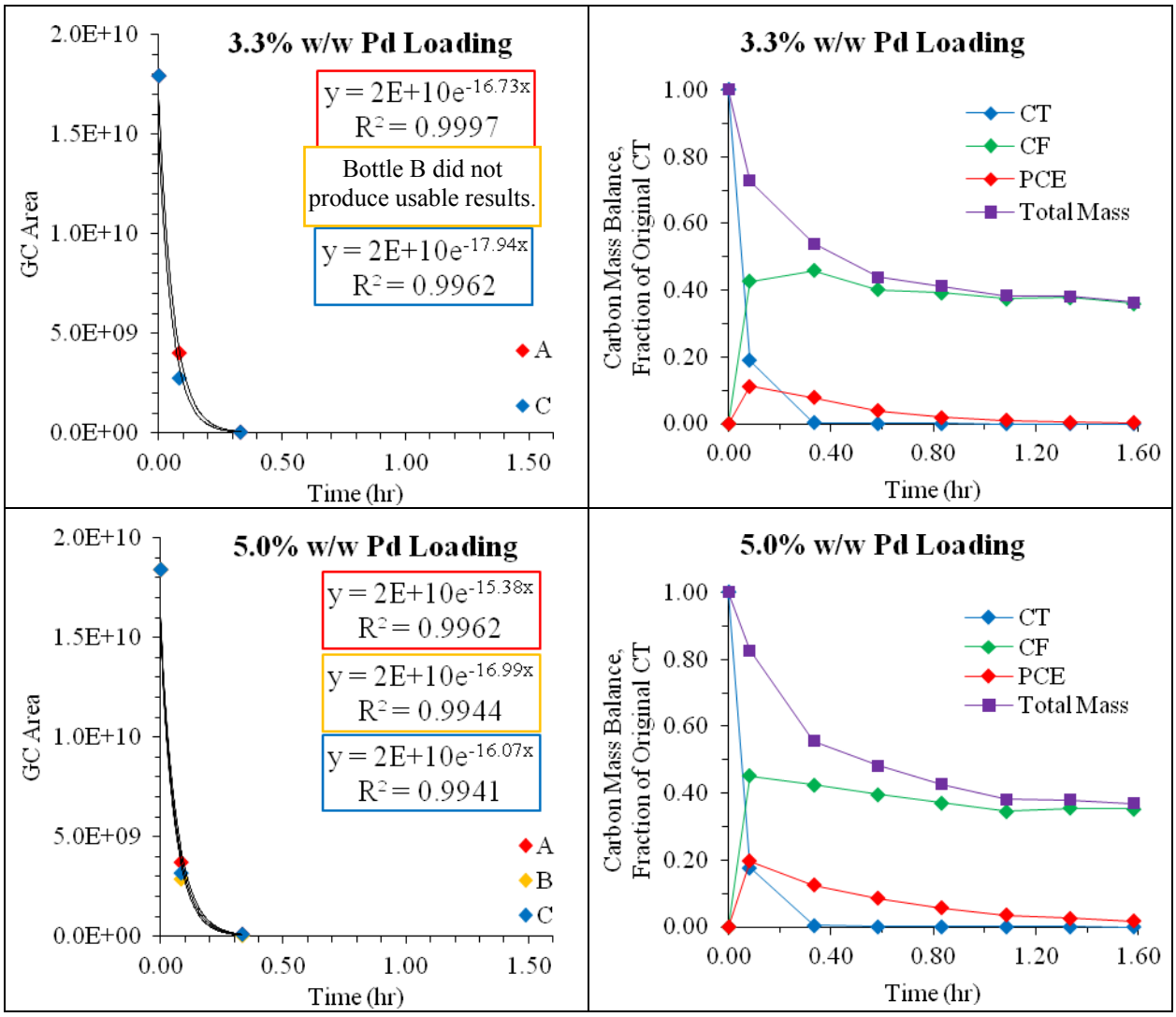

Table A.4. Pd loading experiments, 0.01 g/L nZVI loading, CT (5 of 5).

Table A.5. Pd loading experiments, 0.10 g/L nZVI loading, CF (1 of 4).

Group #7: Varying Pd Loading				k_{obs}	$k_{average}$	k_m	Std.	Fraction Original Carbon Mass at End of Sampling						
Experimental Conditions		#	Condition	(1/hr)	(1/hr)	(L/g/hr)	Dev.	CF	DCM	Methane	–	–	–	Total
$NaBH_4$: $FeSO_4$	6 : 1	**37**	0.00 %w/w Pd Loading	0.51	0.48	4.8E+00	0.04	0.32	0.18	0.05	–	–	–	**0.55**
				0.48										
nZVI Loading	0.1			0.44										
		41	0.50 %w/w Pd Loading	0.89	0.69	6.9E+00	0.17	0.31	0.20	0.06	–	–	–	**0.57**
pH	7			0.61										
				0.57										
TAPSO	7.81 mM	**38**	1.00 %w/w Pd Loading	0.94	0.88	8.8E+00	0.05	0.23	0.17	0.09	–	–	–	**0.49**
				0.86										
CMC	8 g/L			0.85										
		39	2.00 %w/w Pd Loading	1.05	0.99	9.9E+00	0.08	0.18	0.24	0.13	–	–	–	**0.55**
Pd Loading	Variable			0.90										
				1.01										
CAH of Study	CF	**31**	3.33 %w/w Pd Loading	1.56	1.62	1.6E+01	0.15	0.13	0.18	0.23	–	–	–	**0.54**
				1.79										
[Contaminant]	1754 ppb			1.52										
		40	4.00 %w/w Pd Loading	1.81	1.70	1.7E+01	0.13	0.07	0.34	0.15	–	–	–	**0.56**
				1.74										
				1.56										
		32	6.66 %w/w Pd Loading	1.85	1.85	1.9E+01	0.10	0.05	0.21	0.23	–	–	–	**0.49**
				1.96										
				1.76										

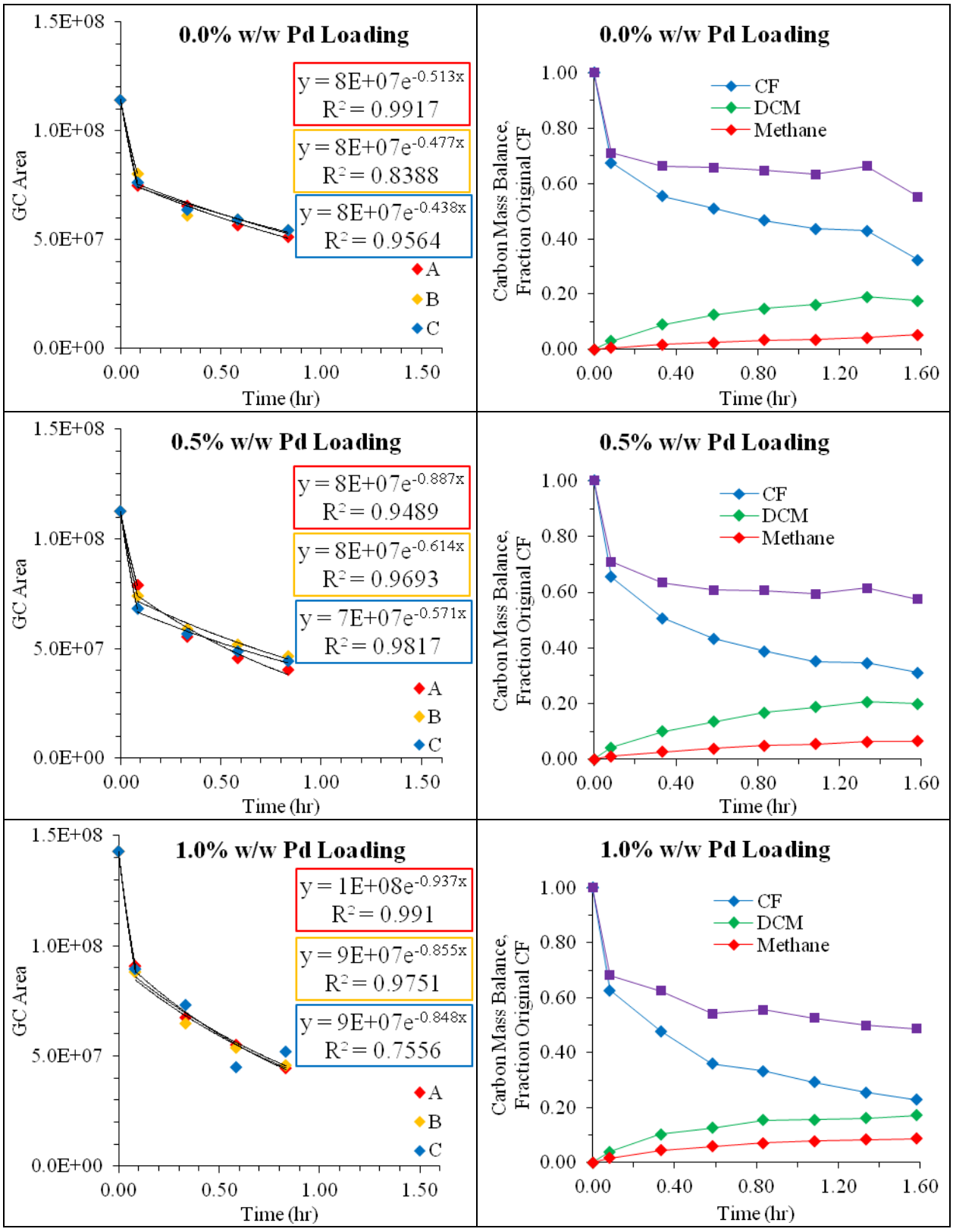

Table A.5. Pd loading experiments, 0.10 g/L nZVI loading, CF (2 of 4).

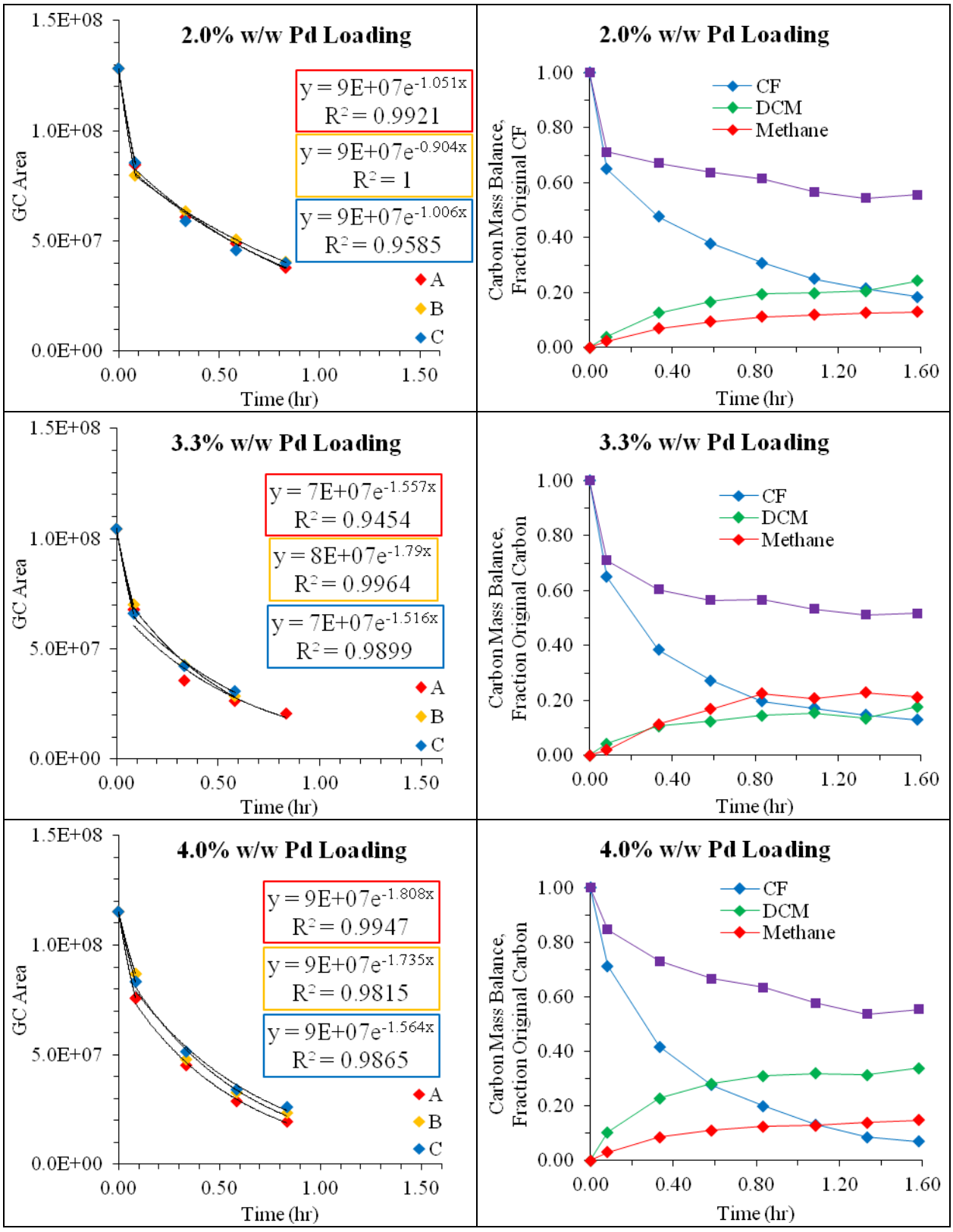

Table A.5. Pd loading experiments, 0.10 g/L nZVI loading, CF (3 of 4).

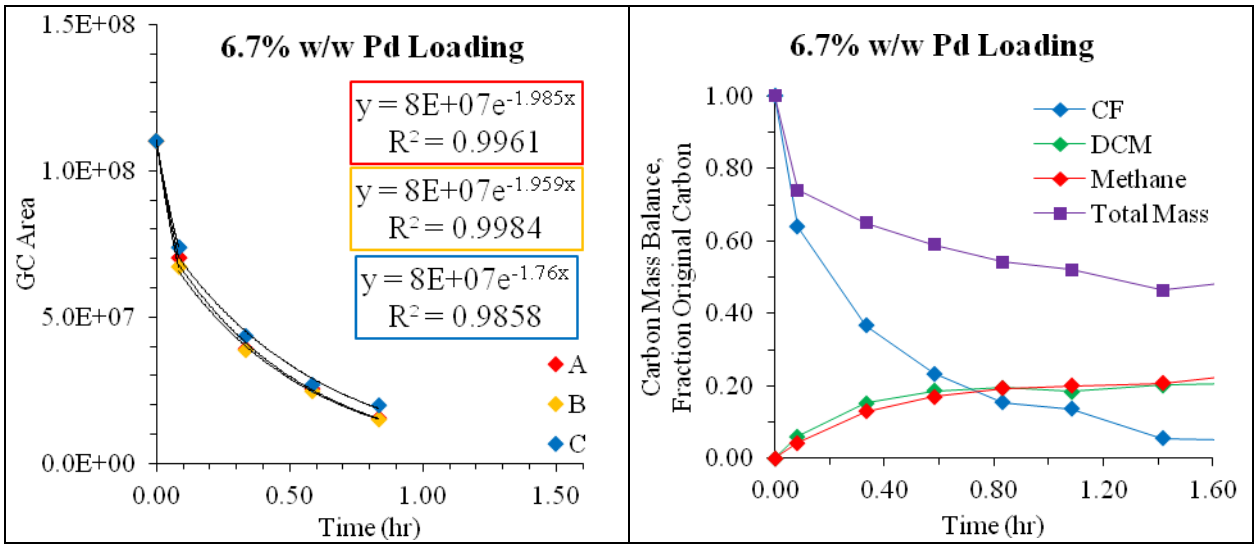

Table A.5. Pd loading experiments, 0.10 g/L nZVI loading, CF (4 of 4).

Table A.6. PCE & TCE experiments, 0.10 g/L nZVI loading (1 of 3).

Group #6: PCE & TCE Degradation				k_{obs}	$k_{average}$	k_m	Std.	Fraction Original Carbon Mass at End of Sampling						
Experimental Conditions		#	Condition	(1/hr)	(1/hr)	(L/g/hr)	Dev.	PCE	TCE	Ethane	Ethene	1,1,2-TCA	–	Total
$NaBH_4$: $FeSO_4$	6 : 1	**33**	0.01 g/L nZVI, PCE	1.25	1.33	1.3E+02	0.17	0.19	0.00	0.30	0.00	0.04	–	**0.53**
				1.21										
nZVI Loading	0.01		3.3% Pd Loading	1.52										
		42	0.01 g/L nZVI, PCE	0.48	0.58	5.8E+01	0.11	0.65	0.02	0.13	0.04	0.00	–	**0.84**
pH	7			0.55										
			0% Pd Loading	0.70										
TAPSO	7.81 mM	**34**	0.01 g/L nZVI, TCE	12.30	14.00	1.4E+03	1.51	–	0.00	0.98	0.00	0.00	–	**0.98**
				14.51										
CMC	8 g/L		3.3% Pd Loading	15.18										
		43	0.01 g/L nZVI, TCE	–	2.88	2.9E+02	0.00	–	0.01	0.63	0.08	0.00	–	**0.72**
Pd Loading	3.2% w/w			2.88										
			0% Pd Loading	2.87										
CAH of Study	PCE & TCE													
[Contaminant]	1833 & 1509 ppb, respect.													

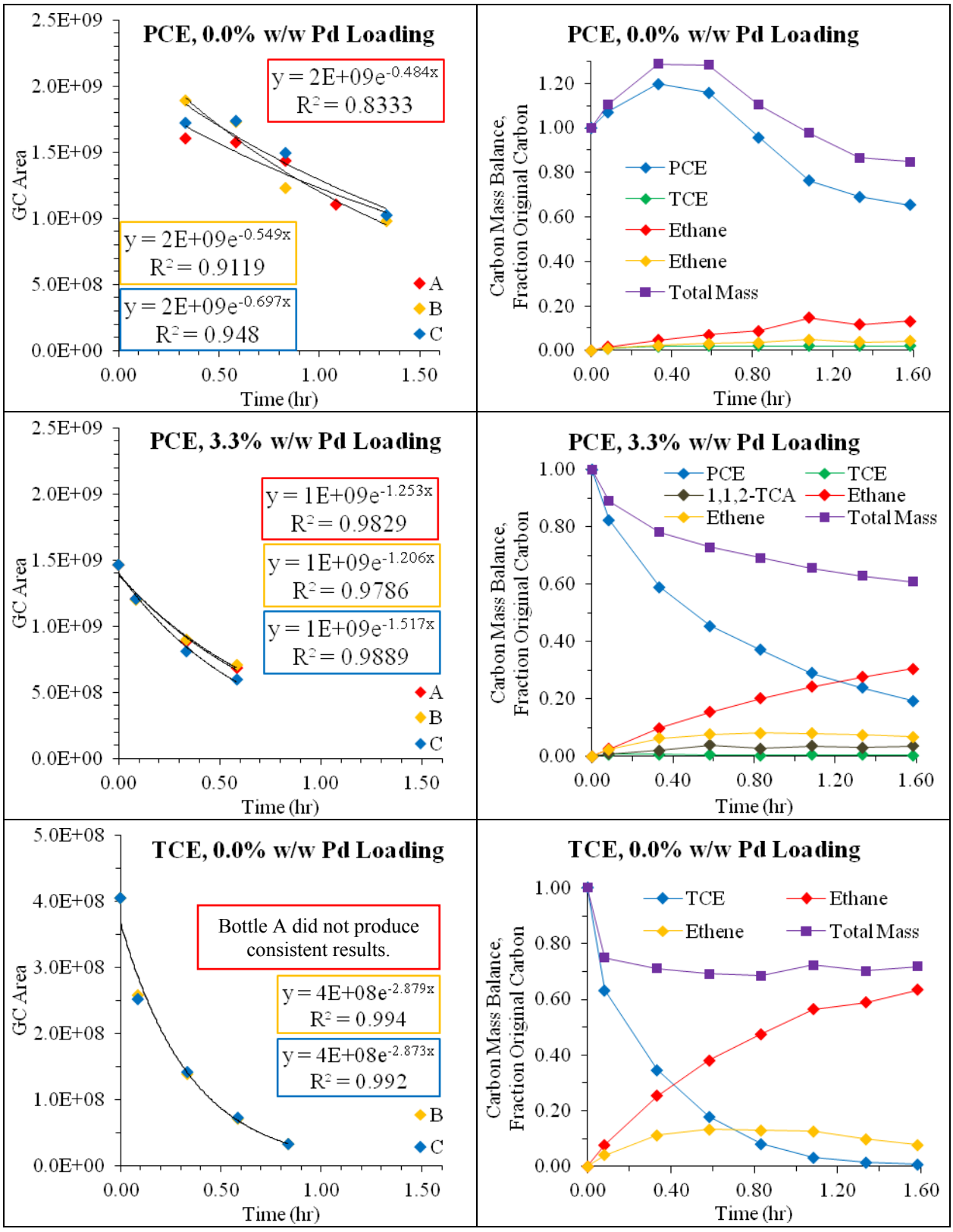

Table A.6. PCE & TCE experiments, 0.10 g/L nZVI loading (2 of 3).

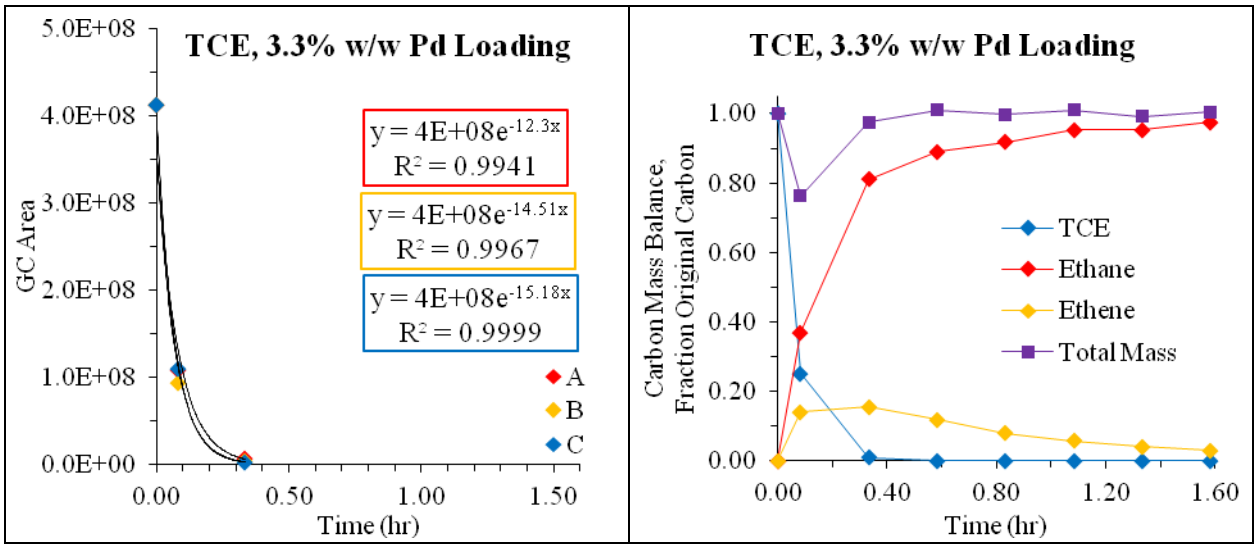

Table A.6. PCE & TCE experiments, 0.10 g/L nZVI loading (3 of 3).

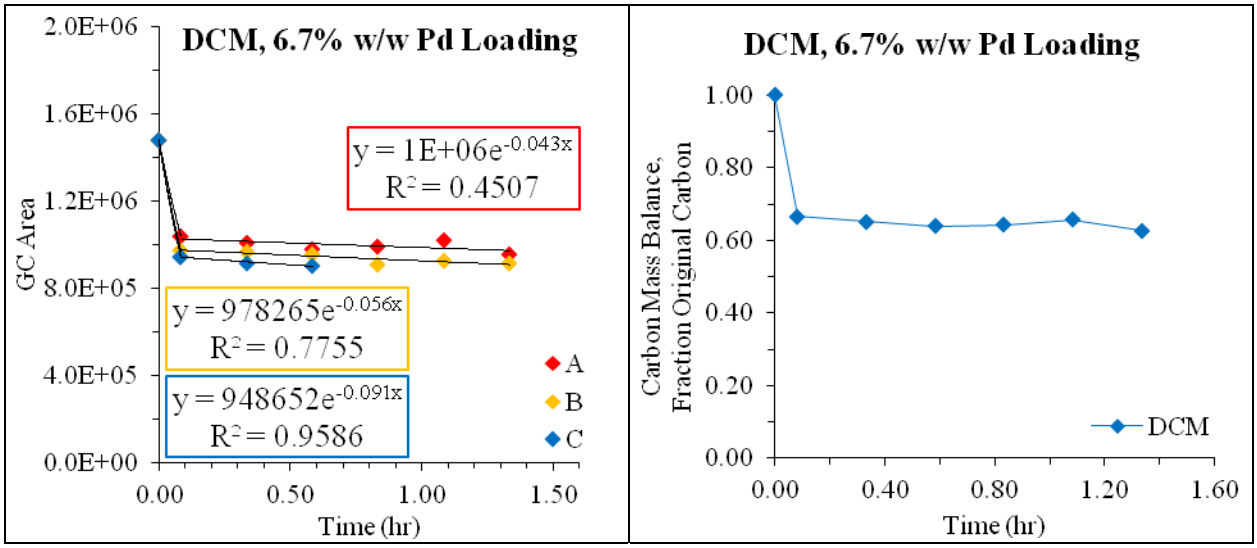

Table A.7. DCM experiments, 0.10 g/L nZVI loading.

Appendix B. Effect of Increasing nZVI Loading on CF Degradation and Byproducts

Group #5: Varying nZVI Loading, CF				k_{obs} (1/hr)	$k_{average}$ (1/hr)	k_m (L/g/hr)	Std. Dev.	Fraction Original Carbon Mass at End of Sampling					
Experimental Conditions		#	Condition					CF	DCM	Methane	–	–	–	Total
$NaBH_4$: $FeSO_4$	6 : 1	**36**	0.01 g/L nZVI	0.18	0.16	1.6E+01	0.09	0.71	0.05	0.08	–	–	–	**0.83**
				0.24										
				0.07										
nZVI Loading	Variable													
pH	7	**30**	0.05 g/L nZVI	0.65	0.56	1.1E+01	0.07	0.33	0.08	0.20	–	–	–	**0.61**
				0.53										
				0.51										
TAPSO	7.81 mM	**31**	0.10 g/L nZVI	1.56	1.62	1.6E+01	0.15	0.13	0.18	0.23	–	–	–	**0.54**
				1.79										
				1.52										
CMC	8 g/L			1.07	1.12	5.6E+00	0.07	0.15	0.12	0.14	–	–	–	**0.41**
Pd Loading	3.3% w/w	**35**	0.20 g/L nZVI	1.20										
				1.08										
CAH of Study	CF													
[Contaminant]	1754 ppb													

Table B.1. Effect of increasing nZVI loading on CF degradation and byproducts.

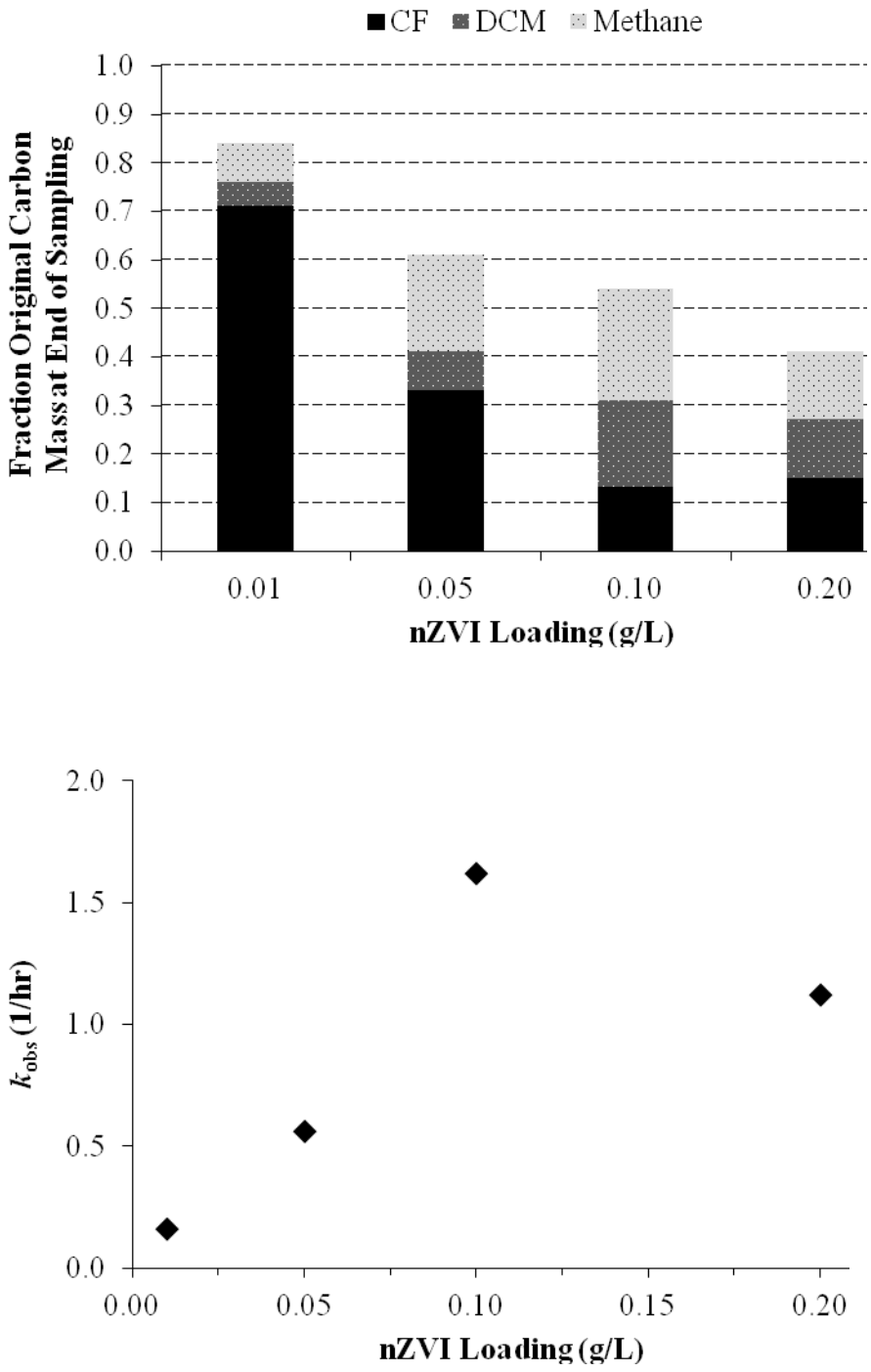

Figure B.1. Effect of increasing nZVI loading on CF (a) degradation and (b) byproducts.

Bibliography

Sources referenced here are those used within the introduction and conclusion. References for the scholarly articles are omitted here, and instead included with their respective manuscripts to preserve the utility of in-text citations.

1. Chun, C.L., D.R. Baer, D.W. Matson, J.E. Amonette, and R.L. Penn. "Characterization and Reactivity of Iron Nanoparticles Prepared With Added Cu, Pd, and Ni," *Environmental Science & Technology*, 44: 5079-5085 (2010).

2. Crane, R.A. and T.B. Scott. "Nanoscale Zero-Valent Iron: Future Prospects for an Emerging Water Treatment Technology," *Journal of Hazardous Materials*, Preprint, Accepted for Publication (2010), doi:10.1016/j.jhazmat.2011.11.073.

3. Feng, Jing and Teik-Thye Lim. "Pathways and Kinetics of Carbon Tetrachloride and Chloroform Reductions by Nano-Scale Fe and Fe/Ni Particles: Comparison With Commercial Micro-Scale Fe and Zn," *Chemosphere*, 59: 1267-1277 (2005).

4. Henderson, Andrew D. and Avery H. Demond. "Long-Term Performance of Zero-Valent Iron Permeable Reactive Barriers: A Critical Review," *Environmental Engineering Science*, 24: 401-423 (2007).

5. Karn, Barbara, Todd Kuiken, and Martha Otto. "Nanotechnology and in Situ Remediation: A Review of the Benefits and Potential Risks," *Environmental Health Perspectives*, 117: 1823-1831 (December 2009).

6. Naval Facilities Engineering Command. *Cost and Performance Report, Nanoscale Zero-Valent Iron Technologies for Source Remediation*. Contract Report; CR-05-007-ENV. Port Hueneme: NAVFAC, 2005.

7. Quinn, Jacqueline and others. "Use of Nanoscale Iron and Bimetallic Particles for Environmental Remediation: A Review of Field-scale Appications," in Environmental Applications of Nanoscale and Microscale Reactive Metal Particles. Ed. Cherie L. Geiger and Kathleen M. Carvalho-Knighton: American Chemical Society, 2009.

8. Song, Hocheol and Elizabeth R. Carraway. "Reduction of Chlorinated Methanes by Nano-Sized Zero-Valent Iron: Kinetics, Pathways, and Effect of Reaction Conditions," *Environmental Engineering Science*, 23: 272-284 (2006).

9. U.S. Government Accountability Office. *Groundwater Contamination, DOD Uses and Develops a Range of Remediation Technologies to Clean Up Military Sites*. Report to Congressional Committees; GAO-05-666. Washington: GAO, 30 June 2005.

10. Wang, Chuan-Bao and Wei-Xian Zhang. "Synthesizing Nanoscale Iron Particles for Rapid and Complete Dechlorination of TCE and PCBs," *Environmental Science & Technology*, 31: 2154-2156 (1997).

Vita

2Lt Andrew McPherson graduated from Kellogg High School in Kellogg, Idaho. In 2006, he entered undergraduate studies at the United States Air Force Academy in Colorado Springs, CO, where he studied Environmental Engineering. In May, 2010, he graduated and commissioned in the U.S. Air Force. His place in the top 15% of his class earned him the opportunity to study for his Master's degree at the Air Force Institute of Technology. In July, 2010, he entered the Graduate School of Engineering and Management, where he earned a Master's of Science degree in Environmental Engineering and Science with a focus in Water Resources. Upon graduation, he will be assigned to the 374th Civil Engineering Squadron, Yokota Air Base, Japan.

REPORT DOCUMENTATION PAGE

Form Approved
OMB No. 074-0188

PLEASE DO NOT RETURN YOUR FORM TO THE ABOVE ADDRESS.

1. REPORT DATE *(DD-MM-YYYY)*	2. REPORT TYPE	3. DATES COVERED *(From – To)*
22-03-2012	Master's Thesis	July 2011 – March 2012

4. TITLE AND SUBTITLE
Optimization of Nanoscale Zero-Valent Iron for the Remediation of Groundwater Contaminants

5a. CONTRACT NUMBER

5b. GRANT NUMBER

5c. PROGRAM ELEMENT NUMBER

6. AUTHOR(S)
McPherson, Andrew W.E., Second Lieutenant, USAF

5d. PROJECT NUMBER
12V293I

5e. TASK NUMBER

5f. WORK UNIT NUMBER

7. PERFORMING ORGANIZATION NAMES(S) AND ADDRESS(S)
Air Force Institute of Technology
Graduate School of Engineering and Management (AFIT/EN)
2950 Hobson Way, Building 640
WPAFB OH 45433-7765

8. PERFORMING ORGANIZATION REPORT NUMBER
AFIT/GES/ENV/12-M01

9. SPONSORING/MONITORING AGENCY NAME(S) AND ADDRESS(ES)
Naval Facilities Engineering Service Center
Nancy E. Ruiz, Ph.D., Environmental Engineer
1100 23rd Ave. EV 31
Port Hueneme, CA 93043
Phone: (805) 982-1155, DSN: 551-1155, Email: Nancy.Ruiz@navy.mil

10. SPONSOR/MONITOR'S ACRONYM(S)
NFESC

11. SPONSOR/MONITOR'S REPORT NUMBER(S)

12. DISTRIBUTION/AVAILABILITY STATEMENT
APPROVED FOR PUBLIC RELEASE; DISTRIBUTION UNLIMITED

13. SUPPLEMENTARY NOTES

14. ABSTRACT

Nanoscale zero-valent iron (nZVI) is an emerging tool for the remediation of groundwater contaminants. The nanoparticles are capable of reductively destroying or immobilizing a wide range of contaminants. Their small size results in a high surface area to mass ratio, making them much more reactive compared to their more-coarse predecessors. Small particle size also allows nZVI particles to be injected directly into contaminated areas via a well, limiting the above-ground footprint and allowing access to contaminated areas that are beyond the reach of some conventional methods. nZVI technology has the potential to facilitate remediation in difficult situations, improve remediation outcomes, and reduce remediation costs. Using bench-scale laboratory experiments, this research investigates three methods for improving the reactivity and transport characteristics of nZVI, including: optimizing the nanoparticle synthesis process, addition of a polyelectrolyte stabilizer, and amendment of the particles with a palladium catalyst. Optimizing the synthesis method improved reactivity by 72%. Addition of a polyelectrolyte stabilizer further increased nZVI reactivity by 452%, while decreasing mean particle size from 29.3 to 4.6 nm and inhibiting aggregation. Finally, amendment with an optimized amount of 3.3% (w/w) palladium catalyst increased reactivity by another 375% while decreasing the formation of toxic byproducts during contaminant degradation.

15. SUBJECT TERMS
nZVI; Groundwater Remediation; Zero-Valent Iron; Chlorinated Methanes; Chlorinated Ethenes

16. SECURITY CLASSIFICATION OF:			17. LIMITATION OF ABSTRACT	18. NUMBER OF PAGES	19a. NAME OF RESPONSIBLE PERSON
a. REPORT	b. ABSTRACT	c. THIS PAGE			AFIT Faculty, Mark N. Goltz, LtCol (Ret.), Ph.D.
U	U	U	UU	114	19b. TELEPHONE NUMBER *(Include area code)* (937) 255-6565, x4638 (Mark.Goltz@afit.edu)